

NASA/TM—2003-212487



Results of Mechanical Testing for PyroceramTM Glass-Ceramic

Sung R. Choi
Ohio Aerospace Institute, Brook Park, Ohio

John P. Gyekenyesi
Glenn Research Center, Cleveland, Ohio

The NASA STI Program Office . . . in Profile

Since its founding, NASA has been dedicated to the advancement of aeronautics and space science. The NASA Scientific and Technical Information (STI) Program Office plays a key part in helping NASA maintain this important role.

The NASA STI Program Office is operated by Langley Research Center, the Lead Center for NASA's scientific and technical information. The NASA STI Program Office provides access to the NASA STI Database, the largest collection of aeronautical and space science STI in the world. The Program Office is also NASA's institutional mechanism for disseminating the results of its research and development activities. These results are published by NASA in the NASA STI Report Series, which includes the following report types:

- **TECHNICAL PUBLICATION.** Reports of completed research or a major significant phase of research that present the results of NASA programs and include extensive data or theoretical analysis. Includes compilations of significant scientific and technical data and information deemed to be of continuing reference value. NASA's counterpart of peer-reviewed formal professional papers but has less stringent limitations on manuscript length and extent of graphic presentations.
- **TECHNICAL MEMORANDUM.** Scientific and technical findings that are preliminary or of specialized interest, e.g., quick release reports, working papers, and bibliographies that contain minimal annotation. Does not contain extensive analysis.
- **CONTRACTOR REPORT.** Scientific and technical findings by NASA-sponsored contractors and grantees.

- **CONFERENCE PUBLICATION.** Collected papers from scientific and technical conferences, symposia, seminars, or other meetings sponsored or cosponsored by NASA.
- **SPECIAL PUBLICATION.** Scientific, technical, or historical information from NASA programs, projects, and missions, often concerned with subjects having substantial public interest.
- **TECHNICAL TRANSLATION.** English-language translations of foreign scientific and technical material pertinent to NASA's mission.

Specialized services that complement the STI Program Office's diverse offerings include creating custom thesauri, building customized databases, organizing and publishing research results . . . even providing videos.

For more information about the NASA STI Program Office, see the following:

- Access the NASA STI Program Home Page at <http://www.sti.nasa.gov>
- E-mail your question via the Internet to help@sti.nasa.gov
- Fax your question to the NASA Access Help Desk at 301-621-0134
- Telephone the NASA Access Help Desk at 301-621-0390
- Write to:
NASA Access Help Desk
NASA Center for AeroSpace Information
7121 Standard Drive
Hanover, MD 21076

NASA/TM—2003-212487



Results of Mechanical Testing for PyroceramTM Glass-Ceramic

Sung R. Choi
Ohio Aerospace Institute, Brook Park, Ohio

John P. Gyekenyesi
Glenn Research Center, Cleveland, Ohio

National Aeronautics and
Space Administration

Glenn Research Center

September 2003

Acknowledgments

The authors are grateful to Ralph Pawlik for the experimental work done during the course of this investigation. This work was conducted under Space Act Agreement No. SAA3-298 with Science and Applied Technology, Inc., Woodland Hills, California 91367.

This report is a formal draft or working paper, intended to solicit comments and ideas from a technical peer group.

Trade names or manufacturers' names are used in this report for identification only. This usage does not constitute an official endorsement, either expressed or implied, by the National Aeronautics and Space Administration.

The Propulsion and Power Program at NASA Glenn Research Center sponsored this work.

Available from

NASA Center for Aerospace Information
7121 Standard Drive
Hanover, MD 21076

National Technical Information Service
5285 Port Royal Road
Springfield, VA 22100

Available electronically at <http://gltrs.grc.nasa.gov>

Results of Mechanical Testing for Pyroceram™ Glass-Ceramic

Sung R. Choi and John P. Gyekenyesi
National Aeronautics and Space Administration
Glenn Research Center
Cleveland, OH 44135

Abstract

Mechanical testing for Pyroceram™ 9606 glass-ceramic fabricated by Corning was conducted to determine mechanical properties of the material including slow crack growth (or life prediction parameters), flexure strength, tensile strength, compressive strength, shear strength, fracture toughness, and elastic modulus. Significantly high Weibull modulus in flexure strength, ranging from $m=34$ to 52 , was observed for the ‘fortified’ test specimens; while relatively low Weibull modulus (but comparable to most ceramics) of $m=9-19$ were obtained from the ‘unfortified’ as-machined test specimens. The high Weibull modulus for the ‘fortified’ test specimens was attributed to the chemical etching process. The slow crack growth parameter n were found to be $n = 21.5$ from constant stress-rate (“dynamic fatigue”) testing in flexure in room-temperature distilled water. Fracture toughness was determined as $K_{IC}=2.3-2.4 \text{ MPa}\sqrt{\text{m}}$ (an average of $2.35 \text{ MPa}\sqrt{\text{m}}$) both by SEPB and SEVNB methods. Elastic modulus, ranging from $E=109$ to 122 GPa , was almost independent of test temperature, material direction, and test method (strain gauging or impulse excitation technique) within in the experimental scope, indicating that the material was homogeneous and isotropic. The existence of the ‘fortified’ layer played a crucial role in controlling and determining strength, strength distribution and slow crack growth behavior. It also acted as a protective layer. Valid testing was not achieved in tension, compression and shear testing due to inappropriate test specimen configurations (in compression and shear) provided and primarily due to the existence of ‘fortified’ layer (in tension).

I. OBJECTIVES AND TEST MATRIX

Mechanical testing for Pyroceram™ 9606 glass-ceramic fabricated by Corning was performed to determine mechanical properties of the material including slow crack growth (or life prediction parameters), tensile strength, compressive strength, shear strength, fracture toughness and elastic modulus. Test specimens with different geometries/treatments were provided by Science & Applied Technology, Incorporated, via Corning. The overall, original test matrix is shown in Table 1.

II. EXPERIMENTAL PROCEDURES

1. Material and Test Specimens

The material used in this work was Pyroceram™ 9606 glass ceramic, fabricated by Corning, Inc., (Corning, NY). The glass-ceramic material has been reported to be processed from a magnesium aluminosilicate glass containing titania as a nucleating agent, and cordierite ($2\text{MgO}-2\text{Al}_2\text{O}_3-5\text{SiO}_2$) is reported as the major crystalline phase in the material [1]. Test specimens were machined from billet(s) in accordance with the test matrix and were chemically etched to ‘fortify’ their surfaces. Both machining and etching of test specimens were made by the manufacturer, Corning. The *apparent* (not *real*) thickness of test specimens was all 2.5 mm ($0.1''$), with a fortified layer thickness of around 0.2 mm . In some cases, testing was performed with test specimens that were not chemically etched, termed ‘as-machined’ test specimens. These ‘unfortified,’ as-machined test specimens were used in part in constant stress testing, fracture toughness and elastic modulus testing.

2. Slow Crack Growth (Life Prediction) Testing: Constant Stress-Rate Testing

A). *Basics*

Constant stress-rate (also called "dynamic fatigue") testing has been utilized for several decades to quantify the slow crack growth behavior of glass and ceramic materials at both ambient and elevated temperatures. The merit of constant stress-rate testing over other methods lies in its simplicity: Strengths of test specimens are determined in a routine manner at four to five stress rates by applying constant crosshead speeds (displacement-control) or constant loading rates (load-control). The slow crack growth (SCG) parameters required for life prediction/reliability are simply calculated from a relationship between failure strength and stress rate. Because of its unique advantages, constant stress-rate flexural testing has been developed as ASTM test standards to determine SCG parameters of advanced ceramics at ambient temperature (Test Method C 1368 [2] and elevated temperatures (Test Method C 1465 [3]).

Slow crack growth of glass and ceramics under mode I loading above the fatigue limit is generally described by the following empirical power-law relation [4]:

$$v = \frac{da}{dt} = A \left[\frac{K_I}{K_{IC}} \right]^n \quad (1)$$

where v , a , t are crack velocity, crack size, and time, respectively. A and n are the material/environment-dependent SCG parameters. K_I is the mode I stress intensity factor (SIF), and K_{IC} is the critical stress intensity factor or fracture toughness of the material, subjected to mode I loading. Under constant stress-rate ("dynamic fatigue") loading using either constant displacement rate or constant loading rate, the corresponding failure strength (σ_f) can be derived as a function of stress rate ($\dot{\sigma}$) as follows [5,6]:

$$\sigma_f = [B(n+1) \sigma_i^{n-2}]^{\frac{1}{n+1}} \dot{\sigma}^{\frac{1}{n+1}} \quad (2)$$

where $B = 2K_{IC}^2 / AY^2(n-2)$ with Y being a crack geometry factor in the expression of $K_I = Y\sigma\sqrt{a}$ with σ being a remote applied stress, and σ_i is the inert strength. By taking the logarithm both sides of Equation (2) yields [2]

$$\log \sigma_f = \frac{1}{n+1} \log \dot{\sigma} + \log D \quad (3)$$

where $\log D = [1/(n+1)] \log[B(n+1)\sigma_i^{n-2}]$. The SCG parameters n and D can be obtained from the slope and the intercept, respectively, of Equation (3) by using a linear regression analysis of $\log \sigma_f$ versus $\log \dot{\sigma}$. The parameter A is determined from D together with appropriate constants. Equation (3) is the commonly utilized SCG solution, from which the SCG parameters required for life prediction of structural components are determined with experimental data of strength versus stress rate.

B). *Testing*

Constant stress-rate testing for 'fortified' test specimens was carried out in flexure at room temperature in distilled water (100% R.H.). A stainless steel, four-point flexure fixture with 20 mm-inner and 40 mm-outer spans was used with alumina roller pins. The *apparent* dimensions of flexure-beam test specimens were 2.5 mm by 5.1 mm by 46 mm, respectively, for thickness (depth), width and overall length. Six different (*apparent*) stress rates of 50, 5, 0.5, 0.05, 0.005 and 0.0005 MPa/s were employed under load control using an electromechanical test frame (Model 8562, Instron, Canton, MA). A total of 30 test specimens were used at each test rate, from 0.005 to 50 MPa/s, while a total 22 test specimens

were tested at the lowest test rate of 0.0005 MPa/s. All testing was conducted in accordance with ASTM Test Method C 1368 [2]. Inert strength (strength without slow crack growth) was also evaluated in an inert environment (silicon oil, 704 Diffusion Pump Fluid, Dow Corning, Midland, MI) at a test rate of 50 MPa/s with a total of 30 test specimens. It was found from the fracture surface examinations of tested specimens that the average ‘fortified’ layer thickness was about 0.17 mm. Hence, the *true* stress or *true* strength (or *true* stress-rate) was calculated based on the actual specimen dimensions with the ‘fortified’ layer thickness being subtracted from the apparent dimensions. The ‘fortified’ layer will be discussed in more detail in the Results & Discussion section.

Additional constant stress-rate testing was performed for comparison in distilled water with ‘unfortified’ test specimens that were not chemically etched but as-machined. The apparent dimensions of as-machined test specimens were 2.5 mm by 5.1 mm by 46 mm in thickness (depth), width and overall length, respectively. Two test rates of 70 and 0.07 MPa/s were used with a total 20 test specimens at each test rate. Inert strength was also determined in silicon oil at 70 MPa/s using 20 test specimens. Test fixture and test frame used for the ‘unfortified’ test specimens were the same as those for the ‘fortified’ test specimens. A typical test fixture/specimen configuration used in slow-crack-growth flexure testing is shown in Figure 1.

3. Tensile Testing

Tensile strength testing of the material was conducted using ‘fortified,’ flat, shoulder-loaded tensile test specimens in accordance with ASTM Test Method C 1273 [7]. The apparent, overall dimensions of tensile test specimens were 2.5 mm by 3.2 mm by 89 mm, respectively, in thickness, width and overall length. The gage section had the apparent dimensions of 2.5 mm by 3.2 mm in cross section and about 50 mm in length. Each test specimen was loaded via four loading roller-pins (two for each end) that were in contact with the upper and lower shoulder regions of a specimen. Three different test temperature/environment conditions were used in tensile testing: room temperature in distilled water, 93 °C (200 °F) in distilled water, and 274 °C (525 °F) in ambient air. The number of test specimens used was 16, 15 and 15, respectively, at room temperature, 93 °C and at 274 °C. Test rates close to 70 MPa/s were used in load control using the electromechanical test frame (Model 8562, Instron).

Originally, alignment of each test specimen was intended by using strain gages attached to the specimen surfaces. However, a great difficulty was encountered in this approach after the finding of the existence of the ‘fortified’ layer on specimen surfaces, produced by a unique surface treatment by chemical etching that had left a ‘*soft*’ powdered layer on the specimen surface. This ‘fortified’ but soft layer was not appropriate to the application of strain gages. One might consider that the layer could be removed by careful scraping, sanding or polishing. However, this approach was vulnerable to generate new flaws by changing original flaw populations on *brittle* specimen surfaces. (The typical flaw size of ‘fortified’ test specimens was estimated to be about 50µm based on the inert strength (=303 MPa, Table 1) in flexure and fracture toughness (=2.35 MPa√m, Table 6) data.). Hence, because of this unique feature of test specimens, imposed through chemical etching, rigorous tensile strength testing with strain gages both to determine strength and elastic modulus was not feasible for the test specimens provided. Tensile testing was performed with the test specimens in as-provided condition. Figure 2 shows the tensile test set-up used in this work.

4. Compression Testing

Compression testing was conducted in room-temperature distilled water with ‘fortified,’ flat, rectangular cross-section test specimens in accordance with Test Method SACMA SRM-1 [8], derived from ASTM Test Method D 695 [9]. The apparent dimensions of test specimens were 2.5 mm by 12.5 mm by 81 mm, respectively, in thickness, width and overall length. Test specimens were supplied with three different material axes: Directions 1, 2 and 3. The use of a proper tapping material in strength testing, as recommended in Test Method SACMA SRM-1, was not feasible, again due to the existence of the *soft*, ‘fortified’ layer on the specimen surfaces. A copper or aluminum shim was placed between the

loading plate (of the upper push rod) and the top-end of a test specimen, to minimize localized stress. It was intended that compressive strength was to be determined at each material axis and that elastic modulus was to be evaluated for Direction 1. However, each individual specimen tested, due to its unique geometrical configuration, failed ('crushed') from the top end where a compression load was locally applied, resulting in localized failure leading to an invalid test. This will be discussed in the Results and Discussion section. Since strain gages could not be attachable ('bonded') to the *soft* 'fortified' layer, one specimen from each material axis was polished to remove the 'fortified' layer so that strain gages were applied to determine corresponding elastic modulus. All testing was conducted in displacement control with a test rate of 1.27 mm/min using the electromechanical test frame (Model 8562, Instron). The compression test set-up utilized is shown in Figure 3.

5. Shear Testing

Shear testing was carried out in room-temperature distilled water with 'fortified,' flat, V-notched test specimens in accordance with ASTM Test Method D 5379 [10], based on the asymmetric Iosipescu test. The apparent dimensions of test specimens were 2.5 mm by 20.3 mm by 76 mm, respectively, in thickness, depth and overall length. Again, due to the existence of the soft 'fortified' layer, strain gauging to determine shear modulus was not applicable to the test specimens. Testing was performed under displacement control with a test rate of 0.25 mm/min using the electromechanical test frame (Model 8562, Instron). Test set-up used in shear testing is shown in Figure 4.

6. Fracture Toughness Testing

Two different test methods were used in determining fracture toughness of the material. One was the single edge precracked beam (SEPB) method as specified in ASTM Test Method C 1421 [11]. The other was the single edge V-notched beam (SEVNB) method. The latter method has been recently practiced and appeared as a valid test technique through an international (VAMAS) round robin on fracture toughness [12]. The 'fortified' specimens with the apparent dimensions of 2.5 mm x 3.6 mm x 46 mm (width, depth and overall length) were used in SEPB method, while the 'unfortified' as-machined specimens with the dimensions of 2.5 mm x 5.1 mm x 46mm (width, depth and overall length) were used in SEVNB method. In SEPB method, a starting, indent crack was placed at the center of the 2.5 mm side of each test specimen (after removing the layer in a small area appropriate). The indented specimen was then placed onto a specially designed precracking fixture and then loaded via the fixture until the indent crack popped-in to form a sharp through-the-thickness crack [13], see Figure 5. In SEVNB method, a sharp razor blade with 1 μm diamond compound was placed into a precut straight saw notch to subsequently cut a very sharp V-notch with its root radius of typically less than 10 μm . A typical example of a SEVNB test specimen thus V-notch prepared is presented in Figure 6. A four-point flexure fixture with 20 mm-inner and 40 mm-outer spans was used to determine fracture load. A test rate of 0.5 mm/min was used via the electromechanical test frame (Model 8562, Instron) with a small load cell with a capacity of 1000 N. Silicon oil was used to minimize slow crack growth effect. Precrack sizes were optically determined from fracture surfaces of test specimens. A total of 10 and 9 test specimens were used, respectively, in SEPB and SEVNB methods.

7. Elastic Modulus Testing

Elastic modulus of the material was determined by methods including impulse excitation (ASTM C 1259 [14]) and strain gauging. It was found that the excitation impulse of vibration method was not applicable to the 'fortified' specimens due to their *soft* layer that acted as a damping medium by quickly diminishing vibration of test specimens. The determination of elastic modulus by the impulse excitation technique had to be made with test specimens without 'fortified' layer, that is, with as-machined test specimens. A total of 39 as-machined flexure beam test specimens, measured 2.5 mm by 5.1 mm by 46 mm, respectively, in depth, width and overall length, were used to determine elastic modulus at room temperature in ambient air by the impulse excitation method. A total of 10 specimens (out of the 39 as-

machined flexure test specimens) were used to determine elastic modulus at three different temperatures of room temperature, 93 °C (200 °F) and 274 °C (525 °F) in ambient air by a high-temperature excitation rig. This testing was a substitute to the originally planned tensile testing in which elastic modulus (together with strength) was intended to be determined by strain gauging at the three temperatures, but which later appeared inappropriate due to the *soft*, ‘fortified’ layer on the tensile test specimens provided.

As stated in the Compression Testing section, elastic modulus by strain gauging could not be obtained in compression testing with the test specimens provided, again due to the ‘fortified’ layer. One compression test specimen from each material axis -a total of three specimens in all three material directions- was polished to remove the ‘fortified’ layer from its major sides to be able to attach strain gage. With these strain-gauged specimens, elastic modulus was determined in compression in accordance with Test Method SACMA SRM-1 [8] as well as in four-point flexure (both in tension and in compression by reversing test specimens upside down) with 20/40 mm spans. Hence, three values of elastic modulus were obtainable by this approach with one test specimen.

III. RESULTS AND DISCUSSION

1. Slow Crack Growth Testing: Constant Stress-Rate Testing

A summary of the results of constant stress-rate testing for both ‘fortified’ and ‘unfortified’ test specimens is presented in Table 2, where test conditions, mean (arithmetic average) strength and Weibull parameters are included. Also included are inert strength data determined in silicon oil. The Weibull parameters (m and $m \ln \sigma_o$) were evaluated using strength data obtained at each test condition, based on the following two-parameter Weibull formula

$$\ln \ln \frac{1}{1-F} = m \ln \sigma_f - m \ln \sigma_o \quad (4)$$

where F is failure probability, m is Weibull modulus, σ_o is the characteristic strength. The Weibull mean strength in Table 2 corresponds to the strength when $F = 0.5$ or 50 %. It is also noteworthy to mention that an excellent relationship between Weibull modulus and coefficient of variation ($C.V$) for a given test condition holds

$$m \approx \frac{1.2}{C.V} = \frac{1.2}{s / \bar{\sigma}_f} \quad (4-a)$$

where s is the (± 1.0) standard deviation and $\bar{\sigma}_f$ is the arithmetic mean strength. The above relation can be checked using the data given in Table 2.

The results of constant stress-rate testing are also summarized in Figure 7, where each individual fracture strength was plotted as a function of the corresponding applied stress rate in a form of \log (*fracture stress*) vs. \log (*stress rate*) based on Equation 3. Also presented are the inert strength data for comparison as well as the best-fit regression line. As can be seen from the figure, strength decreases with decreasing stress rate, which represents the susceptibility to slow crack growth, a unique feature typical of glasses and advanced ceramics. Based on Equation (3), a linear regression analysis of \log (*individual fracture stress* in MPa) versus \log (*true stress rate* in MPa/s), as specified in ASTM C 1368 [2], for a total of 172 data points determined from *true* stress rates ranging from 71 MPa/s to 0.00071 MPa/s, yields the following result

$$\log \sigma_f = 0.04455 \log \dot{\sigma} + 2.27207; \quad r_{coef}^2 = 0.9743 \quad (5)$$

where r_{coef}^2 is the square of the coefficient of correlation in regression. Using Equations (5) and (3), the slow crack growth (SCG) parameters n and D can be determined as follows:

$$n = 21.45 \text{ and } D = 187.1 \quad (6)$$

The units of D , rather complicated, can be evaluated from Equations (3) and (5). It is noted that the value ($n = 21$) of SCG parameter determined from this material is close to the value of soda-lime glass that has been known as one of materials highly susceptible to stress corrosion in a moisture environment. Because of this high SCG susceptibility to the environment, the inert strength (with no slow crack growth) degrades significantly when the specimen is loaded in distilled water. For example, the inert strength (=303 MPa) degraded by 25 % at the fastest test rate of 71 MPa/s, whereas it degraded by 55 % at the lowest test rate of 0.00071 MPa/s (see Table 2). This slow crack growth behavior of the material controls the life of structural components so that component design should be performed in conjunction with an appropriate reliability/life-prediction methodology.

Also as can be seen in Figure 7, the strength scatter was very small and almost consistent regardless of test rate or type of test environment. As seen from Table 2, except for the strength determined at the lowest stress rate of 0.00071 MPa/s (but note that the number of test specimens was only 22 at this test rate), the corresponding Weibull modulus ranged from $m=41$ to $m=52$, which is significantly greater than those ($m=10-20$) of typical advanced ceramics such as silicon nitrides, silicon carbides and aluminas. This significantly high Weibull modulus exhibited by the test material compares well with Weibull modulus ($m=50-100$) of polymer-coated optical fused-silica glass fibers. A summary of all the Weibull strength distributions based on Equation (4), including inert strength, is shown in Figure 8. Evident from the figure are consistent Weibull modulus (slope) and systematic strength degradation with respect to decreasing test rate. Individual Weibull strength plots as well as the raw test data are included in the Appendix.

The reason for the significantly high Weibull modulus can be explored from fractographic analysis. A typical example of the fracture surface of a ‘fortified’ specimen tested is shown in Figure 9. A red dye-penetrant, customarily utilized in our lab to reveal cracks in ceramics (e.g., a SEPB crack such as in Figure 5), was placed around the specimen close to the fracture surface. Due to the existence of the surrounding *soft* ‘fortified’ layer, the dye quickly penetrated into the soft layer, thus revealing a clear demarcation between the base material and the soft layer. In fact, this was the way we determined the thickness of ‘fortified’ layers for different test specimens. Figure 9 clearly shows that fracture originated from the boundary between the base material and the layer. In other word, fracture was initiated from the *surface* of the base material. Further in-depth examinations of fracture surfaces for many tested specimens drew the same conclusion. The chemical etching process applied to the test specimens generated entirely new surface-flaw populations at the base material with a very tight distribution in flaw sizes by removing loosely distributed machining flaws.

The generation of new flaw populations by chemical etching can be further verified by comparing with the Weibull strength data obtained from the as-machined (‘unfortified’) test specimens. The strength and Weibull-parameter data for the as-machined specimens tested at 70 MPa/s, 0.07 MPa/s and in silicon oil (inert) are shown in Table 2, as well as in Figure 10. It should be noted that the Weibull modulus ranged from $m=9$ to 19, appreciably lower compared to $m=40$ to 50 for the ‘fortified’ test specimens. A comparison in strength between the ‘fortified’ and the as-machined test specimens is also illustrated in Figure 11: The strength scatter for the as-machined test specimens was greater than that of the ‘fortified’ counterparts. Also note that strength was lower for the as-machined test specimens than for the ‘fortified’ counterparts. A typical fracture surface of an as-machined specimen tested is presented in Figure 12, showing that fracture originated from a predominant machining flaw, typical of many ceramic materials. The machining damage was a primary failure source for the as-machined test specimens, resulting in both lower Weibull modulus due to *loosely* distributed flaw sizes. This compares well with the behavior of many as-machined advanced ceramic specimens that typically exhibit Weibull modulus of $m = 10$ to 20.

Therefore, based on the above observations and results, it can be concluded that the outcome of the significantly high Weibull modulus for the ‘fortified’ test specimens was attributed to extremely tightly distributed flaw sizes, formed as a result of the chemical etching process.

Finally, it should be noted that the soft ‘fortified’ layer cannot sustain any external loading so that when calculating accurate stress or strength, the layer thickness must be subtracted from the apparent specimen dimensions. In four-point flexure testing, strength (σ_f) can be calculated from the following equation

$$\sigma_f = \frac{3P_f (L_o - L_i)}{2bh^2} \quad (7)$$

where P_f is the fracture load, L_o and L_i are outer and inner spans, respectively, b is the specimen width, and h is the specimen depth. The values of b and h in order to obtain *true* strength (or *true* stress rate) should be determined as follows:

$$b = b_n - 2t \text{ and } h = h_n - 2t \quad (8)$$

where b_n and h_n are apparent width and depth of a test specimen (measured, for example, with a micrometer), respectively, and t is the average ‘fortified’ layer thickness determined from fractography or any other appropriate methods. The value of the average ‘fortified’ layer thickness was found to be $t=0.17$ mm, estimated from about 10 flexure test specimens.

2. Tensile Strength

As mentioned in the Experimental Procedures section, rigorous alignment of test specimens in tensile testing was not feasible due to the existence of the soft ‘fortified’ layer that made the use of strain gages infeasible. Tensile strength testing was conducted under this imperfect condition. A summary of test results determined at three different temperature/environment conditions is presented in Table 3. Corresponding Weibull strength distributions are presented in Figure 13. Contrary to the case for the ‘fortified’ flexure test specimens, no consistent, high Weibull modulus was observed in tensile testing. Instead, Weibull modulus changed considerably from $m=45$ at room temperature to $m=6-8$ at 93 and 274 °C, indicative of some inconsistent factors associated with tensile testing. Figure 14 depicts strength as a function of temperature. The average strength was highest in 274 °C air, intermediate in room temperature distilled water and lowest in 93 °C -distilled water. The highest strength at 274 °C could be understood by the fact that the high temperature would have reduced the moisture content of the ambient air surrounding inside the test furnace. It is well known that strength of a brittle material susceptible to slow crack growth depends on relative humidity: The higher strength yields at the lower relative humidity, and *vice versa*. The lower strength in 93 °C -distilled water, as compared with the room temperature strength, may be attributed to the effect of temperature. For the given environment (distilled water here), strength is known to decrease with increasing temperature, due to increased crack velocity by the relation of $v \sim \alpha [K_I]^n e^{-Q/RT}$ with v , α , Q , R and T being crack velocity, parameter, activation energy, gas constant, and temperature, respectively.

Figure 15 shows two typical fracture patterns associated with tensile failure: gage-section failure and transition-region failure. Transition (or ‘neck’) region failure might have occurred due to geometrical discontinuity of test specimens between the end of shoulder region and the end of gage section. This type of failure has been observed frequently in many dog-boned tensile ceramic specimens, primarily due to improper specimen machining. Because of its possible severe machining damage, discontinuity and/or subsequent higher stress concentration, this transition region acts as a failure origin, resulting in inaccurate strength measurements. About 46 % of all the tensile specimens tested failed from this

transition region. Nevertheless, the strength data of those transition-region-failed specimens were not excluded from the data pool for a description purpose.

As aforementioned, the existence of the soft ‘fortified’ layer hindered the use of strain gages for specimen alignment in tensile testing. It also worsened the alignment of specimens because of its thinning effect of specimen thickness. It was found that the average ‘fortified’ layer thickness for the tensile test specimens was about 0.21 mm. This gives an actual specimen thickness of 2.1 mm (=2.5 mm –0.42 mm) from 2.5 mm. This thickness would not be sufficient for supporting tensile loading under shoulder-loading configuration. Small deviation in parallelism between loading pins can result in significant misalignment, occurring undesirable failure such as loading-pin region failure that in turn would give under- or overestimated strength values. In fact, about 26 % of all the tensile specimens tested failed from the loading-pin contact region, giving rise to lower strength values (e.g, the three lower data points at 274 °C in Figure 14). Moreover, the non-uniform ‘fortified’ layer thickness around a test specimen would result in an additional source toward misalignment. Because of these limiting factors associated with tensile testing, it is recommended that the tensile strength data should not be used as design data (but for information purpose only).

Figure 16 represents a typical example of fracture surface showing fracture originating from a surface flaw. Despite several limiting factors, surface flaws were dominant strength-limiting flaws in tensile specimens. When a material highly susceptible to slow crack growth is exposed to an (SCG) environment, the material surface is most susceptible to failure because of slow crack growth. By contrast, flaws inside the bulk material –i.e, volume flaws- would remain in inert condition, giving much less chance to failure. Even in terms of size, surface flaws formed by chemical etching seemed to be greater than inherent volume flaws in view of all the flexure and tension testing results in this work.

3. Compression Testing

A typical example of a specimen tested in compression testing is shown in Figure 17. The specimen failed from the top end where compression load was applied and where localized stress(es) occurred. All the test specimens tested (a total of 11 test specimens) showed the same failure mode leading to load-point failure. A few of them exhibited the pulverization of top end. As a result, all compression testing conducted was of invalid testing. It is recommended that short, dumbbell-type, cylindrical compression test specimens, as recommended in ASTM Test Method C 1424 [15], be used to determine compression strength of the material. The test results, although invalid, are shown in Table 4 and Figure 18. The average ‘fortified’ layer thickness of compression test specimens was estimated as $t=0.22$ mm.

4. Shear Testing

A typical failure pattern of a test specimen subjected to asymmetric Iosipescu shear testing is presented in Figure 19. It is apparent that a desirable shear fracture did not occur. Instead, fracture originated from the notch roots at approximately 45 degree (to the shear force direction) where a maximum, principal tensile stress existed, resulting in tensile failure. Failure of brittle ceramics and glasses, in general, is governed by the maximum-principal-tensile-stress criterion even under multiaxial state of stresses. A total of 6 test specimens were tested and their failure patterns were all the same as that shown in the figure. Occurrence of pure-shear failure is rarely expected to this brittle test material under the current test fixture/specimen configuration. Shear test results, although not valid, are shown in Table 5 and Figure 20. The average ‘fortified’ layer thickness of shear test specimens was estimated to be $t=0.21$ mm.

5. Fracture Toughness

A summary of the results of fracture toughness testing using SEPB and SEVNB methods is shown in Table 6 and Figure 21. The values of fracture toughness were $K_{IC} = 2.3\pm 0.05$ MPa \sqrt{m} and 2.4 ± 0.08 MPa \sqrt{m} , respectively, by SEPB and SEVNB methods. The two methods yield excellent

agreement in fracture toughness, thereby confirming the accuracy of the values of fracture toughness determined in this work. The average value of fracture toughness is $K_{IC} = 2.35 \text{ MPa}\sqrt{\text{m}}$

6. Elastic Modulus

A summary of elastic modulus determinations is presented in Table 7. Elastic modulus determined using a room-temperature test rig was $E=122\pm 2 \text{ GPa}$ with a total of 39 as-machined flexure test specimens. Using a high-temperature test rig by impulse excitation, elastic modulus was found as $E=118\pm 2 \text{ GPa}$, $115\pm 2 \text{ GPa}$, and $122\pm 2 \text{ GPa}$, respectively, at room temperature, $93 \text{ }^\circ\text{C}$ and $274 \text{ }^\circ\text{C}$. Figure 22 shows a summary of elastic modulus determined by these two different test rigs. The variation of elastic modulus with temperature was insignificant.

Effect of material direction (axis) on elastic modulus is shown in Figure 23 (also in Table 7), where compression test specimens, with ‘fortified’ layer removed and strain gages attached, were subjected to pure compression (by Test Method SACMA SRM-1), four-point flexure tension and four-point flexure compression. No appreciable effect of material axis on elastic modulus was observed, indicative of material’s homogeneity and/or isotropy. The compression specimen of ‘Direction 1’ was additionally subjected to impulse excitation. The value was found as $E = 116 \text{ GPa}$, consistent with the values determined by strain gauging. An overall comparison of elastic modulus at room temperature determined using the three different techniques (impulse, resonance and strain gauging) is shown in Figure 24, from which a conclusion -a homogeneous and isotropic nature of the material- would be drawn.

IV. SIMPLIFIED LIFE PREDICTION

In this section, a simplified life prediction is made based on the slow crack growth data determined in this work. Time to failure (or life) of brittle ceramic, glass, or glass-ceramic components under a constant stress is expressed [6]

$$t_f = B \sigma_i^{n-2} \sigma^{-n} \quad (9)$$

where t_f is time to failure, σ_i is the inert strength, and σ is the applied stress. The parameter B and n are already defined in Equations (1) and (2). The two-parameter Weibull formula for the inert strength can be rewritten from Equation (4)

$$\ln \ln \frac{1}{1-F} = m \ln \sigma_i - m \ln \sigma_{io} \quad (10)$$

where σ_{io} is the characteristic inert strength. Solving for σ_i from Equation (10) and substituting it into Equation (9) yield

$$t_f = B \left\{ \exp \left[\frac{1}{m} \left(\ln \ln \frac{1}{1-F} + m \ln \sigma_{io} \right) \right] \right\}^{n-2} \sigma^{-n} \quad (11)$$

From Equations (2) and (3), B can be solved as follows:

$$B = \frac{D^{n+1}}{(n+1) \sigma_i^{n-2}} \quad (12)$$

From the slow crack growth data in Table 2, $n=21.45$, $D=187.1$ (both from (6)) and $\sigma_i = 303$ MPa (mean inert strength, from Table 2), giving $B = 24.3897$. Substitute $B (=24.3897)$, $m=50$ (inert Weibull modulus from Table 2) and $m \ln \sigma_o = 285.4$ (inert Weibull intercept from Table 2) into Equation (11):

$$t_f = 24.3897 \left\{ \exp \left[0.02 \ln \ln \frac{1}{1-F} + 5.7082 \right] \right\}^{19.45} \sigma^{-21.45} \quad (13)$$

where units are second in t_f and MPa in σ . The use of Equation (13) allows one to estimate a component life (with the component having the same geometry as the test coupons) for a given applied stress and failure probability. An example of a life prediction diagram based on Equation (13) is shown in Figure 25, where lifetime (time to failure) is plotted as a function of applied stress for five different levels of failure probabilities of $F = 0.5, 0.1, 1 \times 10^{-2}, 1 \times 10^{-5}, 1 \times 10^{-6}$ and 1×10^{-8} . For example, for an applied stress of 100 MPa with a failure probability of 1×10^{-6} , a component life would be about 23,000 s, which is about 6.5 h. Of course, different level of failure probability yields different lifetime.

The above approach to life prediction is based on a simple loading condition in which a constant stress is applied. Since static loading (constant stress) gives the shortest component life as compared to the case of cyclic loading or any time-varying loading as long as a peak value of time-varying load is the same as the static load, the above approach can be considered as a conservative estimate (Cyclic fatigue, a dominant crack propagation in most metals or polymers, is rarely operative in many ceramics). Although simplified, this approach has been used in life prediction for optical glass fibers (typically yielding very high Weibull modulus ranging from $m = 50$ to 100), glasses and other advanced ceramics both at room and elevated temperatures. Since the slow crack growth data in this work were obtained in the worst environment (i.e., distilled water) with 100 % relative humidity, they also can be utilized as conservative data since ambient air contains much less humidity than distilled water. In general, slow crack growth parameter n remains unchanged but D (through increase in strength) increases with decreasing humidity, thus increasing life, as reflected in Equations (11) and (12) (B increases with increasing D , and *vice versa*). Decreasing temperature exhibits the similar effect (due to the relation of $v \sim \alpha [K_I]^n e^{-Q/RT}$, as reasoned in Section III-2).

If a component is complicated in its shape giving rise to complex stress distributions, which is typical of most structural components, an appropriate life prediction tool such as the **CARES/Life** design code (developed by NASA Glenn Research Center, Cleveland, OH) in conjunction with finite element modeling should be used to predict accurate reliability/life-prediction of the components concerned.

V. CONCLUSIONS AND SUGGESTIONS

1. Six different testing for Pyroceram™, including slow crack growth flexure testing, tensile strength, compression, shear, fracture toughness, and elastic modulus testing, was conducted in various test conditions. Valid testing was not achieved in tension, compression and shear testing due to inappropriate test specimen configurations (in compression and shear) and primarily due to the existence of ‘fortified’ layer (in tension).

2. In slow crack growth testing, considerably high Weibull modulus ranging from $m=34$ to 52 was observed for the ‘fortified’ test specimens; while relatively low Weibull modulus (but comparable to most ceramics) of $m=9-19$ were obtained from the ‘unfortified’ as-machined test specimens. Fractography and strength data on the ‘unfortified’ as-machined test specimens verified that the high Weibull modulus for the ‘fortified’ test specimens was attributed to the chemical etching process that had generated new surface-flaw populations with extremely tightly distributed sizes of flaws.

3. The slow crack growth parameters n and D , required in component design, were found to be $n = 21.45$ and $D = 187.1$ from a total of 172 ‘fortified’ test specimens. Six different stress rates of 71, 7.1, 0.71, 0.071, 0.0071, and 0.00071 MPa/s were used.

4. Fracture toughness was determined as $K_{IC}=2.3-2.4 \text{ MPa}\sqrt{\text{m}}$ (an average of $2.35 \text{ MPa}\sqrt{\text{m}}$) both by SEPB and SEVNB methods.

5. Elastic modulus, ranging from $E=109$ to 122 GPa , was almost independent of test temperature, material direction, and test method (strain gauging or excitation technique) within in the experimental scope, indicating that the material was homogeneous and isotropic.

6. The existence of the 'fortified' layer plays a crucial role in controlling and determining strength, strength distribution and slow crack growth behavior. It also acts as a protective layer. Therefore, it is very important to keep this layer intact from any deteriorative scratching, rubbing with hard surface or mishandling. Furthermore, consistent etching from batch to batch or from lot to lot is a prerequisite for the reproducibility of strength and slow crack growth behavior.

7. Use of an appropriate life prediction tool such as the NASA Glenn **CARES/Life** code in conjunction with finite element modeling is recommended for accurate reliability/life-prediction of the components related.

REFERENCES

1. P. W. McMillan, *Glass-Ceramics*, Academic Press, New York (1964).
2. ASTM C1368, Test Method for Determination of Slow Crack Growth Parameters of Advanced Ceramics by Constant Stress-Rate Flexural Testing at Ambient Temperature, *Annual Book of ASTM Standards*, Vol. 15.01, ASTM, West Conshohocken, PA (2000).
3. ASTM C 1465, Test Method for Determination of Slow Crack Growth Parameters of Advanced Ceramics by Constant Stress-Rate Flexural Testing at Elevated Temperature, *Annual Book of ASTM Standards*, Vol. 15.01, ASTM, West Conshohocken, PA (2001).
4. S. M. Wiederhorn, Subcritical Crack Growth in Ceramics, pp. 613-646 in *Fracture Mechanics of Ceramics*, Vol. 2, Edited by R.C. Bradt, D.P.H. Hasselman, and F.F. Lange, Plenum Publishing Co., NY (1978).
5. A. G. Evans, Slow Crack Growth in Brittles under Dynamic Loading Conditions, *Int. J. Fracture*, 251-259, Vol. 10 (1974).
6. J. E. Ritter, Engineering Design and Fatigue of Brittle Materials, pp. 667-686 in *Fracture Mechanics of Ceramics*, Vol. 4, Edited by R.C. Bradt, D.P.H. Hasselman, and F.F. Lange, Plenum Publishing Co., NY (1978).
7. ASTM C 1273, Test Method for Tensile Strength of Monolithic Advanced Ceramics at Ambient Temperature, *Annual Book of ASTM Standards*, Vol. 15.01, ASTM, West Conshohocken, PA (2000).
8. SACMA SRM-1, Test Method for Compressive Properties of Oriented Fiber-Resin Composites, SRM 1R-94, Suppliers of Advanced Composite Materials Association.
9. ASTM D 695-96, Standard Test Method for Compressive Properties of Rigid Plastics, *Annual Book of ASTM Standards*, Vol. 08.01, ASTM, Philadelphia, PA.
10. ASTM D 5379/D5379M-93, Test Method for Shear Properties of Composite Materials by the V-Notched Beam Method, *Annual Book of ASTM Standards*, Vol. 08.01, ASTM, Philadelphia, PA.
11. ASTM C 1421, Test Method for Determination of Fracture Toughness of Advanced Ceramics at Ambient Temperature, *Annual Book of ASTM Standards*, Vol. 15.01, ASTM, West Conshohocken, PA (2000).
12. J. Kübler, Fracture Toughness of Ceramics Using the SEVNB Method: Round Robin, VAMAS Report No. 37, ESIS Document D2-99, EMPA Swiss Federal Laboratories for Material Testing and Research, Dübendorf, Switzerland (1999).
13. S. R. Choi, A. Chulya and J. A. Salem, Analysis of Precracking Parameters for Ceramic Single Edge Precracked Beam Specimens, pp. 73-88 in *Fracture Mechanics of Ceramics*, Vol. 10, Edited by R. C. Bradt, D.P.H. Hasselman, D. Munz, M. Sakai, and V. Ya. Shevchenko, Plenum Press, NY (1992).
14. ASTM C 1259, Test Method for Dynamic Young's Modulus, Shear Modulus, and Poisson's Ratio for Advanced Ceramics by Impulse Excitation of Vibration, *Annual Book of ASTM Standards*, Vol. 15.01, ASTM, West Conshohocken, PA (2000).
15. ASTM C 1424, Test Method for Monotonic Compressive Strength of Advanced Ceramics at Ambient Temperature, *Annual Book of ASTM Standards*, Vol. 15.01, ASTM, West Conshohocken, PA (2000).

Table 1.—Test Matrix for Pyroceram™ Testing

March/2000

Type of Tests	Parameters Determined	Specimen Dimensions, mm (inch)	Test Method	Test Conditions			Remarks/Others	
				Temp	Environment	Test Rates		
Pure Tension	σ , E	89x3.2x2.5 (3.5x0.125x0.1)	ASTM C1273 [7]	RT	R/H100%	(300N/s)	Strain-gauging; fractography	
	σ , E			-65F	-	(300N/s)		Strain gauging; fractography
	σ , E			200F	R/H100	(300N/s)		Strain gauging; fractography
	σ , E			525F	-	(300N/s)		Strain gauging; fractography
Pure Compression	σ	81x12.5x2.5 (3.2x0.5x0.1)	SACMA SRM-1 (ASTM D695) [8]	RT	R/H100	(1.27mm/min)	Direction 1; No strain gauging; fractography	
	σ			RT	R/H100	(1.27mm/min)		Direction 2; No strain gauging; fractography
	σ			RT	R/H100	(1.27mm/min)		Direction 3; No strain gauging; fractography
	E			RT	R/H100	(1.27mm/min)		Direction 1; strain gauging
Shear	τ , G	76x20.3x2.5 (3.0x0.8x0.1)	ASTM D5379 [10]	RT	R/H100	(0.25mm/min)	Strain gauging; fractography	
Slow Crack Growth (SCG) ("Dynamic Fatigue")	σ	46x5.1x2.5 (1.8x0.2x0.1)	ASTM C1368 [2]	RT	R/H100	(50 MPa/s)	Fractography; (strain gauging)	
	σ			RT	R/H100	(5 MPa/s)		Fractography; (strain gauging)
	σ			RT	R/H100	(0.5 MPa/s)		Fractography; (strain gauging)
	σ			RT	R/H100	(0.05 MPa/s)		Fractography; (strain gauging)
	σ			RT	R/H100	(0.005 MPa/s)		Fractography; (strain gauging)
Fracture Toughness	σ /SCG parameters	46x3.6x2.5 (1.8x0.14x0.1)	ASTM C1421 [11]	RT	Inert (silicon oil, N ₂ , or L-N)	(50 MPa/s)	Fractography; (strain gauging)	
	K _{IC} (SEPB)			RT	Inert	(0.5 mm/min)		Fractography
	K _{IC} (SEVNB)			RT	Inert	(0.5 mm/min)	Fractography	

Notes:

1. The exact test rate(s) for a given type of testing will be determined after slow crack growth ("dynamic fatigue") testing, based on the degree of slow crack growth of the material.
2. The type of inert environment to be used will also be determined based on the results of slow crack growth testing.
3. Elastic modulus ("E") and/or shear modulus ("G") of the material will also be determined by the impulse excitation method (ASTM C1259 [14]) using the compression and slow-crack-growth test specimens (in rectangular flexure-beam configuration). In this case, the use of strain gages in the slow-crack-growth test specimens will be minimized.
4. Fracture toughness will be determined by the two methods of SEPB and SEVNB. The use of two test rates, originally planned in SEPB testing, is to be changed to the use of only one test rate, since no test-rate effect is expected for ceramics in inert environment.
5. Concern about the specimen machining employed – discussion needed.
6. Concern about some surface treatment of test specimens (after machining), observable from their fracture surfaces.
7. Period of testing: April-June/2000.
8. Test matrix may be changeable and/or adjustable depending on the individual test results as testing proceeds.

Table 2.—Summary of Constant Stress-Rate (“Dynamic Fatigue”) Testing Results

Specimen Configurations	Test Method	Test Conditions			Mean Strength (MPa)	Weibull Parameters			Remarks
		Temp (°C)	Environment	Test Rate (MPa/s)		No. of Test Specimens	Weibull Modulus, m	Intercept, $\ln \sigma_0$ (MPa)	
Nominal 5.1x2.5x46 (mm ³); Fortified	ASTM C1368 [2]	RT	100% RH	7.1x10 ¹	228.1(5.3)	52.42	285.19	228.9	
		RT	100% RH	7.1x10 ⁰	*	49.60	264.00	203.4	
		RT	100% RH	7.1x10 ⁻¹	202.7(5.0)	41.44	216.51	184.2	
		RT	100% RH	7.1x10 ⁻²	183.5(5.4)	47.95	245.90	167.4	
		RT	100% RH	7.1x10 ⁻³	166.9(4.3)	45.75	229.92	151.0	
		RT	100% RH	7.1x10 ⁻⁴	150.5(4.1)	34.32	169.06	136.4	
		RT	Oil (inert)	7.1x10 ¹	135.6(4.8)	49.85	285.41	304.3	
		303.2(7.4)							
Nominal 5.1x2.5x45(mm ³); Not-Fortified	ASTM C1368 [2]	RT	100% RH	70	216.6(23.6)	10.66	57.81	218.9	Specimen edges polished Specimen edges not-polished Specimen edges polished Specimen edges polished
		RT	100% RH	70	6)	-	-	-	
		RT	100% RH	0.07	180.1(6.3)	18.80	95.13	154.6	
		RT	Oil (inert)	70	153.3(9.3)	8.57	47.32	239.6	
				235.7(30.9)					

Notes:

1. Four-point flexure with 20 mm-inner and 40 mm-outer spans used.
2. Test mode under load control.
3. Test environments: 100% relative humidity (distilled water) in fatigue testing, and silicon oil in inert testing.
4. Average fortified layer estimated to be 0.17 mm.
5. Specimen-edge polishing for the unfortified, as-machined specimens were made prior to testing, except for the testing with five specimens.
6. The parentheses in the mean-strength column indicate ± 1.0 standard deviations.
7. Two-parameter Weibull statistics was used: $\text{Lnln} [1/(1-F)] = m \ln \sigma_f - m \ln \sigma_0$, where F is failure probability, σ_f fracture stress, σ_0 characteristic strength, and $m \ln \sigma_0$ is the intercept in the Weibull plot. The Weibull mean strength corresponds to the strength when $F = 0.5$ or 50 %.

Table 3.—Summary of Tensile Strength Testing Results

Specimen Configurations	Test Method	Test Conditions				Mean Strength (MPa)	Weibull Parameters			Remarks
		Temp (°C)	Environment	Test Rate (MPa/s)	No. of Test Specimens		Weibull Modulus, m	Intercept, $m \ln \sigma_0$	Weibull Mean Strength (MPa)	
Nominal 3.2x2.5x89 (in mm); Fortified	ASTM C1273 [7]	RT	100% RH	70	16	172.3(4.6)*	45.23	233.78	174.3	
		93 (200F)	100% RH	82	15	133.1(20.4)	7.50	37.17	135.3	
		274(525F)	Air	82	15	212.6(37.5)	5.82	31.66	216.3	

Notes:

1. Specimens in shoulder-loading configuration.
2. Test mode under load control.
3. Test environments: 100% relative humidity (distilled water) at RT (25 °C) and 93 °C (200F), and ambient air at 274 °C (525F).
4. Average fortified layer estimated to be 0.21 mm.
5. The parentheses in the mean-strength column indicate ± 1.0 standard deviations.
6. Two-parameter Weibull statistics was used: $L \ln [1/(1-F)] = m \ln \sigma_f - m \ln \sigma_0$, where F is failure probability, σ_f fracture stress, σ_0 characteristic strength, and $m \ln \sigma_0$ is the intercept in the Weibull plot. The Weibull mean strength corresponds to the strength when $F = 0.5$ or 50 %.

Table 4.—Summary of Compression Testing Results

Specimen Configurations	Test Method	Test Conditions			Mean Strength (MPa)	Weibull Parameters			Remarks
		Temp (°C)	Environment	Test Rate (mm/min)		No. of Test Specimens	Weibull Modulus, m	Intercept, $\ln \sigma_0$ (MPa)	
Nominal 12.5x2.5x81 (in mm); Fortified	SACMA SRM-1 [8]	RT	100% RH	1.27	[748(176)]	-	-	-	Direction 1
		RT	100% RH	1.27	[722(164)]	-	-	-	Direction 2
		RT	100% RH	1.27	[982(57)]	-	-	-	Direction 3

Notes:

1. Test mode under displacement control.
2. Test environments: 100% relative humidity (distilled water).
3. Average fortified layer estimated to be 0.22 mm.
4. All the specimens tested failed from the top portion of specimens where compression load was applied via an aluminum shim. Crushing from the top portion of test specimens was a typical exclusive failure mode. Invalid testing, hence unable to determine the valid compressive strength of the material.

Table 5.—Summary of Shear Testing Results

Specimen Configurations	Test Method	Test Conditions			Mean Strength (MPa)	Weibull Parameters			Remarks
		Temp (°C)	Environment	Test Rate (mm/min)		No. of Test Specimens	Weibull Modulus, m	Intercept, $\ln \sigma_0$ (MPa)	
Nominal 20.3x2.5x76 (in mm) with Double Notches; Fortified	ASTM D 5379 [10]	RT	100% RH	0.25	[86.0 (5.0)]	-	-	-	

Notes:

1. Test mode under displacement control.
2. Test environments: 100% relative humidity (distilled water).
3. Average fortified layer estimated to be 0.21 mm.
4. All the specimens tested failed in a mode of the principal-stress-failure criterion in which a crack propagated from the maximum-tensile stress direction at the root of each notch. Hence, no valid shear testing was obtained, and unable to determine the valid shear strength of the material.

Table 6.—Summary of Fracture Toughness Testing Results

Specimen Configurations	Test Method	Test Conditions				Mean Fracture Toughness, K_{Ic} (MPa \sqrt{m})	Remarks
		Temp (°C)	Environment	Test Rate (mm/min)	No. of Test Specimens		
3.6x2.5x46 (in mm); Fortified	SEVNB	RT	Oil (inert)	0.5	9	2.4 (0.08)	
5.1x2.5x46 (in mm); Not-Fortified	SEPB (ASTM C 1421 [11])	RT	Oil (inert)	0.5	10	2.3 (0.05)	

Notes:

1. Four-point flexure with 20 mm-inner and 40 mm-outer spans used for both SEVNB (single edge v-notched beam) and SEPB (single edge precracked beam) methods.
2. Test mode under displacement control.
3. Test environment: silicon oil (inert).
4. The fortified test specimens were used for the SEPB method, while the not-fortified, as-machined test specimens used for the SEVNB method.

Table 7.—Summary of Elastic Modulus Determinations

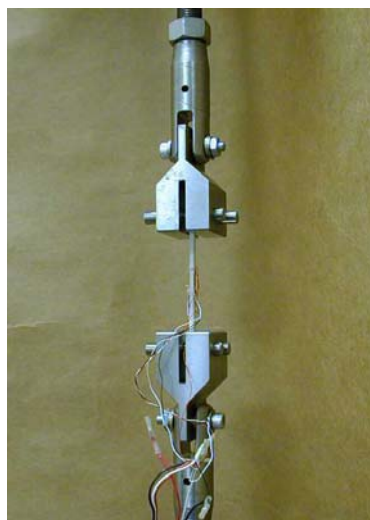
Specimen Configurations	Method	Test Conditions			E (GPa)	Remarks
		Temp (°C)	Environment	No. of Test Specimens		
5.1x2.5x46 (in mm); As-machined, not-fortified	Impulse excitation (by RT rig); ASTM C 1259 [14]	RT	Air	39	122.3 (2.1)	
		RT	Air	10	118.1 (2.4)	
		93 (200F)	Air	10	114.6 (2.3)	
		274 (525F)	Air	10	121.7 (2.4)	
Direction 1	Pure compression/strain gauging	RT	Air	3	115.6	
	Flexure compression/strain gauging	RT	Air	3	116.9	
Direction 2	Flexure tension/strain gauging	RT	Air	3	114.1	
	Pure compression/strain gauging	RT	Air	3	112.3	
Direction 3	Flexure compression/strain gauging	RT	Air	3	109.0	
	Flexure tension/strain gauging	RT	Air	3	109.1	
	Pure compression/strain gauging	RT	Air	3	114.7	
Direction 1	Flexure compression/strain gauging	RT	Air	3	115.4	
	Flexure tension/strain gauging	RT	Air	3	114.3	
Direction 1	Impulse/ASTM C 1259	RT	Air	1	116.1	
	Impulse/ASTM C 1259 (For shear modulus)	RT	Air	1	G = 45.0	

Notes:

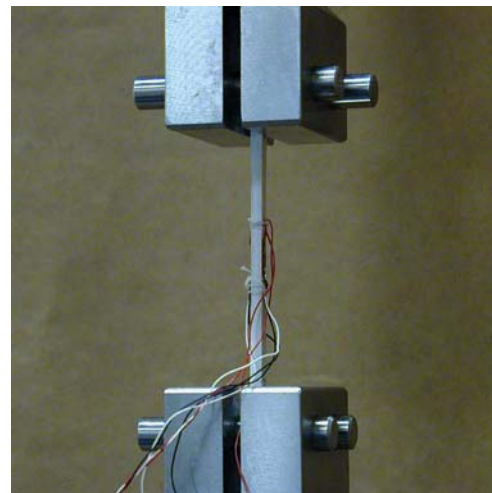
1. The fortified layers of the compression specimens were removed by polishing the specimens. Strain gages were attached to the as-removed surface of the specimens to determine elastic modulus as a function of direction. Elastic modulus for each direction was determined in three different loading configurations such as pure compression, four-point (20/40 mm spans) flexural tension, and four-point (20/40 mm spans) flexural compression.



Figure 1.—Four-point flexure test fixture with a test specimen placed, used in flexure strength and slow crack growth (“dynamic fatigue”) testing for Pyroceram at ambient temperature.



(a)



(b)

Figure 2.—Shoulder-loaded tensile test fixture with a test specimen placed, used in tension testing for Pyroceram: (a) overall view; (b) closed-up view.

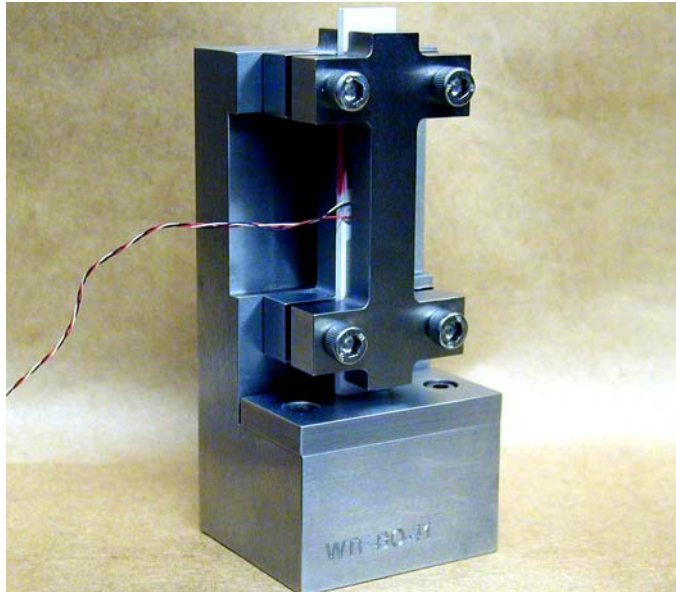


Figure 3.—Compression test fixture with a test specimen placed, used in compression testing for Pyroceram at ambient temperature.

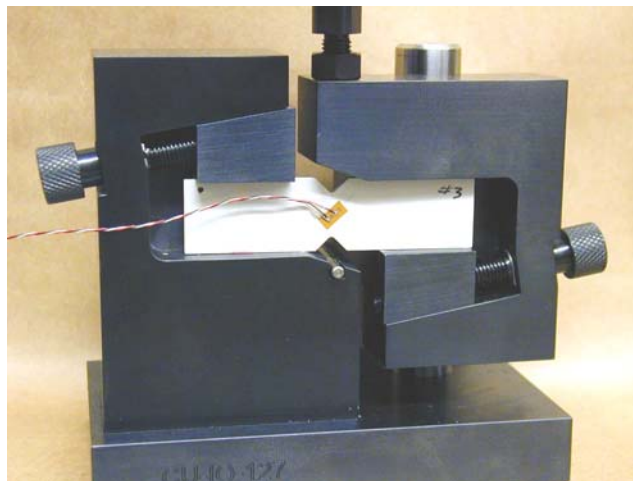


Figure 4.—Shear test fixture with a test specimen placed, used in shear testing for Pyroceram at ambient temperature.

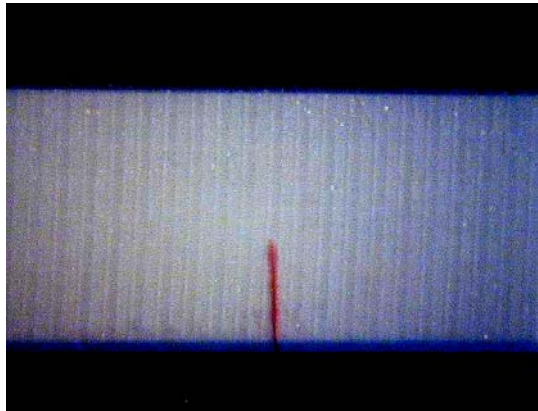


Figure 5.—A typical example of a precracked SEPB fracture toughness specimen. A precrack is shown as a (red) line revealed through dye penetrant.



(a)



(b)

Figure 6.—A typical example of a sharp notch produced in a SEVNB fracture toughness specimen: (a) overall view; (b) enlarged view of notch

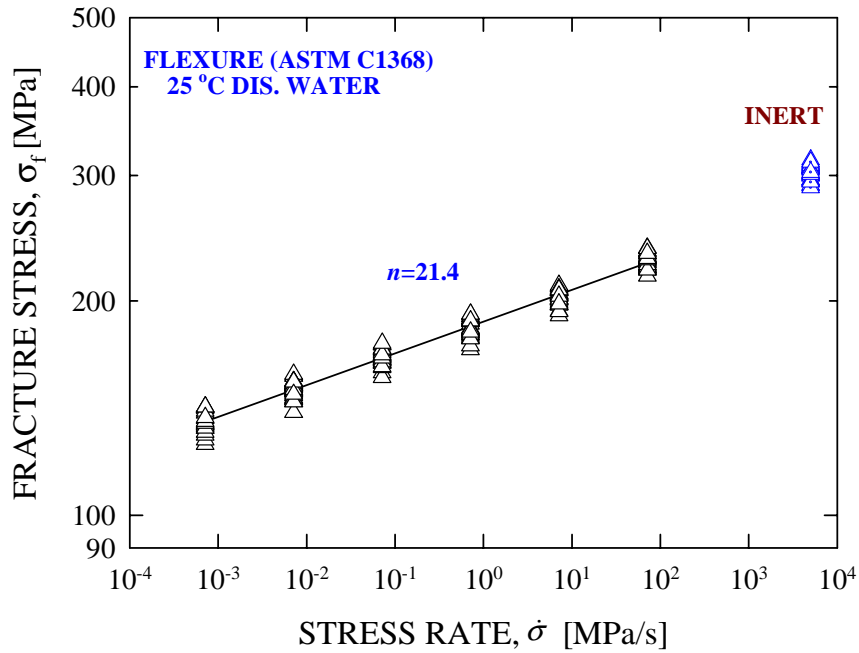


Figure 7.—Results of constant stress-rate (“dynamic fatigue”) testing for ‘fortified’ Pyroceram test specimens in room-temperature distilled water in flexure. The best-fit regression line was included with a slow crack parameter of $n=21.4$. Inert strength determined in oil was included for comparison.

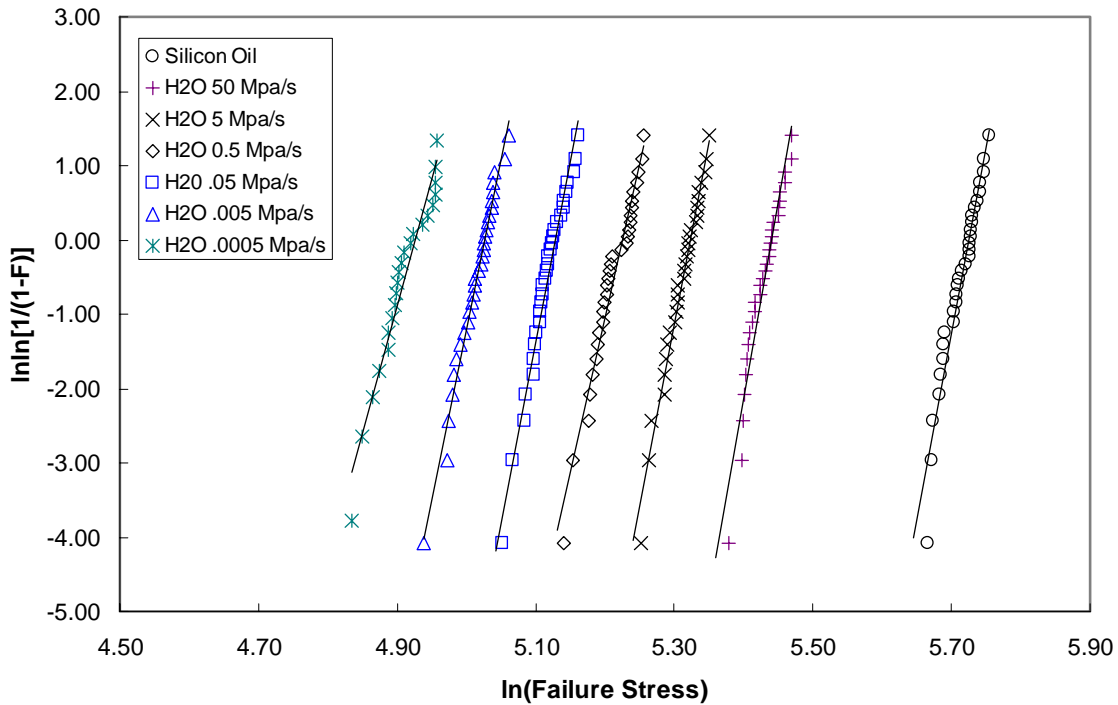


Figure 8.—Summary of Weibull strength distributions in constant stress-rate (“dynamic fatigue”) testing in flexure in room-temperature distilled water for ‘fortified’ Pyroceram test specimens. Inert strength determined in oil was included for comparison



Figure 9.—Typical fracture surface of a ‘fortified’ Pyroceram specimen tested in slow crack growth testing in flexure in room-temperature distilled water. ‘Fortified’ layer is seen outside of the specimen as a red band revealed through dye penetrant.

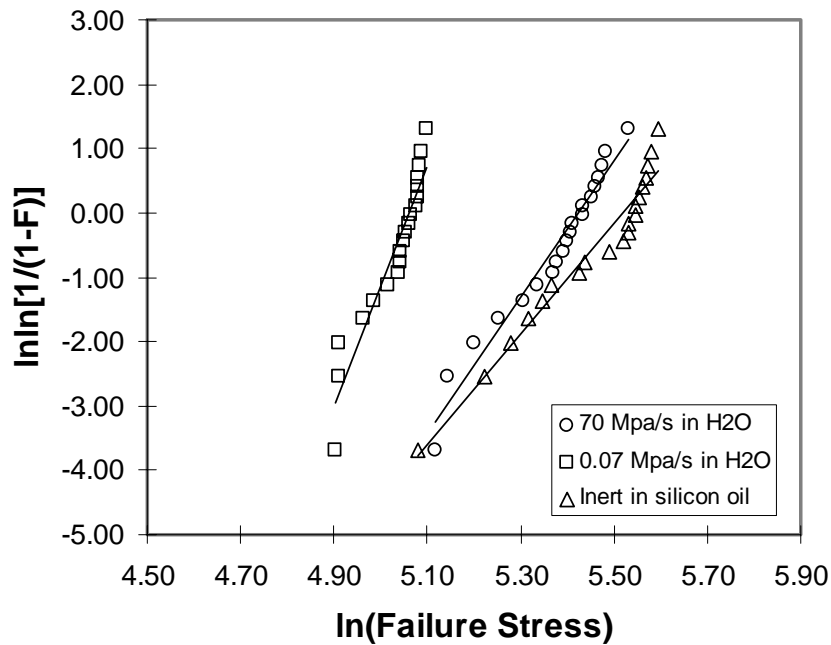


Figure 10.—Summary of Weibull strength distributions for ‘unfortified’, as-machined Pyroceram test specimens in flexure at ambient temperature.

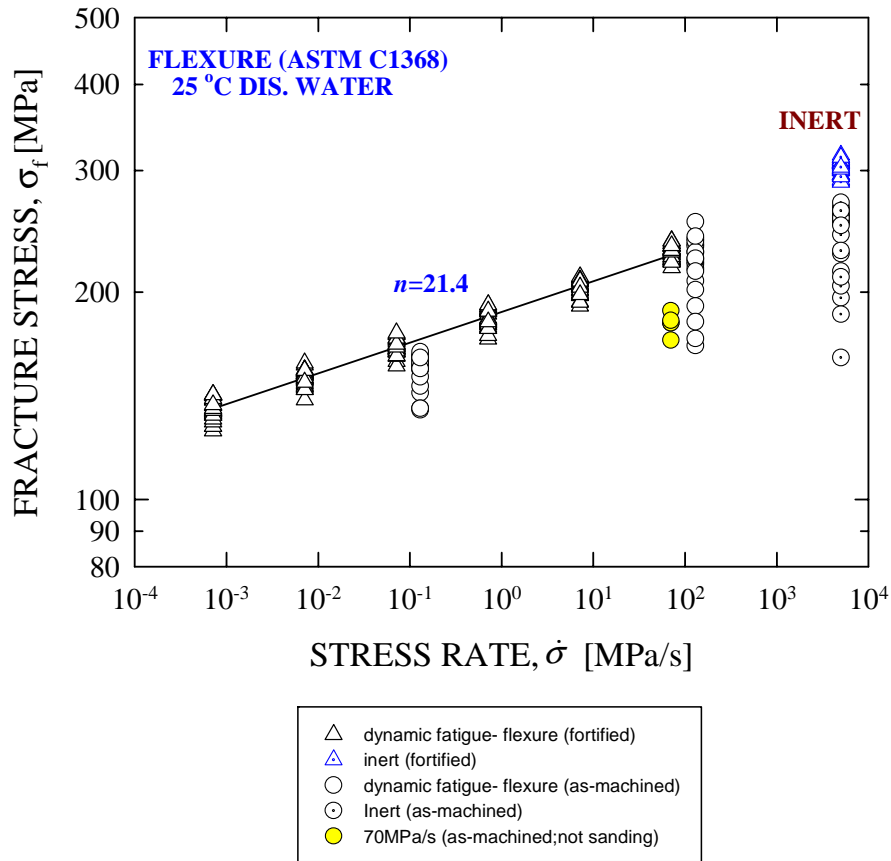


Figure 11.—Results of constant stress-rate (“dynamic fatigue”) testing in flexure for as-machined Pyroceram test specimens in room-temperature distilled water. The data (‘triangle’ marks with $n=21.4$) on the ‘fortified’ Pyroceram test specimens are included for comparison.



Figure 12.—A typical fracture surface of an as-machined Pyroceram flexure specimen tested in room temperature distilled water.

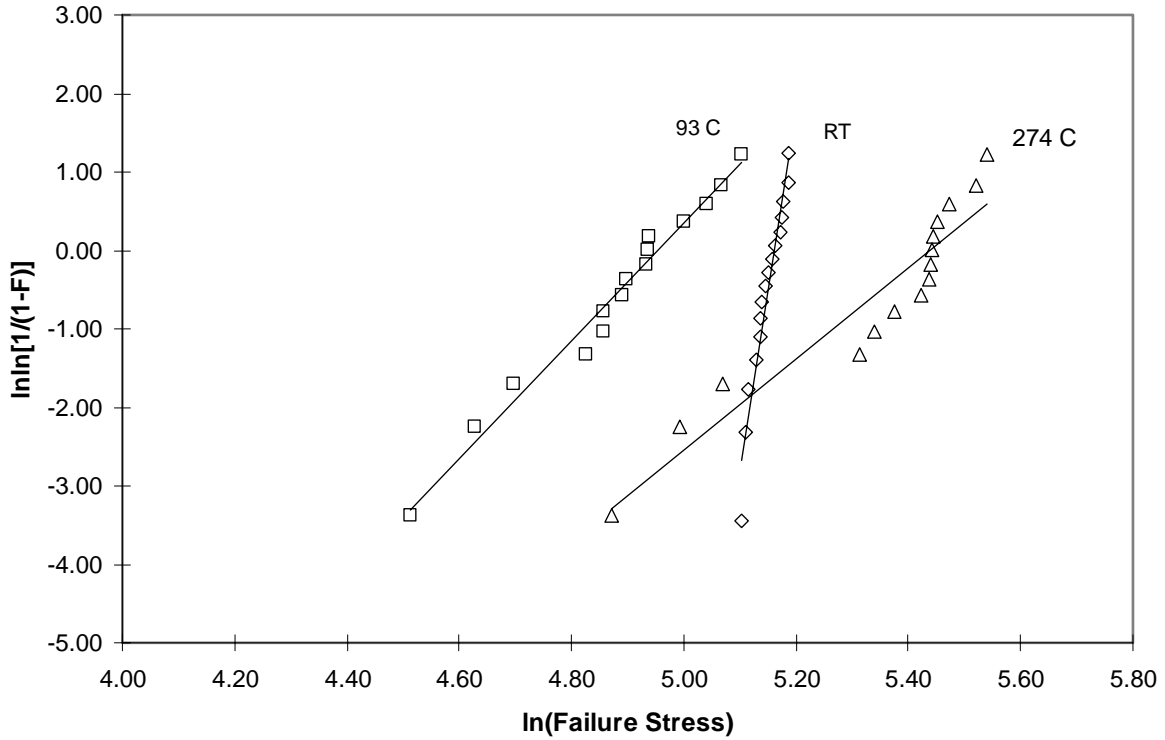


Figure 13.—Summary of Weibull strength distributions for ‘fortified’ Pyroceram test specimens in tension at three different test temperature-environment conditions of 25 °C (RT) in distilled water, 93 °C in distilled water, and 274 °C in ambient air.

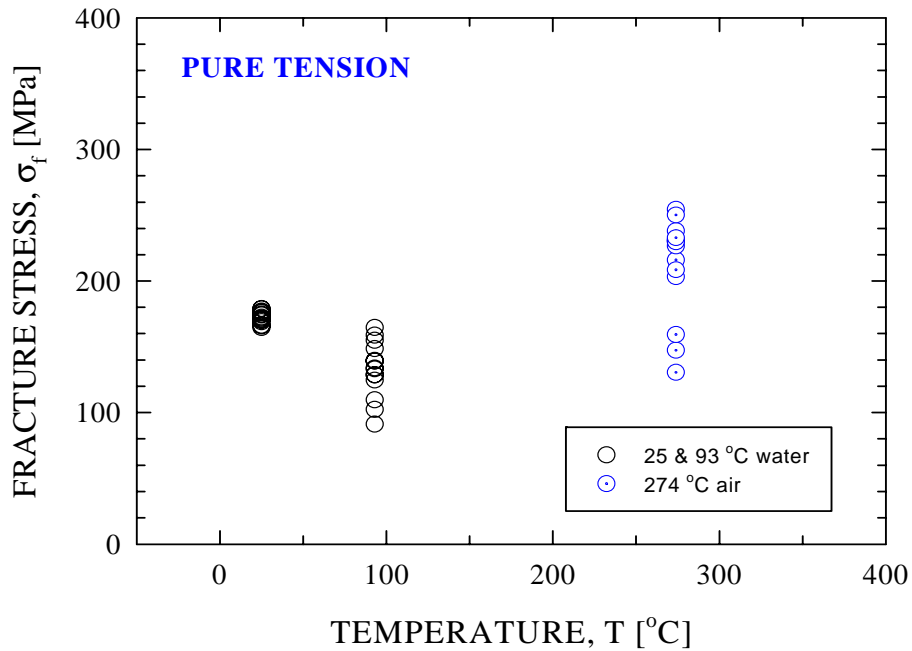


Figure 14.—Tensile strength as a function of temperature for ‘fortified’ Pyroceram test specimens. Test temperature-environments were 25 and 93 °C in distilled water, and 274 °C in ambient air.

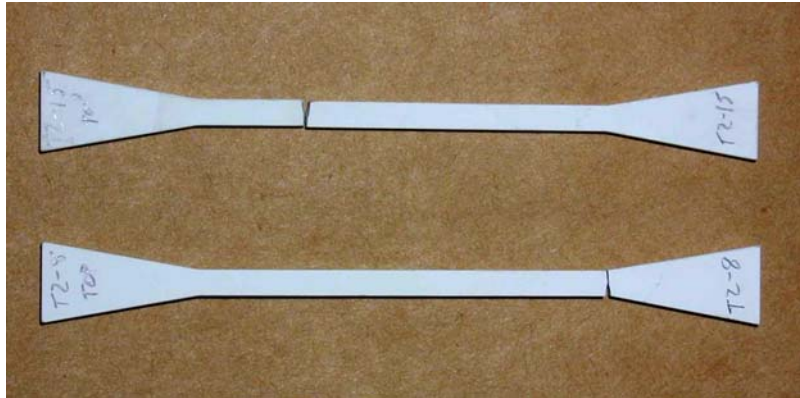


Figure 15.—Typical Pyroceram tensile specimens showing two different failure locations: gage-section failure (top) and transition-region failure (bottom).



Figure 16.—A typical fracture surface of a 'fortified' test specimen in tension, showing fracture origin and 'fortified' layer. The 'fortified' layer is seen outside of the specimen as a red band revealed through dye penetrant.

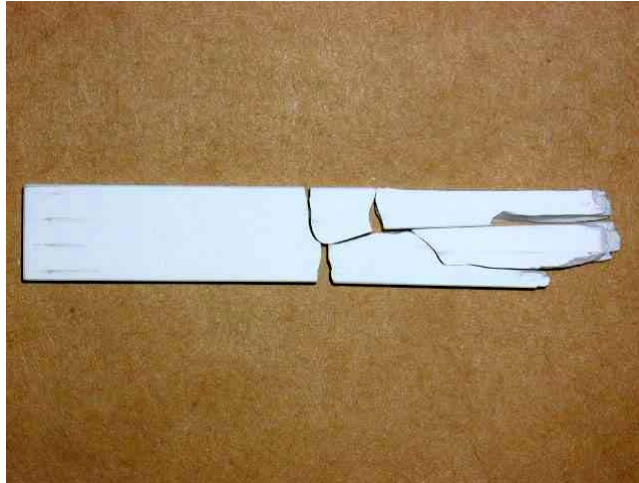


Figure 17.—A typical fracture pattern of a Pyroceram compression specimen tested in pure compression testing at ambient temperature

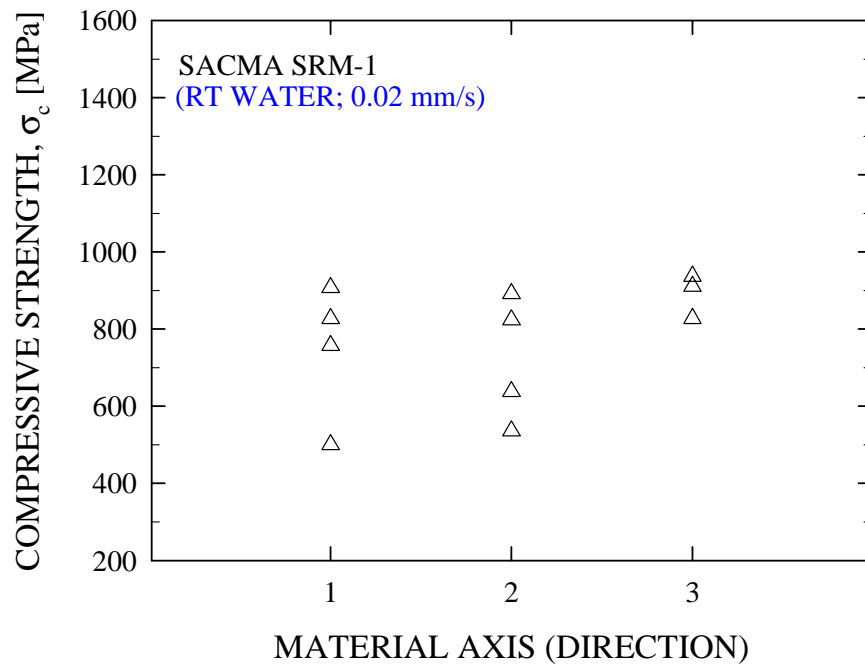


Figure 18.—Compressive strength as a function of material direction (axis) for ‘fortified’ Pyroceram test specimens, determined in room-temperature distilled water.

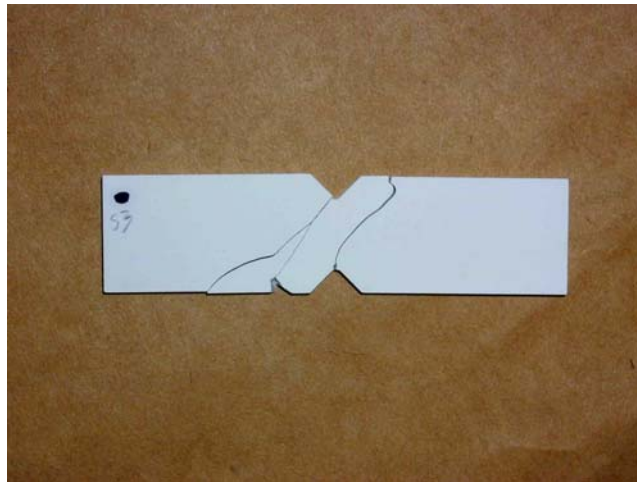


Figure 19.—A typical fracture pattern of a Pyroceram shear specimen tested in shear testing at ambient temperature.

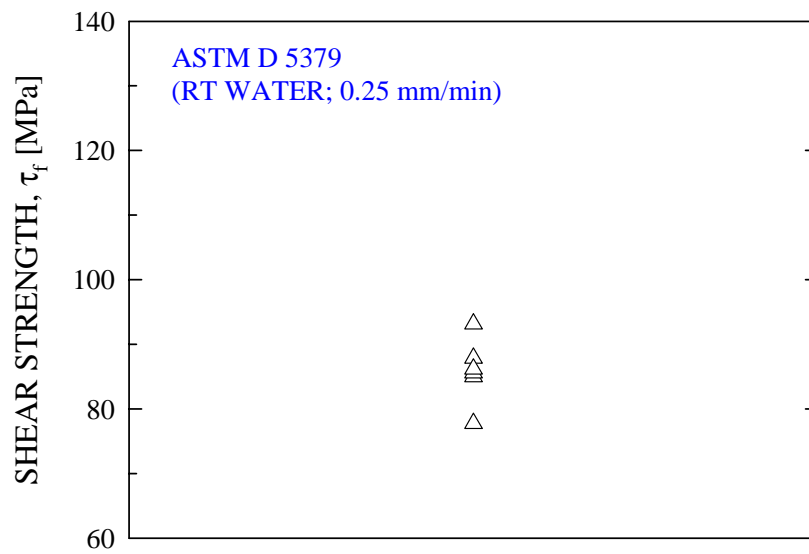


Figure 20.—Results of shear strength testing for ‘fortified’ Pyroceram shear test specimens, tested in room-temperature distilled water.

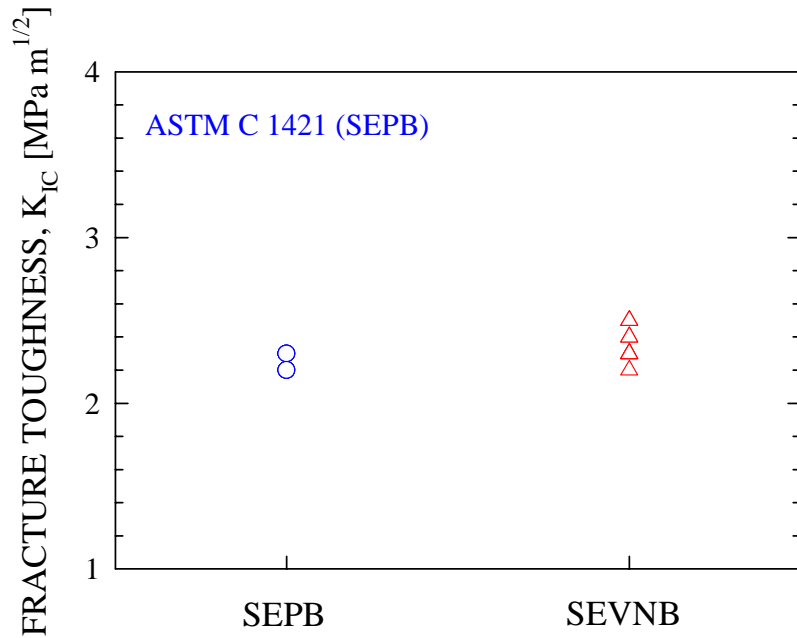


Figure 21.—A summary of fracture toughness determined for Pyroceram by SEPB and SEVNB methods.

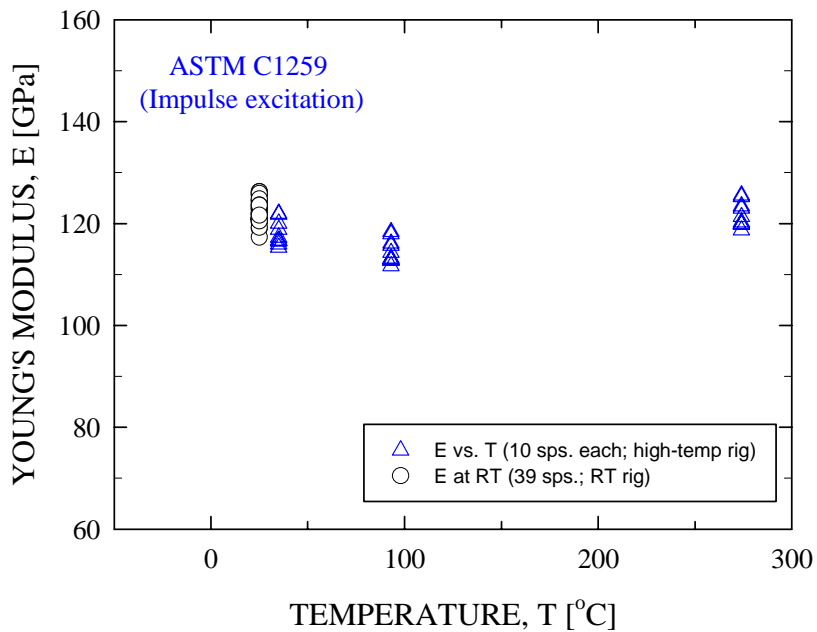


Figure 22.—Elastic modulus (E) as a function of temperature (T), determined for as-machined Pyroceram flexure test specimens. Two different test rigs (room-temperature(RT) rig and high-temperature rig) by impulse excitation method [14] were used.

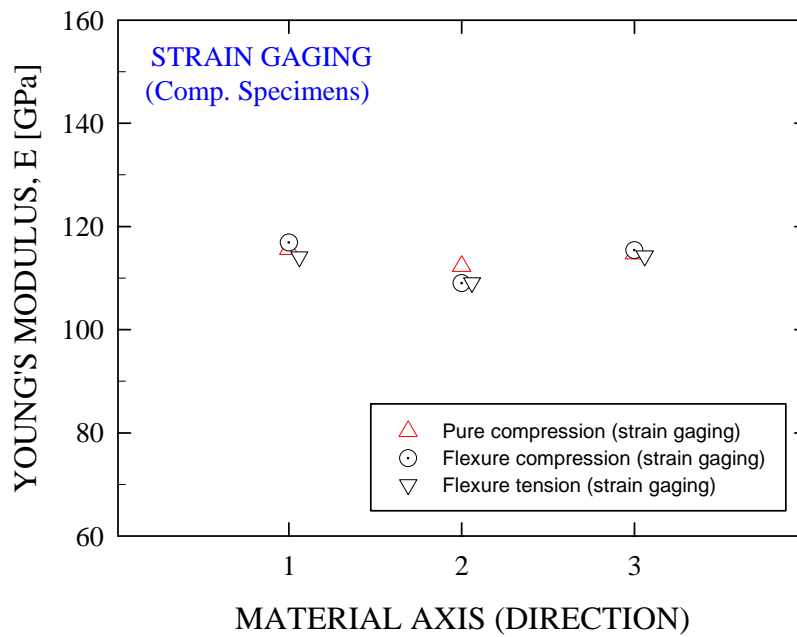


Figure 23.—Results of elastic modulus by strain gauging as a function of material axis for Pyroceram, determined at room temperature by three different loading configurations in compression, flexure tension, and flexure compression.

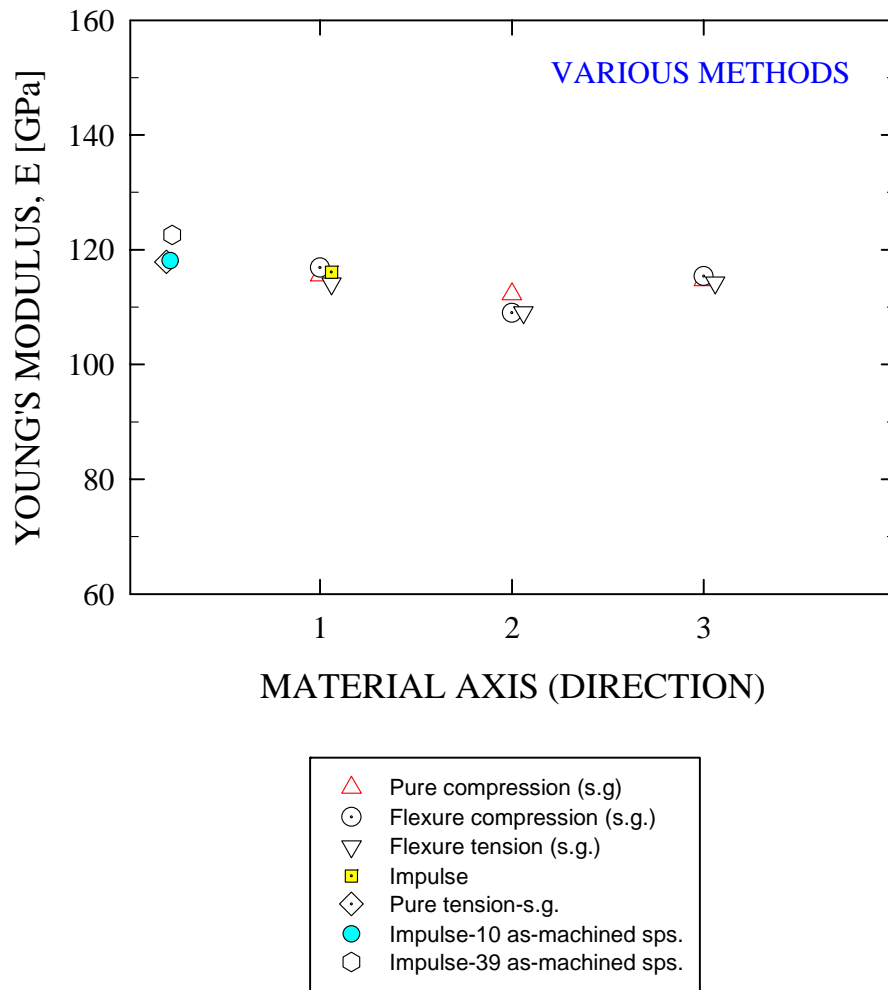


Figure 24.—Comparison of elastic modulus of Pyroceram, determined at room temperature by various methods of strain gauging and impulse excitation. “s.g.” represents strain gauging.

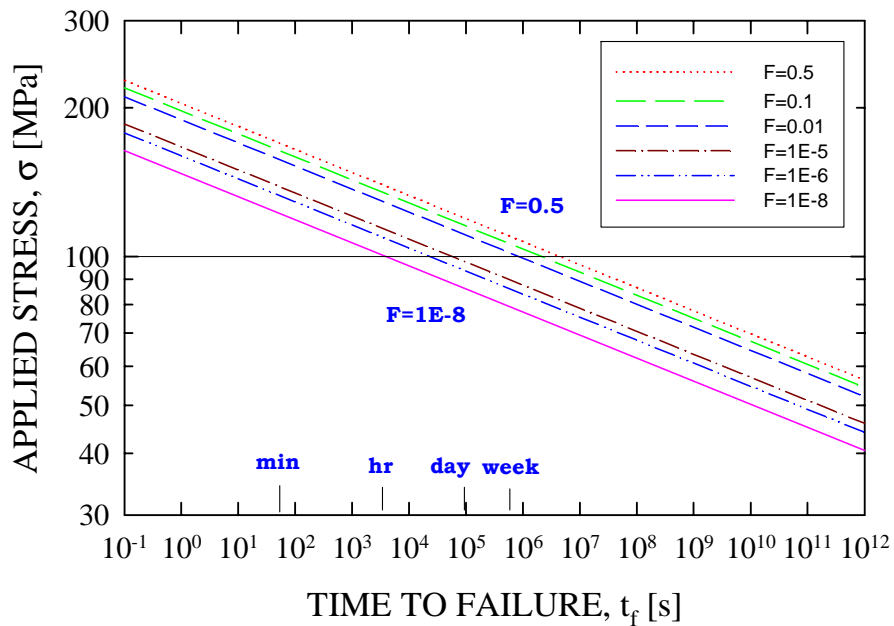


Figure 25. Simplified life prediction diagram for ‘fortified’ Pyroceram flexure test specimens, based on the slow crack growth data determined in flexure in room-temperature distilled water. The solid horizontal line, as an example, represents a case for an applied stress of 100 MPa. F: probability of failure.

APPENDIX

1. Individual Weibull plots and raw strength data in slow crack growth testing in flexure: 'Fortified' Pyroceram test specimens
2. Individual Weibull plots and raw strength data in slow crack growth testing in flexure: 'Unfortified' Pyroceram test specimens
3. Individual Weibull plots and raw strength data in tension: 'Fortified' Pyroceram test specimens
4. Raw strength data in compression testing
5. Raw strength data in shear testing
6. Raw fracture toughness data
7. Raw elastic modulus data

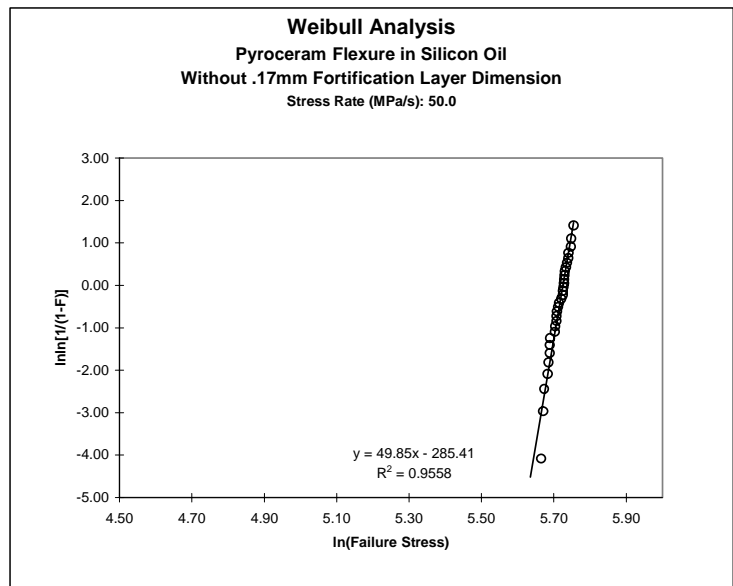
1. Individual Weibull Plots and Raw Strength Data in Slow Crack Growth Testing in flexure: 'Fortified' Test Specimens

Weibull Plot

Material: Pyroceram
 n: 30 Specimens
 Average Failure Stress: 303.19 (MPa)
 Std. Dev. +/-: 7.42 (MPa)

Stress Rate (MPa/s): 50.000
 Temperature: rt
 Environment: Oil

Rank	Failure Stress (MPa)	F	ln(Failure Stress)	lnln[1/(1-F)]
1	288.55	0.02	5.665	-4.086
2	290.31	0.05	5.671	-2.970
3	291.01	0.08	5.673	-2.442
4	293.81	0.12	5.683	-2.087
5	294.57	0.15	5.686	-1.817
6	295.69	0.18	5.689	-1.597
7	295.69	0.22	5.689	-1.410
8	295.76	0.25	5.690	-1.246
9	299.82	0.28	5.703	-1.099
10	299.94	0.32	5.704	-0.966
11	301.26	0.35	5.708	-0.842
12	301.29	0.38	5.708	-0.727
13	301.57	0.42	5.709	-0.618
14	302.39	0.45	5.712	-0.514
15	303.31	0.48	5.715	-0.415
16	305.16	0.52	5.721	-0.319
17	306.53	0.55	5.725	-0.225
18	306.62	0.58	5.726	-0.133
19	306.91	0.62	5.727	-0.042
20	307.53	0.65	5.729	0.049
21	307.64	0.68	5.729	0.140
22	307.79	0.72	5.729	0.232
23	308.22	0.75	5.731	0.327
24	309.14	0.78	5.734	0.425
25	310.08	0.82	5.737	0.529
26	311.19	0.85	5.740	0.640
27	311.39	0.88	5.741	0.765
28	313.30	0.92	5.747	0.910
29	313.46	0.95	5.748	1.097
30	315.81	0.98	5.755	1.410

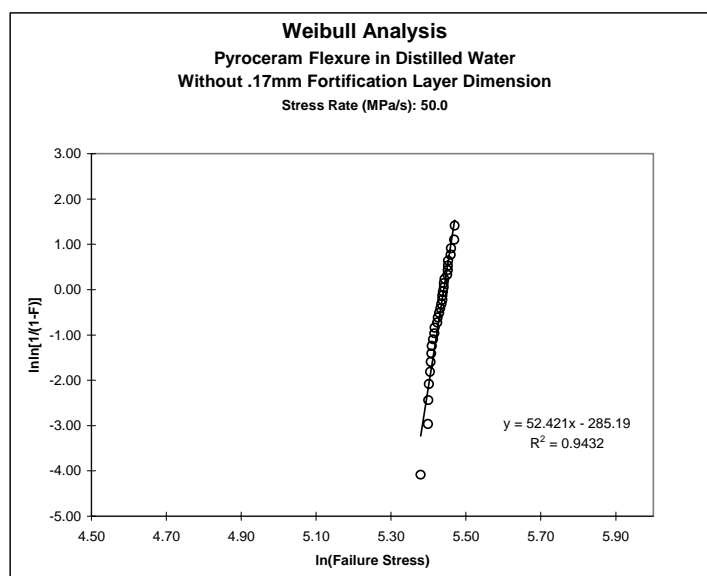


Weibull Plot

Material: Pyroceram
 n: 30 Specimens
 Average Failure Stress: 228.12 (MPa)
 Std. Dev. +/-: 5.29 (MPa)

Stress Rate (MPa/s): 50.000
 Temperature: rt
 Environment: Distilled Water

Rank	Failure Stress (MPa)	F	ln(Failure Stress)	lnln[1/(1-F)]
1	216.79	0.02	5.379	-4.086
2	221.04	0.05	5.398	-2.970
3	221.26	0.08	5.399	-2.442
4	221.67	0.12	5.401	-2.087
5	222.25	0.15	5.404	-1.817
6	222.66	0.18	5.406	-1.597
7	223.04	0.22	5.407	-1.410
8	223.31	0.25	5.409	-1.246
9	224.16	0.28	5.412	-1.099
10	224.86	0.32	5.415	-0.966
11	225.08	0.35	5.416	-0.842
12	226.64	0.38	5.423	-0.727
13	226.88	0.42	5.424	-0.618
14	227.79	0.45	5.428	-0.514
15	228.49	0.48	5.432	-0.415
16	229.08	0.52	5.434	-0.319
17	229.69	0.55	5.437	-0.225
18	229.72	0.58	5.437	-0.133
19	230.11	0.62	5.439	-0.042
20	230.57	0.65	5.441	0.049
21	230.65	0.68	5.441	0.140
22	231.06	0.72	5.443	0.232
23	232.87	0.75	5.450	0.327
24	233.05	0.78	5.451	0.425
25	233.22	0.82	5.452	0.529
26	233.37	0.85	5.453	0.640
27	234.87	0.88	5.459	0.765
28	235.13	0.92	5.460	0.910
29	237.08	0.95	5.468	1.097
30	237.37	0.98	5.470	1.410

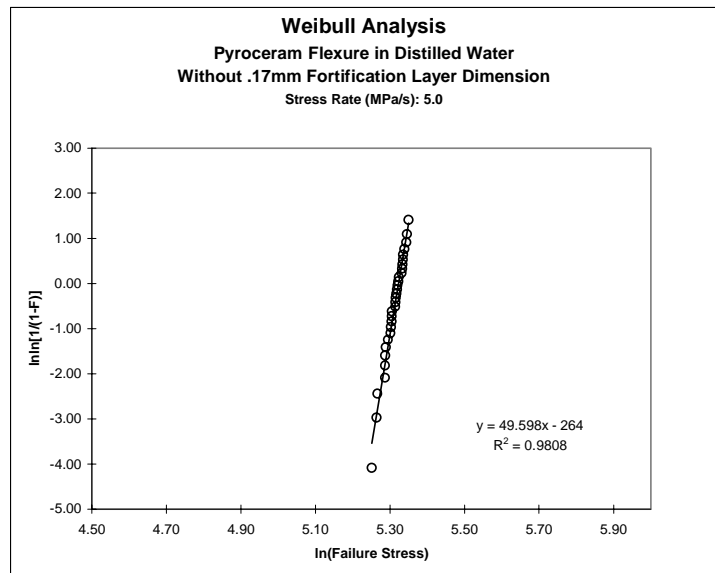


Material: Pyroceram
 n: 30 Specimens
 Average Failure Stress: 202.67 (MPa)
 Std. Dev. +/-: 5.04 (MPa)

Stress Rate (MPa/s): 5.000
 Temperature: rt
 Environment: Distilled Water

Rank	Failure Stress (MPa)	F	ln(Failure Stress)	ln[1/(1-F)]
1	190.81	0.02	5.251	-4.086
2	193.25	0.05	5.264	-2.970
3	193.67	0.08	5.266	-2.442
4	197.67	0.12	5.287	-2.087
5	197.71	0.15	5.287	-1.817
6	197.84	0.18	5.287	-1.597
7	198.20	0.22	5.289	-1.410
8	199.23	0.25	5.294	-1.246
9	200.66	0.28	5.302	-1.099
10	200.85	0.32	5.303	-0.966
11	201.21	0.35	5.304	-0.842
12	201.33	0.38	5.305	-0.727
13	201.37	0.42	5.305	-0.618
14	203.23	0.45	5.314	-0.514
15	203.27	0.48	5.315	-0.415
16	203.42	0.52	5.315	-0.319
17	203.90	0.55	5.318	-0.225
18	204.21	0.58	5.319	-0.133
19	204.43	0.62	5.320	-0.042
20	204.93	0.65	5.323	0.049
21	205.17	0.68	5.324	0.140
22	206.79	0.72	5.332	0.232
23	206.98	0.75	5.333	0.327
24	207.16	0.78	5.333	0.425
25	207.44	0.82	5.335	0.529
26	207.51	0.85	5.335	0.640
27	208.21	0.88	5.339	0.765
28	209.33	0.92	5.344	0.910
29	209.70	0.95	5.346	1.097
30	210.55	0.98	5.350	1.410

Weibull Plot

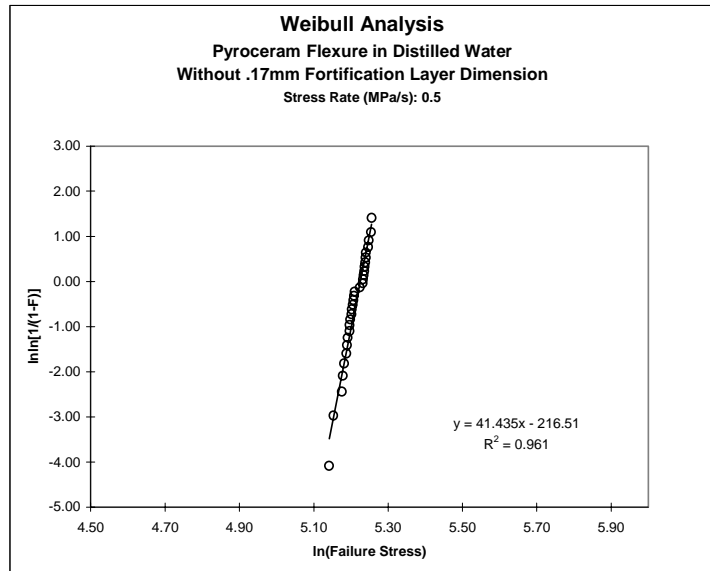


Material: Pyroceram
 n: 30 Specimens
 Average Failure Stress: 183.47 (MPa)
 Std. Dev. +/-: 5.41 (MPa)

Stress Rate (MPa/s): 0.500
 Temperature: rt
 Environment: Distilled Water

Rank	Failure Stress (MPa)	F	ln(Failure Stress)	ln[1/(1-F)]
1	170.94	0.02	5.141	-4.086
2	172.97	0.05	5.153	-2.970
3	177.03	0.08	5.176	-2.442
4	177.34	0.12	5.178	-2.087
5	178.02	0.15	5.182	-1.817
6	179.07	0.18	5.188	-1.597
7	179.46	0.22	5.190	-1.410
8	179.78	0.25	5.192	-1.246
9	180.66	0.28	5.197	-1.099
10	180.72	0.32	5.197	-0.966
11	180.98	0.35	5.198	-0.842
12	181.62	0.38	5.202	-0.727
13	181.83	0.42	5.203	-0.618
14	182.15	0.45	5.205	-0.514
15	182.51	0.48	5.207	-0.415
16	182.81	0.52	5.208	-0.319
17	183.16	0.55	5.210	-0.225
18	185.66	0.58	5.224	-0.133
19	187.18	0.62	5.232	-0.042
20	187.30	0.65	5.233	0.049
21	187.66	0.68	5.235	0.140
22	187.99	0.72	5.236	0.232
23	188.03	0.75	5.237	0.327
24	188.51	0.78	5.239	0.425
25	188.56	0.82	5.239	0.529
26	188.83	0.85	5.241	0.640
27	189.93	0.88	5.247	0.765
28	190.33	0.92	5.249	0.910
29	191.45	0.95	5.255	1.097
30	191.72	0.98	5.256	1.410

Weibull Plot

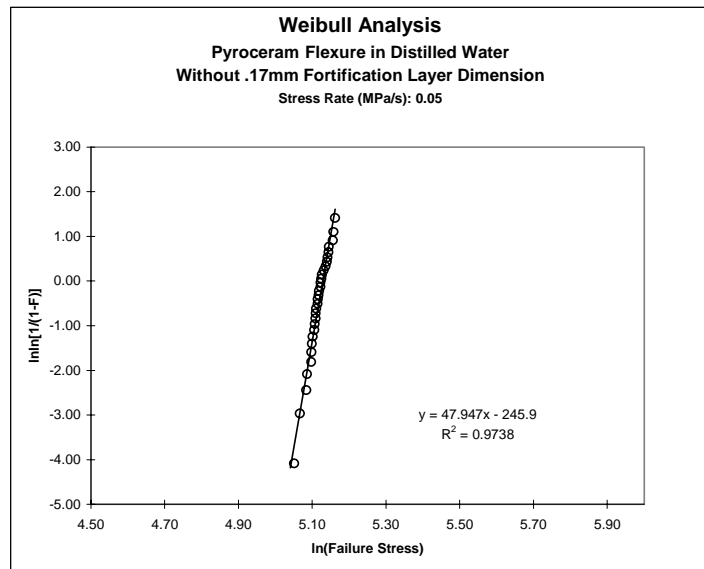


Weibull Plot

Material: Pyroceram
 n: 30 Specimens
 Average Failure Stress: 166.85 (MPa)
 Std. Dev. +/-: 4.28 (MPa)

Stress Rate (MPa/s): 0.050
 Temperature: rt
 Environment: Distilled Water

Rank	Failure Stress (MPa)	F	ln(Failure Stress)	lnln[1/(1-F)]
1	156.24	0.02	5.051	-4.086
2	158.63	0.05	5.067	-2.970
3	161.38	0.08	5.084	-2.442
4	161.76	0.12	5.086	-2.087
5	163.64	0.15	5.098	-1.817
6	163.66	0.18	5.098	-1.597
7	163.92	0.22	5.099	-1.410
8	164.28	0.25	5.102	-1.246
9	164.96	0.28	5.106	-1.099
10	165.14	0.32	5.107	-0.966
11	165.50	0.35	5.109	-0.842
12	165.63	0.38	5.110	-0.727
13	165.81	0.42	5.111	-0.618
14	166.42	0.45	5.115	-0.514
15	166.52	0.48	5.115	-0.415
16	166.95	0.52	5.118	-0.319
17	167.09	0.55	5.119	-0.225
18	167.73	0.58	5.122	-0.133
19	167.80	0.62	5.123	-0.042
20	168.14	0.65	5.125	0.049
21	168.43	0.68	5.127	0.140
22	169.29	0.72	5.132	0.232
23	170.11	0.75	5.136	0.327
24	170.68	0.78	5.140	0.425
25	170.95	0.82	5.141	0.529
26	171.43	0.85	5.144	0.640
27	171.67	0.88	5.146	0.765
28	173.49	0.92	5.156	0.910
29	173.80	0.95	5.158	1.097
30	174.53	0.98	5.162	1.410

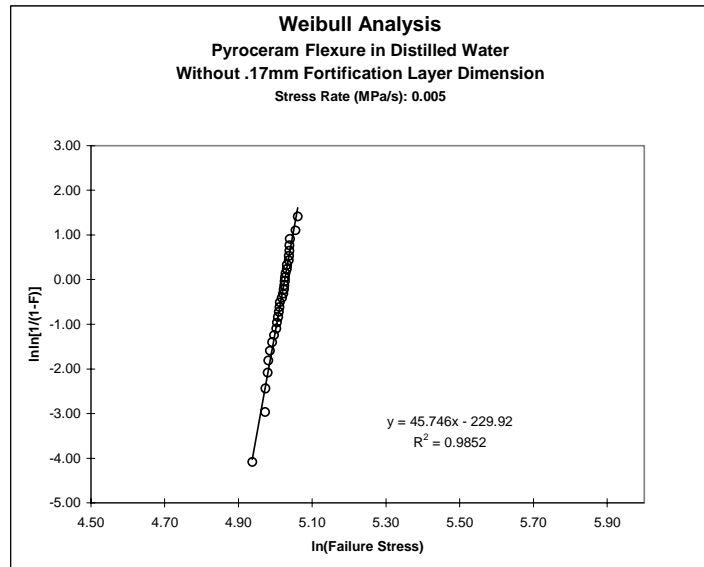


Weibull Plot

Material: Pyroceram
 n: 30 Specimens
 Average Failure Stress: 150.51 (MPa)
 Std. Dev. +/-: 4.06 (MPa)

Stress Rate (MPa/s): 0.005
 Temperature: rt
 Environment: Distilled Water

Rank	Failure Stress (MPa)	F	ln(Failure Stress)	lnln[1/(1-F)]
1	139.50	0.02	4.938	-4.086
2	144.37	0.05	4.972	-2.970
3	144.51	0.08	4.973	-2.442
4	145.46	0.12	4.980	-2.087
5	145.70	0.15	4.982	-1.817
6	146.30	0.18	4.986	-1.597
7	147.18	0.22	4.992	-1.410
8	147.97	0.25	4.997	-1.246
9	148.89	0.28	5.003	-1.099
10	149.16	0.32	5.005	-0.966
11	149.58	0.35	5.008	-0.842
12	149.91	0.38	5.010	-0.727
13	150.12	0.42	5.011	-0.618
14	150.33	0.45	5.013	-0.514
15	151.17	0.48	5.018	-0.415
16	151.63	0.52	5.021	-0.319
17	151.92	0.55	5.023	-0.225
18	152.12	0.58	5.025	-0.133
19	152.33	0.62	5.026	-0.042
20	152.44	0.65	5.027	0.049
21	152.70	0.68	5.028	0.140
22	153.19	0.72	5.032	0.232
23	153.25	0.75	5.032	0.327
24	153.96	0.78	5.037	0.425
25	154.01	0.82	5.037	0.529
26	154.24	0.85	5.039	0.640
27	154.25	0.88	5.039	0.765
28	154.47	0.92	5.040	0.910
29	156.79	0.95	5.055	1.097
30	157.77	0.98	5.061	1.410

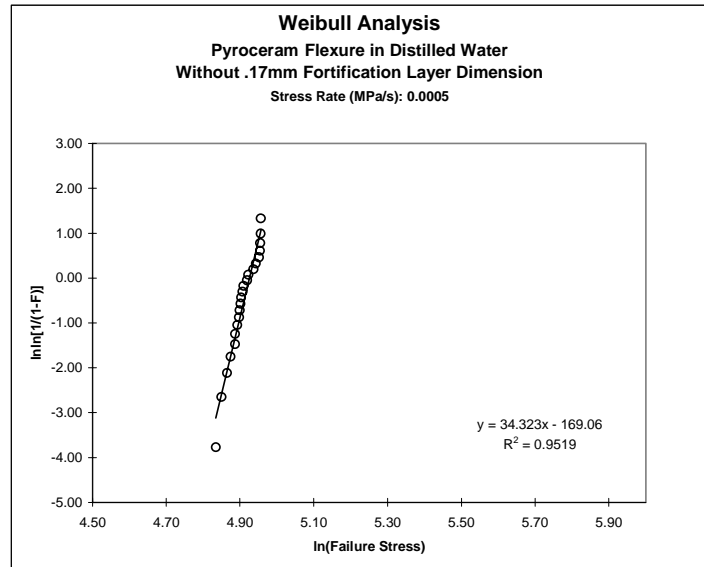


Material: Pyroceram
 n: 22 Specimens
 Average Failure Stress: 135.61 (MPa)
 Std. Dev. +/-: 4.78 (MPa)

Stress Rate (MPa/s): 0.0005
 Temperature: rt
 Environment: Distilled Water

Rank	Failure Stress (MPa)	F	ln(Failure Stress)	lnln[1/(1-F)]
1	125.81	0.02	4.835	-3.773
2	127.71	0.07	4.850	-2.650
3	129.64	0.11	4.865	-2.115
4	130.92	0.16	4.875	-1.753
5	132.52	0.20	4.887	-1.475
6	132.57	0.25	4.887	-1.246
7	133.27	0.30	4.892	-1.049
8	133.93	0.34	4.897	-0.875
9	134.16	0.39	4.899	-0.717
10	134.44	0.43	4.901	-0.570
11	134.72	0.48	4.903	-0.433
12	135.24	0.52	4.907	-0.302
13	135.60	0.57	4.910	-0.175
14	136.86	0.61	4.919	-0.050
15	137.35	0.66	4.923	0.073
16	139.27	0.70	4.936	0.198
17	140.24	0.75	4.943	0.327
18	141.40	0.80	4.952	0.462
19	141.80	0.84	4.954	0.609
20	141.81	0.89	4.955	0.777
21	141.98	0.93	4.956	0.988

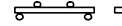
Weibull Plot



FLEXURE DYNAMIC FATIGUE TEST

Advanced Ceramics Test Lab

NASA Glenn Research Center Cleveland, Ohio



Material: <u>Pyroceram</u>	Environment: <u>Dow 704 silicone oil</u>	Load: <u>3280 N/min</u>
Test Temperature (C): <u>rt</u>	Load Frame: <u>M-2 Instron</u>	Rate: _____
Poissons Ratio : _____	Load Cell: <u>1Kn Instron</u>	Rate: <u>50 Mpa/sec</u>
Support Span(mm): <u>40.026</u>	Specimen Prep.: <u>as received</u>	Notes: _____
Load Span (mm): <u>20.065</u>	Annealing: <u>as received</u>	Notes: _____
	Fortification Layer Thickness (mm): <u>0.17</u>	Notes: _____
	Without With	

Completion Date	Specimen Number	Stress Rate (MPa/sec)	Specimen Size		Fracture Load (N)	Fracture Strength (MPa)	Fracture Strength (MPa)	Comments
			Width ↔ (mm)	Depth ↓ (mm)				
4/6/2000	FI-1	50.0	5.069	2.539	236.1	309.1	216.3	1
	2	50.0	5.043	2.546	235.6	308.2	215.8	2
	3	50.0	5.054	2.541	237.5	311.4	217.9	3
	4	50.0	5.038	2.545	237.4	311.2	217.8	4
	5	50.0	5.035	2.548	226.1	295.8	207.1	5
	6	50.0	5.065	2.550	227.9	295.7	207.2	6
	7	50.0	5.025	2.536	231.3	306.5	214.3	7
	8	50.0	5.047	2.545	221.9	290.3	203.2	8
	9	50.0	5.043	2.546	241.4	315.8	221.1	9
	10	50.0	5.037	2.548	235.2	307.5	215.3	10
	11	50.0	5.028	2.554	230.2	299.9	210.2	11
	12	50.0	5.084	2.550	225.2	291.0	204.0	12
	13	50.0	5.091	2.557	235.2	301.6	211.6	13
	14	50.0	5.029	2.547	228.7	299.8	209.9	14
	15	50.0	5.041	2.548	235.6	307.8	215.5	15
	16	50.0	5.043	2.547	239.7	313.3	219.4	16
	17	50.0	5.029	2.546	233.9	306.9	214.8	17
	18	50.0	5.036	2.586	243.4	307.6	216.4	18
	19	50.0	5.041	2.573	225.9	288.6	202.7	19
	20	50.0	5.032	2.547	225.7	295.7	207.0	20
4/10/2000	21	50.0	4.994	2.536	220.8	294.6	205.8	21
	22	50.0	5.154	2.540	241.3	310.1	217.3	22
	23	50.0	5.055	2.540	233.7	306.6	214.6	23
	24	50.0	5.049	2.557	232.9	301.3	211.2	24
	25	50.0	5.168	2.540	236	302.4	211.9	25
	26	50.0	5.031	2.543	223.4	293.8	205.6	26
	27	50.0	5.071	2.550	235.5	305.2	213.8	27
	28	50.0	5.040	2.543	238.8	313.5	219.4	28
	29	50.0	5.087	2.533	229.7	301.3	210.7	29
	30	50.0	5.045	2.486	219.5	303.3	210.8	30

Avg	303.2	212.3
StDev +/-	7.42	5.17
n	30	30

FLEXURE DYNAMIC FATIGUE TEST

Advanced Ceramics Test Lab

NASA Glenn Research Center Cleveland, Ohio

Material: <u>Pyroceram</u>	Environment: <u>Distilled H2O</u>	Load: <u>3280 N/min</u>
Test Temperature (C): <u>rt</u>	Load Frame: <u>M-2 Instron</u>	Rate: <u>50 Mpa/sec</u>
Poissons Ratio : _____	Load Cell: <u>1Kn Instron</u>	Notes: _____
Support Span(mm): <u>40.026</u>	Specimen Prep.: <u>as received</u>	_____
Load Span (mm): <u>20.065</u>	Annealing: <u>as received</u>	_____
	Fortification Layer Thickness (mm): <u>0.17</u>	
	Without With	

Completion Date	Specimen Number	Stress Rate (MPa/sec)	Specimen Size		Fracture Load (N)	Fracture Strength (MPa)	Fracture Strength (MPa)	Comments	
			Width (mm)	Depth (mm)					
	FD50-1	50.0	5.060	2.547	175.9	229.1	160.4		1
	2	50.0	5.062	2.555	171.5	221.7	155.4		2
	3	50.0	5.037	2.543	175.6	230.6	161.4		3
	4	50.0	5.031	2.543	173.2	227.8	159.4		4
	5	50.0	5.063	2.518	166.3	222.2	155.1		5
	6	50.0	5.049	2.486	170.3	235.1	163.4		6
	7	50.0	5.066	2.543	173.8	226.9	158.8		7
	8	50.0	5.060	2.548	177.2	230.6	161.5		8
	9	50.0	5.057	2.539	177.4	232.9	162.9		9
	10	50.0	5.068	2.503	172.3	233.2	162.5		10
	11	50.0	5.000	2.529	173.8	233.0	162.7		11
	12	50.0	5.040	2.532	169.6	224.9	157.2		12
	13	50.0	4.999	2.532	175.6	234.9	164.1		13
	14	50.0	5.015	2.544	171.9	226.6	158.6		14
	15	50.0	5.055	2.483	161.3	223.0	155.0		15
	16	50.0	5.026	2.538	167.3	221.3	154.7		16
	17	50.0	5.028	2.522	167.1	224.2	156.4		17
	18	50.0	5.055	2.549	171.1	222.7	156.0		18
	19	50.0	5.143	2.536	167.7	216.8	151.8		19
	20	50.0	5.132	2.533	182.7	237.4	166.1		20
	21	50.0	5.010	2.531	167.2	223.3	156.0		21
	22	50.0	5.060	2.543	172.2	225.1	157.6		22
	23	50.0	5.022	2.544	167.9	221.0	154.7		23
	24	50.0	5.039	2.535	173.7	229.7	160.6		24
	25	50.0	5.020	2.564	177.9	230.1	161.4		25
	26	50.0	5.047	2.551	175.6	228.5	160.1		26
	27	50.0	5.044	2.523	177.5	237.1	165.5		27
	28	50.0	5.012	2.528	172.6	231.1	161.3		28
	29	50.0	5.034	2.542	174.6	229.7	160.7		29
	30	50.0	5.053	2.545	178.6	233.4	163.4		30

Avg	228.1	159.5
StDev +/-	5.29	3.66
n	30	30

FLEXURE DYNAMIC FATIGUE TEST

Advanced Ceramics Test Lab

NASA Glenn Research Center Cleveland, Ohio

Material: <u>Pyroceram</u>	Environment: <u>Distilled H2O</u>	Load: <u>328.0 N/min</u>
Test Temperature (C): <u>rt</u>	Load Frame: <u>M-2 Instron</u>	Rate: _____
Poissons Ratio : _____	Load Cell: <u>1Kn Instron</u>	<u>5.0 Mpa/sec</u>
Support Span(mm): <u>40.026</u>	Specimen Prep.: <u>as received</u>	Notes: _____
Load Span (mm): <u>20.065</u>	Annealing: <u>as received</u>	_____
	Fortification Layer Thickness (mm): <u>0.17</u>	_____
	Without With	

Completion Date	Specimen Number	Stress Rate (MPa/sec)	Specimen Size		Fracture Load (N)	Fracture Strength (MPa)	Fracture Strength (MPa)	Comments	
			Width (mm)	Depth (mm)					
	FDF5-1	5.0	5.015	2.532	152.5	203.3	142.0		1
	2	5.0	5.029	2.549	148	193.7	135.6		2
	3	5.0	5.060	2.549	154.5	200.8	140.7		3
	4	5.0	5.025	2.538	155.1	205.2	143.5		4
	5	5.0	5.034	2.542	155	203.9	142.7		5
	6	5.0	5.067	2.530	158.5	209.3	146.3		6
	7	5.0	5.046	2.535	158.8	209.7	146.6		7
	8	5.0	5.061	2.545	157.1	204.9	143.5		8
	9	5.0	5.042	2.529	156.1	207.4	144.9		9
	10	5.0	5.055	2.538	153.2	201.4	140.9		10
	11	5.0	5.059	2.476	151.4	210.5	146.2		11
	12	5.0	5.078	2.548	152.5	197.7	138.5		12
	13	5.0	5.061	2.544	155.8	203.4	142.4		13
	14	5.0	5.060	2.552	155.2	201.2	141.0		14
	15	5.0	5.031	2.571	148.8	190.8	134.0		15
	16	5.0	5.022	2.535	150.1	199.2	139.3		16
	17	5.0	5.039	2.543	157.5	206.8	144.7		17
	18	5.0	5.041	2.523	155	207.2	144.6		18
	19	5.0	5.153	2.476	152.7	208.2	144.7		19
	20	5.0	5.017	2.538	156.2	207.0	144.7		20
	21	5.0	5.082	2.547	157.7	204.4	143.2		21
	22	5.0	5.017	2.532	150.6	200.7	140.2		22
	23	5.0	5.062	2.477	145	201.3	139.8		23
	24	5.0	5.144	2.529	157	204.2	142.9		24
	25	5.0	5.042	2.544	158.3	207.5	145.3		25
	26	5.0	5.057	2.552	152.5	197.8	138.6		26
	27	5.0	5.032	2.576	154.9	197.7	138.9		27
	28	5.0	5.170	2.535	150.2	193.3	135.4		28
	29	5.0	5.085	2.550	157.3	203.2	142.4		29
	30	5.0	5.193	2.533	154.5	198.2	138.8		30

Avg	202.7	141.7
StDev +/-	5.04	3.34
n	30	30

FLEXURE DYNAMIC FATIGUE TEST

Advanced Ceramics Test Lab

NASA Glenn Research Center Cleveland, Ohio

Material: <u>Pyroceram</u>	Environment: <u>Distilled H2O</u>	Load: <u>3280 N/min</u>
Test Temperature (C): <u>rt</u>	Load Frame: <u>M-2 Instron</u>	Rate: _____
Poissons Ratio: _____	Load Cell: <u>1Kn Instron</u>	<u>.50 Mpa/sec</u>
Support Span(mm): <u>40.026</u>	Specimen Prep.: <u>as received</u>	Notes: _____
Load Span (mm): <u>20.065</u>	Annealing: <u>as received</u>	_____
	Fortification Layer Thickness (mm): <u>0.17</u>	_____
	Without With	

Completion Date	Specimen Number	Stress Rate (MPa/sec)	Specimen Size		Fracture Load (N)	Fracture Strength (MPa)	Fracture Strength (MPa)	Comments	
			Width (mm)	Depth (mm)					
	FDF0.5-1	0.5	5.049	2.539	130	170.9	119.6		1
	2	0.5	5.042	2.536	142.8	188.6	131.9		2
	3	0.5	5.027	2.539	142.3	188.0	131.5		3
	4	0.5	5.025	2.535	136.2	180.7	126.3		4
	5	0.5	5.035	2.529	139.5	185.7	129.7		5
	6	0.5	5.022	2.532	143	190.3	133.0		6
	7	0.5	5.056	2.487	135.9	187.2	130.1		7
	8	0.5	5.112	2.532	144.6	188.8	132.1		8
	9	0.5	5.023	2.546	135.5	178.0	124.6		9
	10	0.5	5.035	2.545	142.8	187.3	131.1		10
	11	0.5	5.140	2.528	138.7	180.7	126.4		11
	12	0.5	5.041	2.525	136.3	181.8	127.0		12
	13	0.5	5.167	2.537	138	177.3	124.2		13
	14	0.5	5.024	2.545	136.2	179.1	125.3		14
	15	0.5	5.026	2.534	135.2	179.5	125.4		15
	16	0.5	5.044	2.488	136.3	188.0	130.7		16
	17	0.5	5.046	2.551	147.1	191.5	134.1		17
	18	0.5	5.034	2.553	132.8	173.0	121.2		18
	19	0.5	5.060	2.548	140.5	182.8	128.1		19
	20	0.5	5.052	2.541	144.8	189.9	132.9		20
	21	0.5	5.051	2.475	135.2	188.5	130.8		21
	22	0.5	5.046	2.550	140.6	183.2	128.3		22
	23	0.5	5.034	2.531	135.3	179.8	125.6		23
	24	0.5	5.037	2.541	145.7	191.7	134.1		24
	25	0.5	5.061	2.551	140.4	182.2	127.6		25
	26	0.5	5.165	2.533	137.2	177.0	124.0		26
	27	0.5	5.049	2.542	138.5	181.6	127.1		27
	28	0.5	5.142	2.527	140	182.5	127.7		28
	29	0.5	5.046	2.538	142.5	187.7	131.3		29
	30	0.5	5.062	2.550	139.4	181.0	126.8		30

Avg	183.5	128.3
StDev +/-	5.41	3.70
n	30	30

FLEXURE DYNAMIC FATIGUE TEST

Advanced Ceramics Test Lab

NASA Glenn Research Center Cleveland, Ohio

Material: <u>Pyroceram</u>	Environment: <u>Distilled H2O</u>	Load: <u>3280 N/min</u>
Test Temperature (C): <u>rt</u>	Load Frame: <u>M-2 Instron</u>	Rate: _____
Poissons Ratio: _____	Load Cell: <u>1Kn Instron</u>	<u>.050 Mpa/sec</u>
Support Span(mm): <u>40.026</u>	Specimen Prep.: <u>as received</u>	Notes: _____
Load Span (mm): <u>20.065</u>	Annealing: <u>as received</u>	_____
_____	Fortification Layer Thickness (mm): <u>0.17</u>	_____
	Without With	

Completion Date	Specimen Number	Stress Rate (MPa/sec)	Specimen Size		Fracture Load (N)	Fracture Strength (MPa)	Fracture Strength (MPa)	Comments	
			Width (mm)	Depth (mm)					
	FDF0.05-1	0.05	5.086	2.549	122.7	158.6	111.2		1
	2	0.05	5.085	2.547	120.6	156.2	109.5		2
	3	0.05	5.044	2.542	132.4	173.8	121.6		3
	4	0.05	5.091	2.531	128.3	168.4	117.8		4
	5	0.05	5.056	2.472	118.1	165.0	114.5		5
	6	0.05	5.081	2.539	127.5	166.5	116.5		6
	7	0.05	5.035	2.554	131.4	171.0	119.8		7
	8	0.05	5.065	2.543	123.6	161.4	113.0		8
	9	0.05	5.052	2.543	125	163.7	114.6		9
	10	0.05	5.058	2.544	126.4	165.1	115.6		10
	11	0.05	5.083	2.540	128.6	167.7	117.4		11
	12	0.05	5.015	2.537	128.2	170.1	118.9		12
	13	0.05	5.144	2.528	131.1	170.7	119.4		13
	14	0.05	5.021	2.528	124.1	165.8	115.8		14
	15	0.05	5.054	2.539	126.1	165.6	115.9		15
	16	0.05	5.046	2.541	132.1	173.5	121.4		16
	17	0.05	5.058	2.481	121.2	167.8	116.6		17
	18	0.05	5.024	2.539	126.4	167.1	116.9		18
	19	0.05	5.067	2.548	130.3	169.3	118.6		19
	20	0.05	5.187	2.538	128.2	163.9	114.9		20
	21	0.05	5.037	2.543	130.7	171.7	120.1		21
	22	0.05	5.044	2.544	126.3	165.5	115.8		22
	23	0.05	5.062	2.544	127.9	167.0	116.9		23
	24	0.05	5.031	2.541	124.2	163.6	114.5		24
	25	0.05	5.016	2.542	124.4	164.3	114.9		25
	26	0.05	5.049	2.551	131.8	171.4	120.1		26
	27	0.05	5.169	2.535	125.7	161.8	113.3		27
	28	0.05	5.014	2.530	124.6	166.4	116.2		28
	29	0.05	5.010	2.551	128.2	168.1	117.7		29
	30	0.05	5.067	2.537	133	174.5	122.1		30

Avg	166.9	116.7
StDev +/-	4.28	3.00
n	30	30

FLEXURE DYNAMIC FATIGUE TEST

Advanced Ceramics Test Lab

NASA Glenn Research Center Cleveland, Ohio

Material: <u>Pyroceram</u>	Environment: <u>Distilled H2O</u>	Load: <u>3280 N/min</u>
Test Temperature (C): <u>rt</u>	Load Frame: <u>M-2 Instron</u>	Rate: _____
Poissons Ratio : _____	Load Cell: <u>1Kn Instron</u>	<u>.0050 Mpa/sec</u>
Support Span(mm): <u>40.026</u>	Specimen Prep.: <u>as received</u>	Notes: _____
Load Span (mm): <u>20.065</u>	Annealing: <u>as received</u>	_____
	Fortification Layer Thickness (mm): <u>0.17</u>	_____
	Without With	

Completion Date	Specimen Number	Stress Rate (MPa/sec)	Specimen Size		Fracture Load (N)	Fracture Strength (MPa)	Fracture Strength (MPa)	Comments	
			Width (mm)	Depth (mm)					
	FDf.005-1	0.005	5.030	2.540	113.4	149.6	104.6		1
	2	0.005	5.052	2.547	111.5	145.5	101.9		2
	3	0.005	5.147	2.545	118	151.2	106.0		3
	4	0.005	5.166	2.532	113.3	146.3	102.4		4
	5	0.005	5.037	2.551	117.1	152.7	107.0		5
	6	0.005	5.028	2.531	116.1	154.5	107.9	80%PL (90N)	6
	7	0.005	5.041	2.532	115	152.4	106.5		7
	8	0.005	5.054	2.489	114	156.8	109.0	60%PL (69N)	8
	9	0.005	5.076	2.550	113.7	147.2	103.1	70%PL (80N)	9
	10	0.005	5.056	2.480	113.8	157.8	109.6	90%PL	10
	11	0.005	5.152	2.530	117.1	151.9	106.3	90%PL	11
	12	0.005	5.148	2.475	112.9	154.2	107.2		12
	13	0.005	5.064	2.547	116.9	152.1	106.5	60%PL	13
	14	0.005	5.043	2.484	111.2	154.0	107.0	90%PL	14
	15	0.005	5.037	2.548	116.5	152.3	106.7	90%PL	15
	16	0.005	5.063	2.551	115.6	149.9	105.1	90%PL	16
	17	0.005	5.014	2.531	114.8	153.2	107.0	80%PL	17
	18	0.005	5.044	2.548	111.6	145.7	102.0	80%PL	18
	19	0.005	5.011	2.538	115.5	153.2	107.1	80%PL	19
	20	0.005	5.051	2.546	114	148.9	104.3		20
	21	0.005	5.046	2.549	118.3	154.2	108.0	60%PL	21
	22	0.005	5.027	2.537	112.7	149.2	104.3	80%PL	22
	23	0.005	5.039	2.523	113.4	151.6	105.9	70%PL	23
	24	0.005	5.013	2.541	113.5	150.1	105.0	70%PL	24
	25	0.005	5.032	2.534	113.4	150.3	105.1	70%PL	25
	26	0.005	5.020	2.545	117	154.0	107.7	70%PL	26
	27	0.005	5.066	2.542	110.6	144.5	101.2	60%PL	27
	28	0.005	5.178	2.537	108.8	139.5	97.7	60%PL	28
	29	0.005	5.032	2.545	110	144.4	101.1		29
	30	0.005	5.027	2.533	111.4	148.0	103.4		30

Avg	150.5	105.2
StDev +/-	4.06	2.68
n	30	30

FLEXURE DYNAMIC FATIGUE TEST

Advanced Ceramics Test Lab

NASA Glenn Research Center Cleveland, Ohio

Material: <u>Pyroceram</u>	Environment: <u>Distilled H2O</u>	Load <u>3280 N/min</u>
Test Temperature (C): <u>rt</u>	Load Frame: <u>M-2 Instron</u>	Rate: _____
Poissons Ratio : _____	Load Cell: <u>1Kn Instron</u>	<u>.0005 Mpa/sec</u>
Support Span(mm): <u>40.026</u>	Specimen Prep.: <u>as received</u>	Notes: _____
Load Span (mm): <u>20.065</u>	Annealing: <u>as received</u>	_____
	Fortification Layer Thickness (mm): <u>0.17</u>	_____
	Without With	

Completion Date	Specimen Number	Stress Rate (MPa/sec)	Specimen Size		Fracture Load (N)	Fracture Strength (MPa)	Fracture Strength (MPa)	Comments	
			Width (mm)	Depth (mm)					
	FD0005-1	0.0005	5.003	2.531	100.3	134.2	93.7	20 N PL	1
	2	0.0005	5.090	2.531	108	141.8	99.2	80%PL	2
	3	0.0005	5.054	2.550	101.9	132.5	92.8	80%PL	3
	4	0.0005	5.012	2.536	106.7	141.8	99.1	20 N PL	4
	5	0.0005	5.082	2.548	102.9	133.3	93.4	80%PL	5
	6	0.0005	5.041	2.535	101.7	134.4	94.0	80%PL	6
	7	0.0005	5.025	2.549	104.5	136.9	95.8	20 N PL	7
	8	0.0005	5.040	2.531	94.8	125.8	87.9	90%PL	8
	9	0.0005	5.038	2.539	96.9	127.7	89.3	90%PL	9
	10	0.0005	5.053	2.487	102.6	141.4	98.3	90%PL	10
	11	0.0005	5.057	2.545	99.3	129.6	90.8	90%PL	11
	12	0.0005	5.042	2.539	102.7	135.2	94.6	90%PL	12
	13	0.0005	5.042	2.541	99.6	130.9	91.6	80%PL	13
	14	0.0005	5.033	2.540	101.6	133.9	93.7	95% PL	14
	15	0.0005	5.035	2.539	105.6	139.3	97.4	95% PL	15
	16	0.0005	5.067	2.540	101.3	132.6	92.8	95% PL	16
	17	0.0005	5.065	2.540	102.9	134.7	94.3	95% PL	17
	18	0.0005	5.030	2.546	106.9	140.2	98.2	95% PL	18
	19	0.0005	5.057	2.488	103.3	142.1	98.8	20 N PL	19
	20	0.0005	5.060	2.550	104.4	135.6	95.0	20 N PL	20
	21	0.0005	5.061	2.486	103.1	142.0	98.7	20 N PL	21
	22	0.0005	5.054	2.484	99.4	137.3	95.4	20 N PL	22
									23
									24
									25
									26
									27
									28
									29
									30

Avg	135.6	94.8
StDev +/-	4.78	3.22
n	22	22

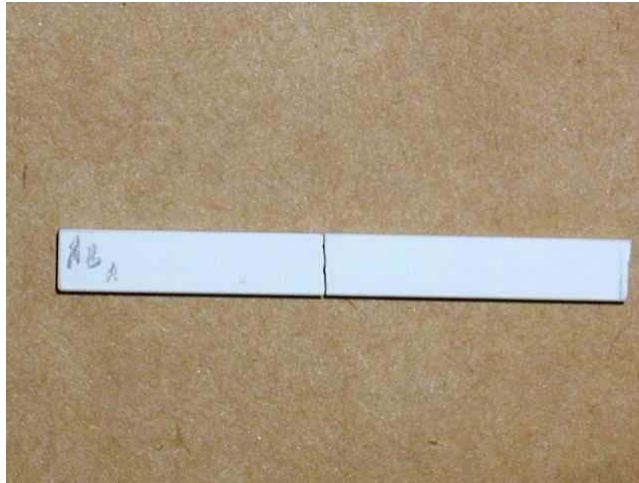


Figure A1-1.—Typical fracture pattern of a Pyroceram specimen tested in constant stress-rate (“dynamic fatigue”) testing in flexure at room-temperature distilled water.

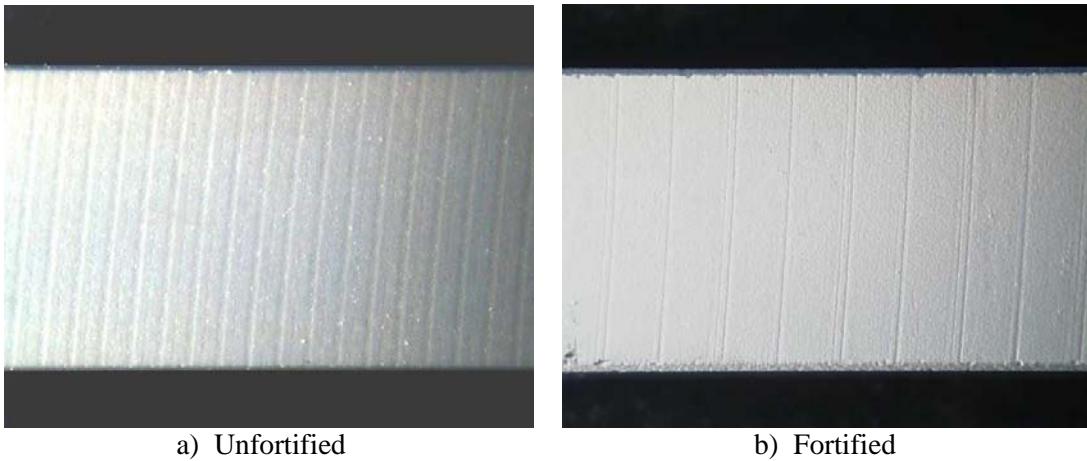


Figure A1-2.—Surface appearances of as-received Pyroceram flexure specimens: (a) ‘Unfortified’ (as-machined) and (b) ‘fortified’ specimens. Machining marks are seen in both specimens; however, for the ‘fortified’ specimens, their machining marks were etched away from the specimens’ surfaces leaving a soft, protective layer.

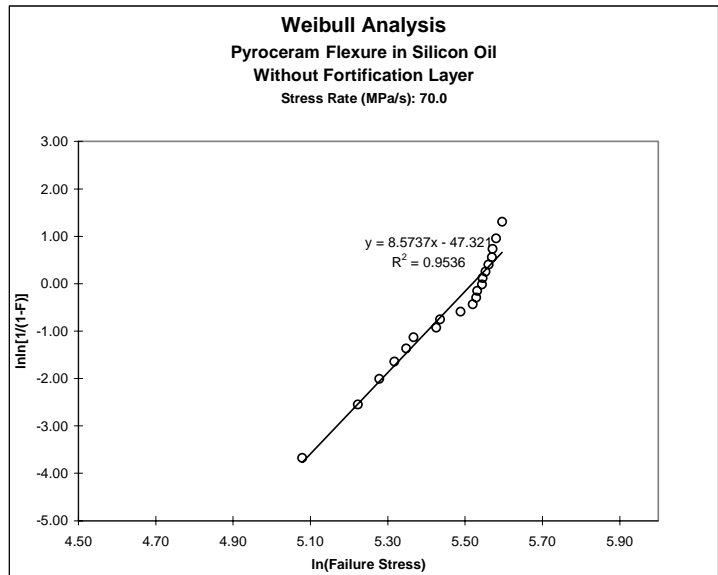
2. Individual Weibull Plots and Raw Strength Data in Slow Crack Growth Testing in Flexure: 'Unfortified' Pyroceram Test Specimens

Weibull Plot

Material: Pyroceram
 n: 20 Specimens
 Average Failure Stress: 235.72 (MPa)
 Std. Dev. +/-: 30.87 (MPa)

Stress Rate (MPa/s): 70 Mpa/s
 Temperature: rt
 Environment: Silicon Oil

Rank	Failure Stress (MPa)	F	ln(Failure Stress)	ln[1/(1-F)]
1	160.73	0.03	5.080	-3.676
2	185.64	0.08	5.224	-2.552
3	196.10	0.13	5.279	-2.013
4	204.01	0.18	5.318	-1.648
5	210.20	0.23	5.348	-1.367
6	214.20	0.28	5.367	-1.134
7	227.16	0.33	5.426	-0.934
8	229.60	0.38	5.436	-0.755
9	242.06	0.43	5.489	-0.592
10	249.67	0.48	5.520	-0.440
11	252.01	0.53	5.529	-0.295
12	252.67	0.58	5.532	-0.156
13	255.90	0.63	5.545	-0.019
14	256.10	0.68	5.546	0.117
15	258.15	0.73	5.554	0.255
16	260.15	0.78	5.561	0.400
17	262.39	0.83	5.570	0.556
18	262.90	0.88	5.572	0.732
19	265.29	0.93	5.581	0.952
20	269.50	0.98	5.597	1.305

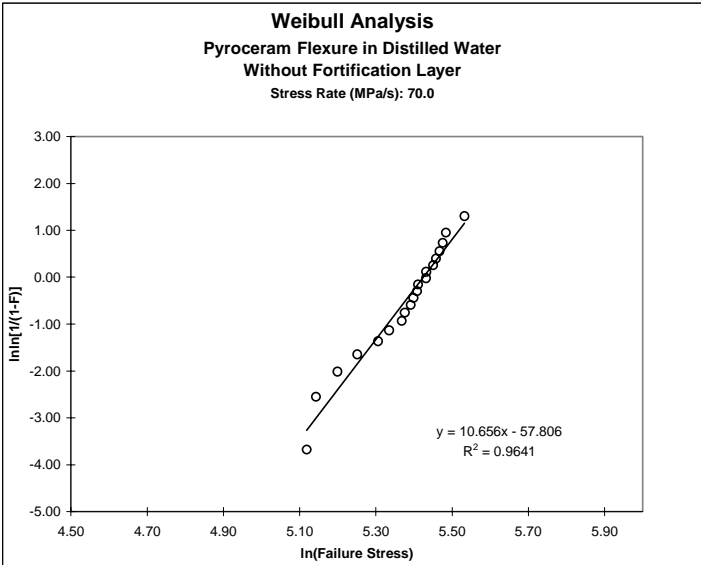


Material: Pyroceram
 n: 20 Specimens
 Average Failure Stress: 216.56 (MPa)
 Std. Dev. +/-: 23.56 (MPa)

Rank	Failure Stress (MPa)	F	ln(Failure Stress)	lnln[1/(1-F)]
1	167.07	0.03	5.118	-3.676
2	171.20	0.08	5.143	-2.552
3	181.15	0.13	5.199	-2.013
4	190.83	0.18	5.251	-1.648
5	201.52	0.23	5.306	-1.367
6	207.50	0.28	5.335	-1.134
7	214.42	0.33	5.368	-0.934
8	216.22	0.38	5.376	-0.755
9	219.53	0.43	5.391	-0.592
10	221.06	0.48	5.398	-0.440
11	223.26	0.53	5.408	-0.295
12	223.72	0.58	5.410	-0.156
13	228.51	0.63	5.432	-0.019
14	228.59	0.68	5.432	0.117
15	232.84	0.73	5.450	0.255
16	234.64	0.78	5.458	0.400
17	236.76	0.83	5.467	0.556
18	238.67	0.88	5.475	0.732
19	240.82	0.93	5.484	0.952
20	252.84	0.98	5.533	1.305

Weibull Plot

Stress Rate (MPa/s): 70 Mpa/s
 Temperature: rt
 Environment: Distilled Water

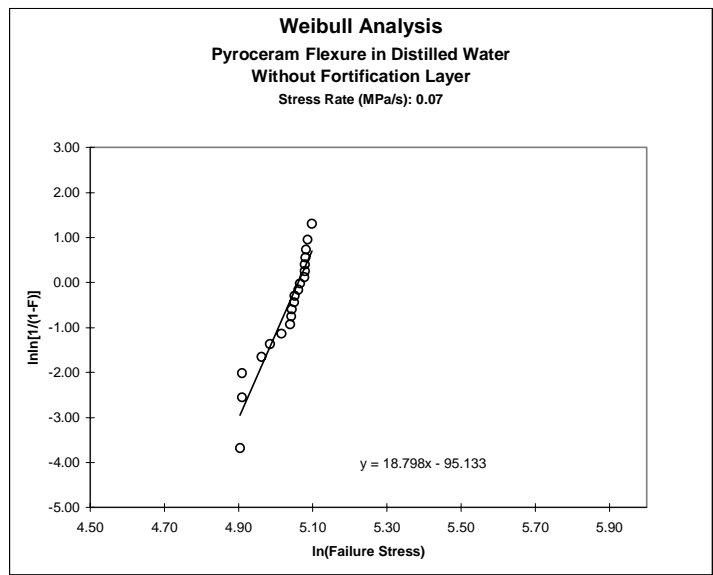


Material: Pyroceram
 n: 20 Specimens
 Average Failure Stress: 153.34 (MPa)
 Std. Dev. +/-: 9.33 (MPa)

Weibull Plot

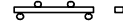
Stress Rate (MPa/s): .07Mpa/s
 Temperature: rt
 Environment: Distilled Water

Rank	Failure Stress (MPa)	F	ln(Failure Stress)	lnln[1/(1-F)]
1	134.86	0.03	4.904	-3.676
2	135.57	0.08	4.910	-2.552
3	135.59	0.13	4.910	-2.013
4	142.83	0.18	4.962	-1.648
5	146.11	0.23	4.984	-1.367
6	150.71	0.28	5.015	-1.134
7	154.33	0.33	5.039	-0.934
8	154.81	0.38	5.042	-0.755
9	154.92	0.43	5.043	-0.592
10	155.97	0.48	5.050	-0.440
11	156.26	0.53	5.052	-0.295
12	157.82	0.58	5.061	-0.156
13	158.40	0.63	5.065	-0.019
14	160.26	0.68	5.077	0.117
15	160.54	0.73	5.079	0.255
16	160.60	0.78	5.079	0.400
17	160.87	0.83	5.081	0.556
18	161.06	0.88	5.082	0.732
19	161.72	0.93	5.086	0.952
20	163.66	0.98	5.098	1.305



FLEXURE DYNAMIC FATIGUE TEST

Advanced Ceramics Test Lab
 NASA Glenn Research Center Cleveland, Ohio



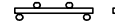
Not Fortified
 Material: Pyroceram
 Test Temperature (C): rt
 Poissons Ratio : _____
 Support Span(mm): 40.026
 Load Span (mm): 20.065
 Environment: Silicon Oil
 Load Frame: M-1 Instron
 Load Cell: 5Kn Instron
 Specimen Prep.: see comments
 Annealing: as received
 Fortification Layer Thickness (mm): 0
 Load 80 N/s = 4800 N/min
 Rate: 70 MPa/s
 Notes: _____
 Without With

Completion Date	Specimen Number	Stress Rate (MPa/sec)	Specimen Size		Fracture Load (N)	Fracture Strength (MPa)	Fracture Strength (MPa)	Comments	
			Width ↔ (mm)	Depth ↓ (mm)					
	NFI-1	0.070	5.082	2.600	225	196.1	196.1		1
	2	0.070	5.100	2.519	220.5	204.0	204.0		2
	3	0.070	5.085	2.563	288	258.2	258.2		3
	4	0.070	5.081	2.591	299.5	262.9	262.9		4
	5	0.070	5.120	2.522	274.1	252.0	252.0		5
	6	0.070	5.116	2.585	302.9	265.3	265.3		6
	7	0.070	5.116	2.526	263.9	242.1	242.1		7
	8	0.070	5.087	2.599	260.7	227.2	227.2		8
	9	0.070	5.087	2.586	306.2	269.5	269.5		9
	10	0.070	5.077	2.577	241.2	214.2	214.2		10
	11	0.070	5.102	2.517	200.4	185.6	185.6		11
	12	0.070	5.096	2.557	289.5	260.2	260.2		12
	13	0.070	5.098	2.509	274.5	256.1	256.1		13
	14	0.070	5.083	2.614	293.1	252.7	252.7		14
	15	0.070	5.090	2.517	275.6	255.9	255.9		15
	16	0.070	5.096	2.516	282.7	262.4	262.4		16
	17	0.070	5.093	2.547	275.5	249.7	249.7		17
	18	0.070	5.100	2.534	229.9	210.2	210.2		18
	19	0.070	5.111	2.514	173.4	160.7	160.7		19
	20	0.070	5.122	2.535	252.4	229.6	229.6		20
									21
									22
									23
									24
									25
									26
									27
									28
									29
									30

Avg 235.7 235.7
 StDev +/- 30.87 30.87
 n 20 20

FLEXURE DYNAMIC FATIGUE TEST

Advanced Ceramics Test Lab
 NASA Glenn Research Center Cleveland, Ohio



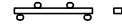
Not Fortified
 Material: Pyroceram Environment: Distilled H2O Load: 80 N/s = 4800 N/min
 Test Temperature (C): rt Load Frame: M-1 Instron Rate: _____
 Poissons Ratio : _____ Load Cell: 5Kn Instron 70 Mpa/sec
 Support Span(mm): 40.026 Specimen Prep.: as received Notes: _____
 Load Span (mm): 20.065 Annealing: as received _____
 Fortification Layer Thickness (mm): 0 _____

Completion Date	Specimen Number	Stress Rate (MPa/sec)	Specimen Size		Fracture Load (N)	Fracture Strength (MPa)		Comments	
			Width ↔ (mm)	Depth ↓ (mm)		Without	With		
7/14/2000	70NDFD-1	70.0	5.103	2.505	270.4	252.8	252.8		1
	2	70.0	5.089	2.549	184.5	167.1	167.1		2
	3	70.0	5.070	2.562	245.7	221.1	221.1		3
	4	70.0	5.094	2.497	181.6	171.2	171.2		4
	5	70.0	5.094	2.510	235.3	219.5	219.5		5
	6	70.0	5.094	2.515	245.9	228.5	228.5		6
	7	70.0	5.084	2.576	233.8	207.5	207.5		7
	8	70.0	5.108	2.519	254	234.6	234.6		8
	9	70.0	5.092	2.545	262.9	238.7	238.7		9
	10	70.0	5.093	2.524	234.3	216.2	216.2		10
	11	70.0	5.085	2.554	211.4	190.8	190.8		11
	12	70.0	5.076	2.592	265.2	232.8	232.8		12
	13	70.0	5.085	2.576	251.6	223.3	223.3		13
	14	70.0	5.096	2.520	255.9	236.8	236.8		14
	15	70.0	5.095	2.503	243.7	228.6	228.6		15
	16	70.0	5.102	2.518	241.7	223.7	223.7		16
	17	70.0	5.097	2.520	231.8	214.4	214.4		17
	18	70.0	5.106	2.504	257.5	240.8	240.8		18
	19	70.0	5.079	2.565	224.9	201.5	201.5		19
	20	70.0	5.094	2.507	193.7	181.1	181.1		20
									21
									22
									23
									24
									25
									26
									27
									28
									29
									30

Avg 216.6 216.6
 StDev +/- 23.56 23.56
 n 20 20

FLEXURE DYNAMIC FATIGUE TEST

Advanced Ceramics Test Lab
 NASA Glenn Research Center Cleveland, Ohio



Not Fortified
 Material: Pyroceram Environment: Distilled H2O Load 80 N/s = 4800 N/min
 Test Temperature (C): rt Load Frame: M-1 Instron Rate: 0.07 MPa/s
 Poissons Ratio : _____ Load Cell: 5Kn Instron
 Support Span(mm): 40.026 Specimen Prep.: see comments Notes: _____
 Load Span (mm): 20.065 Annealing: as received
 Fortification Layer Thickness (mm): 0

Completion Date	Specimen Number	Stress Rate (MPa/sec)	Specimen Size		Fracture Load (N)	Fracture Strength (MPa)	Fracture Strength (MPa)	Comments	
			Width ↔ (mm)	Depth ↓ (mm)					
7/14/2000	NFDF-7	0.070	5.068	2.587	161.8	142.8	142.8		1
	NFDF-8	0.070	5.083	2.536	168.5	154.3	154.3		2
	NFDF-9	0.070	5.100	2.531	170.5	156.3	156.3		3
	NFDF-10	0.070	5.118	2.510	146	135.6	135.6		4
	NFDF-11	0.070	5.099	2.548	177.5	160.5	160.5		5
	NFDF-12	0.070	5.105	2.517	171.1	158.4	158.4		6
	NFDF-13	0.070	5.098	2.506	144.2	134.9	134.9		7
	NFDF-14	0.070	5.104	2.503	171.8	160.9	160.9		8
	NFDF-15	0.070	5.080	2.542	171	156.0	156.0		9
	NFDF-16	0.070	5.079	2.592	184.3	161.7	161.7		10
	NFDF-17	0.070	5.102	2.541	177.2	161.1	161.1		11
	NFDF-18	0.070	5.093	2.607	179.1	154.9	154.9		12
	NFDF-19	0.070	5.083	2.510	171.4	160.3	160.3		13
	NFDF-20	0.070	5.081	2.596	167.1	146.1	146.1		14
	NFDF-21	0.070	5.105	2.595	187.9	163.7	163.7		15
	NFDF-22	0.070	5.079	2.581	170.3	150.7	150.7		16
	NFDF-23	0.070	5.086	2.555	175	157.8	157.8		17
	NFDF-24	0.070	5.085	2.560	172.3	154.8	154.8		18
	NFDF-25	0.070	5.097	2.517	173.2	160.6	160.6		19
	NFDF-26	0.070	5.092	2.499	144	135.6	135.6		20
									21
									22
									23
									24
									25
									26
									27
									28
									29
									30

Avg 153.3 153.3
 StDev +/- 9.33 9.33
 n 20 20

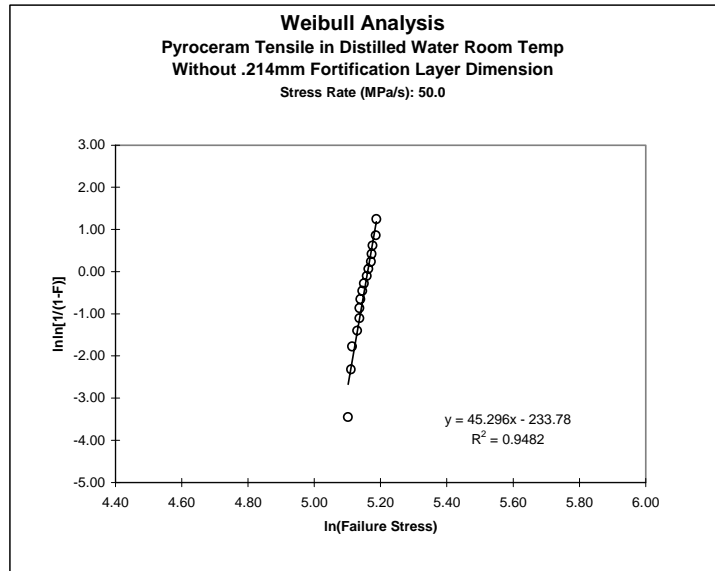
3. Individual Weibull Plots and Raw Strength Data in Tension: 'Fortified' Pyroceram Test Specimens

Material: Pyroceram
 n: 16 Specimens
 Average Failure Stress: 172.29 (MPa)
 Std. Dev. +/-: 4.57 (MPa)

Stress Rate (MPa/s): 60.000
 Temperature: rt
 Environment: Distilled Water

Rank	Failure Stress (MPa)	F	ln(Failure Stress)	ln[1/(1-F)]
1	164.39	0.03	5.102	-3.450
2	165.82	0.09	5.111	-2.318
3	166.32	0.16	5.114	-1.773
4	169.01	0.22	5.130	-1.399
5	170.16	0.28	5.137	-1.108
6	170.21	0.34	5.137	-0.865
7	170.54	0.41	5.139	-0.651
8	171.62	0.47	5.145	-0.458
9	172.47	0.53	5.150	-0.277
10	173.99	0.59	5.159	-0.104
11	174.76	0.66	5.163	0.066
12	176.12	0.72	5.171	0.238
13	176.53	0.78	5.174	0.419
14	176.98	0.84	5.176	0.619
15	178.78	0.91	5.186	0.862
16	178.97	0.97	5.187	1.243
17				
18				
19				
20				
21				
22				
23				
24				
25				
26				
27				
28				
29				
30				

Weibull Plot

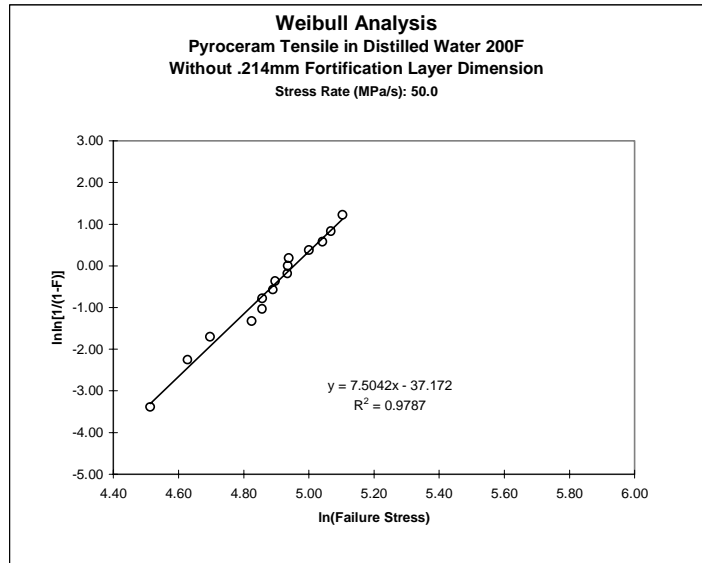


Material: Pyroceram
n: 15 Specimens
Average Failure Stress: 133.08 (MPa)
Std. Dev. +/-: 20.42 (MPa)

Stress Rate (MPa/s): 60.0000
Temperature: 200 F (93 C)
Environment: Distilled Water

Rank	Failure Stress (MPa)	F	ln(Failure Stress)	lnln[1/(1-F)]
1	91.21	0.03	4.513	-3.384
2	102.34	0.10	4.628	-2.250
3	109.62	0.17	4.697	-1.702
4	124.58	0.23	4.825	-1.325
5	128.59	0.30	4.857	-1.031
6	128.67	0.37	4.857	-0.784
7	132.95	0.43	4.890	-0.566
8	133.82	0.50	4.896	-0.367
9	138.97	0.57	4.934	-0.179
10	139.14	0.63	4.935	0.003
11	139.63	0.70	4.939	0.186
12	148.52	0.77	5.001	0.375
13	154.76	0.83	5.042	0.583
14	158.80	0.90	5.068	0.834
15	164.55	0.97	5.103	1.224

Weibull Plot

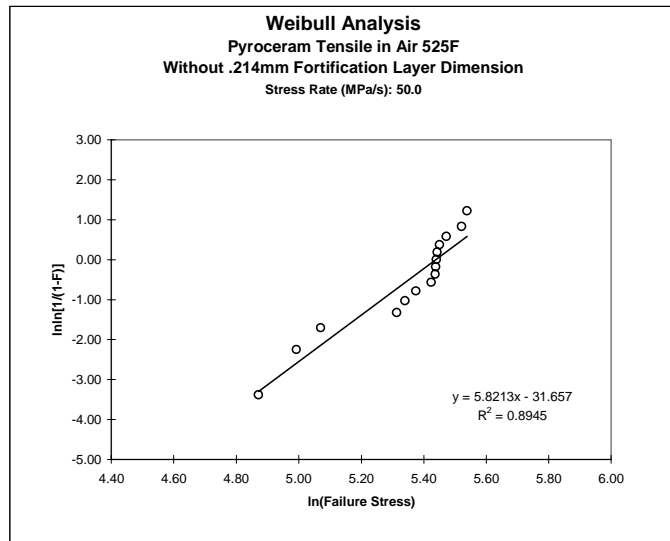


Material: Pyroceram
 n: 15 Specimens
 Average Failure Stress: 212.56 (MPa)
 Std. Dev. +/-: 37.45 (MPa)

Stress Rate (MPa/s): 60.000
 Temperature: 525 F (274 C)
 Environment: Air

Rank	Failure Stress (MPa)	F	ln(Failure Stress)	lnln[1/(1-F)]
1	130.53	0.03	4.872	-3.384
2	147.30	0.10	4.992	-2.250
3	159.25	0.17	5.070	-1.702
4	203.19	0.23	5.314	-1.325
5	208.54	0.30	5.340	-1.031
6	215.90	0.37	5.375	-0.784
7	226.74	0.43	5.424	-0.566
8	229.68	0.50	5.437	-0.367
9	230.13	0.57	5.439	-0.179
10	230.76	0.63	5.441	0.003
11	231.18	0.70	5.443	0.186
12	232.83	0.77	5.450	0.375
13	238.02	0.83	5.472	0.583
14	250.08	0.90	5.522	0.834
15	254.32	0.97	5.539	1.224
16				
17				
18				
19				
20				
21				
22				
23				
24				
25				
26				
27				
28				
29				
30				

Weibull Plot



Tensile Dynamic Fatigue Test

ADVANCED CERAMICS TEST LAB

NASA Glenn Research Center Cleveland, Ohio

Material: Pyroceram Environment: H2O Load: 70 Mpa/sec
 Test Temperature (C): RT Load Frame: M2 Rate: _____
 Poissons Ratio : _____ Load Cell: _____
 _____ Specimen Prep.: _____ Notes: _____
 _____ Annealing: _____
 Fortification Layer Thickness (mm nominal): 0.214

Actual

Completion Date	Specimen Number	Stress Rate (MPa/sec)	Specimen Size		Fracture Load (N)	Fracture Strength (MPa)	Load Rate N/s	Comments	
			Width ↔ (mm)	Depth ↓ (mm)					
	T2		2.543	3.178	983	169.0	0.00	BL#9-028-2035-15.2	1
	T3		2.548	3.182	1002	171.6	0.00	BL#9-028-2035-15.2	2
	T4		2.549	3.186	997.6	170.5	0.00	BL#9-028-2035-15.2	3
	T5		2.551	3.172	968.9	166.3	0.00	BL#9-028-2035-15.2	4
	TC1		2.549	3.189	1010	172.5	0.00	BL#9-028-2035-15.2	5
	T9		2.549	3.188	996.4	170.2	0.00	BL#9-028-2035-15.2	6
	T11		3.170	2.525	1028	178.8	0.00	BL#9-028-2035-15.2	7
	T12		2.764	2.197	1072	176.5	0.00	BL#9-028-2035-15.2 Actmeas	8
	T13		3.179	2.548	967.1	165.8	0.00		9
	T14		3.169	2.548	1040	179.0	0.00		10
	T15		2.180	2.750	1061	177.0	0.00	BL#9-028-2035-15.2 Actmeas	11
	T16		3.180	2.552	1017	174.0	0.00		12
	T17		3.184	2.548	1029	176.1	0.00		13
	T18		3.190	2.548	962.6	164.4	0.00		14
	T19		2.731	2.167	1007	170.2	0.00	BL#9-028-2035-15.2 Actmeas	15
	T20		2.716	2.170	1030	174.8	0.00	BL#9-028-2035-15.2 Actmeas	16
									17
									18
									19
									20
									21
									22
									23
									24
									25
									26
									27
									28
									29
									30

Avg 172.3
 StDev +/- 4.57
 — — n 16

Tensile Dynamic Fatigue Test

ADVANCED CERAMICS TEST LAB

NASA Glenn Research Center Cleveland, Ohio

Material: <u>Pyroceram</u>	Environment: <u>H2O</u>	Load: <u>70 Mpa/sec</u>
Test Temperature (C): <u>93C (200F)</u>	Load Frame: <u>M2</u>	Rate: <u>400 N/sec</u>
Poissons Ratio : _____	Load Cell: _____	Notes: _____
_____	Specimen Prep.: <u>none</u>	_____
_____	Annealing: _____	_____
Fortification Layer Thickness (mm nominal): <u>0.214</u>	_____	_____

Completion Date	Specimen Number	Stress Rate (MPa/sec)	Specimen Size		Fracture Load (N)	Fracture Strength (MPa)	Load Rate N/s	Comments	
			Width ↔ (mm)	Depth ↓ (mm)					
	T2-1		2.672	2.184	727	124.6	0.00	BL#9-028-2035-14.7	1
	T2-2		2.782	2.182	847.6	139.6	0.00	BL#9-028-2035-14.7	2
	T2-3		3.186	2.535	747.7	128.7	0.00	BL#9-028-2035-14.7	3
	T2-4		3.247	2.477	802.7	139.0	0.00	BL#9-028-2035-14.7	4
	T2-5		3.167	2.553	924.3	158.8	0.00	BL#9-028-2035-14.7	5
	T2-6		3.242	2.541	883.1	148.5	0.00	BL#9-028-2035-14.7	6
	T2-7		3.238	2.548	828.9	139.1	0.00	BL#9-028-2035-14.7	7
	T2-8		3.226	2.554	764.9	128.6	0.00	BL#9-028-2035-14.7	8
	T2-9		3.135	2.555	765.5	133.0	0.00	BL#9-028-2035-14.7	9
	T2-10		3.227	2.555	543	91.2	0.00	BL#9-028-2035-14.7	10
	T2-11		3.224	2.557	609.2	102.3	0.00	BL#9-028-2035-14.7	11
	T2-12		3.252	2.553	657.8	109.6	0.00	BL#9-028-2035-14.7	12
	T2-13		3.244	2.550	983.3	164.6	0.00	BL#9-028-2035-14.7	13
	T2-14		3.246	2.555	802.1	133.8	0.00	BL#9-028-2035-14.7	14
	T2-15		3.244	2.548	923.9	154.8	0.00	BL#9-028-2035-14.7	15
									16
									17
									18
									19
									20
									21
									22
									23
									24
									25
									26
									27
									28
									29
									30

Avg 133.1
StDev +/- 20.42
n 15

Tensile Dynamic Fatigue Test

ADVANCED CERAMICS TEST LAB

NASA Glenn Research Center Cleveland, Ohio

Material: <u>Pyroceram</u>	Environment: <u>Air</u>	Load: <u>70 Mpa/sec</u>
Test Temperature (C): <u>274C (525F)</u>	Load Frame: <u>M2</u>	Rate: <u>400 N/s</u>
Poissons Ratio : _____	Load Cell: _____	Notes: _____
_____	Specimen Prep.: <u>none</u>	_____
_____	Annealing: _____	_____
Fortification Layer Thickness (mm nominal): <u>0.214</u>		

Completion Date	Specimen Number	Stress Rate (MPa/sec)	Specimen Size		Fracture Load (N)	Fracture Strength (MPa)	Load Rate N/s	Comments	
			Width ↔ (mm)	Depth ↓ (mm)					
	T5-1		2.551	3.188	863.1	147.3	0.00	BL#9-028-2035-15.2	1
	T5-2		2.569	3.182	939	159.3	0.00	BL#9-028-2035-15.2	2
	T5-3		2.544	3.198	765.1	130.5	0.00	BL#9-028-2035-15.2	3
	T5-4		2.549	3.172	1343	230.8	0.00	BL#9-028-2035-15.2	4
	T5-5		2.550	3.184	1352	231.2	0.00	BL#9-028-2035-15.2	5
	T5-6		2.549	3.180	1186	203.2	0.00	BL#9-028-2035-15.2	6
	T5-7		2.547	3.180	1259	215.9	0.00	BL#9-028-2035-15.2	7
	T5-8		2.554	3.214	1343	226.7	0.00	BL#9-028-2035-15.2	8
	T5-9		2.551	3.181	1345	230.1	0.00	BL#9-028-2035-15.2	9
	T5-10		2.547	3.172	1384	238.0	0.00	BL#9-028-2035-15.2	10
	T5-11		2.547	3.245	1371	229.7	0.00	BL#9-028-2035-14.7	11
	T5-12		2.539	3.113	1182	208.5	0.00	BL#9-028-2035-14.7	12
	T5-13		2.547	3.165	1475	254.3	0.00	BL#9-028-2035-14.7	13
	T5-14		2.560	3.172	1463	250.1	0.00	BL#9-028-2035-14.7	14
	T5-15		2.548	3.236	1386	232.8	0.00	BL#9-028-2035-14.7	15
									16
									17
									18
									19
									20
									21
									22
									23
									24
									25
									26
									27
									28
									29
									30

Avg 212.6
StDev +/- 37.45
n 15

Comparison of Strength Between Tension And Flexure

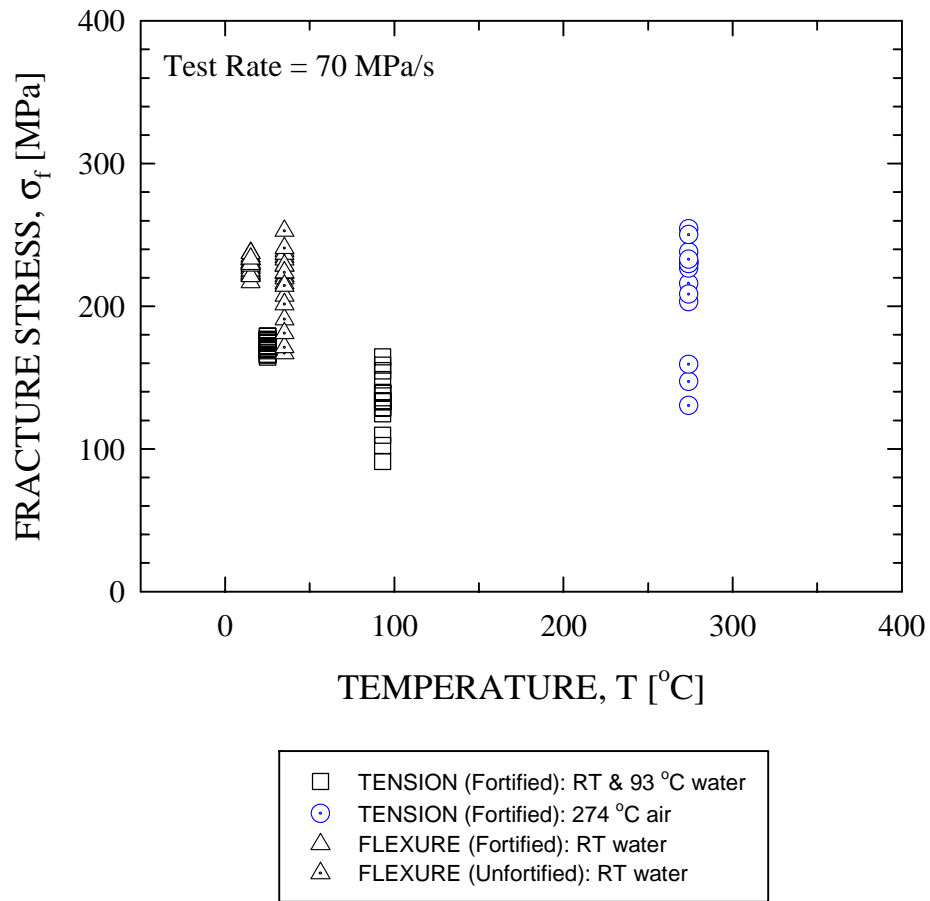


Figure A3-1.—Comparison of strength as a function of test temperature between tension and flexure in Pyroceram.

4. Raw Strength Data in Compression Testing

Compression Strength Test

ADVANCED CERAMICS TEST LAB

NASA Glenn Research Center Cleveland, Ohio

Material: Pyroceram Environment: H2O Load: 1.27 mm/min
 Test Temperature (C): RT Load Frame: M2 Rate: _____
 Poissons Ratio: _____ Load Cell: _____
 _____ Specimen Prep.: _____ Notes: _____
 _____ Annealing: _____
 Fortification Layer Thickness (mm nominal): 0.225 _____

Actual

Completion Date	Specimen Number	Stress Rate (MPa/sec)	Specimen Size		Fracture Load (N)	Fracture Strength (MPa)	Load Rate N/s	Comments	
			Width ↔ (mm)	Depth ↓ (mm)					
	C1-1		12.769	2.555	12970	500.2	0.00		1
	C1-2		12.774	2.549	23480	907.7	0.00		2
	C1-3		12.785	2.545	19580	757.7	0.00		3
	C1-4		12.754	2.534	21200	826.8	0.00		4
						0.0	0.00		5
	C2-1		12.774	2.542	22990	891.7	0.00		6
	C2-2		12.761	2.544	21250	824.3	0.00		7
	C2-3		12.762	2.531	16350	638.1	0.00		8
	C2-4		12.750	2.536	13740	535.5	0.00		9
						0.0	0.00		10
	C3-1		12.763	2.550	21400	827.6	0.00		11
	C3-2		12.756	2.553	24250	937.0	0.00		12
	C3-3		12.772	2.578	23890	911.1	0.00		13
									14
									15
									16
									17
									18
									19
									20
									21
									22
									23
									24
									25
									26
									27
									28
									29
									30

5. Raw Strength Data in Shear Testing Shear Strength Test

ADVANCED CERAMICS TEST LAB
NASA Glenn Research Center Cleveland, Ohio

Material: Pyroceram Environment: H2O Load _____
 Test Temperature (C): RT Load Frame: M2 Rate: _____
 Poissons Ratio : _____ Load Cell: _____
 _____ Specimen Prep.: _____ Notes: _____
 _____ Annealing: _____
 Fortification Layer Thickness (mm nominal): 0.213 _____

Actual

Completion Date	Specimen Number	Stress Rate (MPa/sec)	Specimen Size		Fracture Load (N)	Fracture Strength (MPa)	Load Rate N/s	Comments	
			Width ↔ (mm)	Height ↓ (mm)					
	S1		11.622	2.531	1834	77.8	0.00		1
	S2		11.621	2.602	2070	85.0	0.00		2
	S3		11.584	2.550	2083	87.9	0.00		3
	S4		11.635	2.551	2220	93.2	0.00		4
	S5		11.561	2.544	2019	85.6	0.00		5
	S6		11.600	2.548	2044	86.2	0.00		6
									7
									8
									9
									10
									11
									12
									13
									14
									15
									16
									17
									18
									19
									20
									21
									22
									23
									24
									25
									26
									27
									28
									29
									30

Avg 86.0
 StDev +/- 4.97
 — - n 6

6. Raw Fracture Toughness Data

<div style="text-align: center;"> <h2 style="margin: 0;">S.E.P.B. TEST</h2> <h3 style="margin: 0;">NASA CERAMICS TESTING LAB</h3> </div>											
Material: <u>Pyroceram</u> Temperature: <u>RT</u> Actual upper span (mm): <u>20.065</u> Actual lower span (mm): <u>40.026</u> Actual fixture Wgt (g): <u>227.000</u>				Loading Rate: <u>1/2 mm/min</u> Load Frame: <u>M2</u> Load Cell: <u>1KN Instron</u> Environment: <u>DOW 704 Oil</u> Date: <u>6/12/00</u> Average: <u>2.3</u> St.Dev.+/-: <u>0.0533</u> n= <u>10</u>							
Specimens are without fortification layer											
Spec #	P (N)	\overleftrightarrow{B} (mm)	\updownarrow W (mm)	a1 (mm)	a2 (mm)	a3 (mm)	a _{avg.} (mm)	a/w	F(a/w)	K _{Ic} E+6	
SPNF-1	48.170	2.541	5.094	2.221	2.031	1.738	1.997	0.392	1.2494	2.3	
SPNF-2	47.140	2.507	5.095	2.174	2.076	1.932	2.061	0.404	1.2709	2.3	
SPNF-3	42.990	2.5	5.097	2.378	2.282	2.036	2.232	0.438	1.3361	2.3	
SPNF-4	44.600	2.498	5.089	2.230	2.123	2.033	2.129	0.418	1.2965	2.3	
SPNF-5	43.690	2.516	5.092	2.206	2.143	2.031	2.127	0.418	1.2953	2.2	
SPNF-6	46.110	2.539	5.093	1.987	2.120	2.193	2.100	0.412	1.2853	2.3	
SPNF-7	46.130	2.505	5.102	2.177	2.063	1.854	2.031	0.398	1.2599	2.2	
SPNF-8	41.6	2.503	5.102	2.310	2.222	2.010	2.181	0.427	1.3144	2.2	
SPNF-9	46.2	2.501	5.101	1.910	1.824	2.262	1.999	0.392	1.2492	2.2	
SPNF-10	47.3	2.507	5.1	1.802	1.962	2.071	1.945	0.381	1.2322	2.2	

S.E.V.N.B. TEST

NASA CERAMICS TESTING LAB

Material: <u>Pyroceram</u> Temperature: <u>RT</u> Actual upper span (mm): <u>20.065</u> Actual lower span (mm): <u>40.026</u> Actual fixture Wgt (g): <u>227.000</u> Specimens have fortification layer Linear measurements are without fortification layer	Loading Rate: <u>1/2 mm/min</u> Load Frame: <u>M2</u> Load Cell: <u>1KN Instron</u> Environment: <u>DOW 704 Oil</u> Date: <u>6/12/2000</u> Average: <u>2.4</u> St.Dev.+/-: <u>0.079808032</u> n= <u>9</u>
---	--

Spec #	P (N)	\overleftrightarrow{B} (mm)	\updownarrow W (mm)	a1 (mm)	a2 (mm)	a3 (mm)	a _{avg.} (mm)	a/w	F(a/w)	KIc E+6
SEVNB-1	23.3	2.142	3.255	1.120	1.129	1.116	1.122	0.345	1.1793	2.4
SEVNB-2	26.7	2.149	3.241	1.019	1.020	1.017	1.019	0.314	1.1426	2.5
SEVNB-3	23.3	2.19	3.168	1.051	1.080	1.061	1.064	0.336	1.1681	2.3
SEVNB-4	26.6	2.193	3.197	0.921	0.933	0.932	0.929	0.290	1.1179	2.3
SEVNB-5	21.4	2.149	3.176	1.102	1.047	1.082	1.077	0.339	1.1722	2.2
SEVNB-6	27.8	2.24	3.26	0.955	0.978	0.958	0.964	0.296	1.1229	2.3
SEVNB-7	22.9	2.159	3.214	1.088	1.097	1.095	1.093	0.340	1.1735	2.3
SEVNB-8	27.0	2.165	3.225	0.933	0.949	0.980	0.954	0.296	1.1231	2.4
SEVNB-9	28.0	2.149	3.355	1.067	1.065	1.065	1.066	0.318	1.1464	2.5

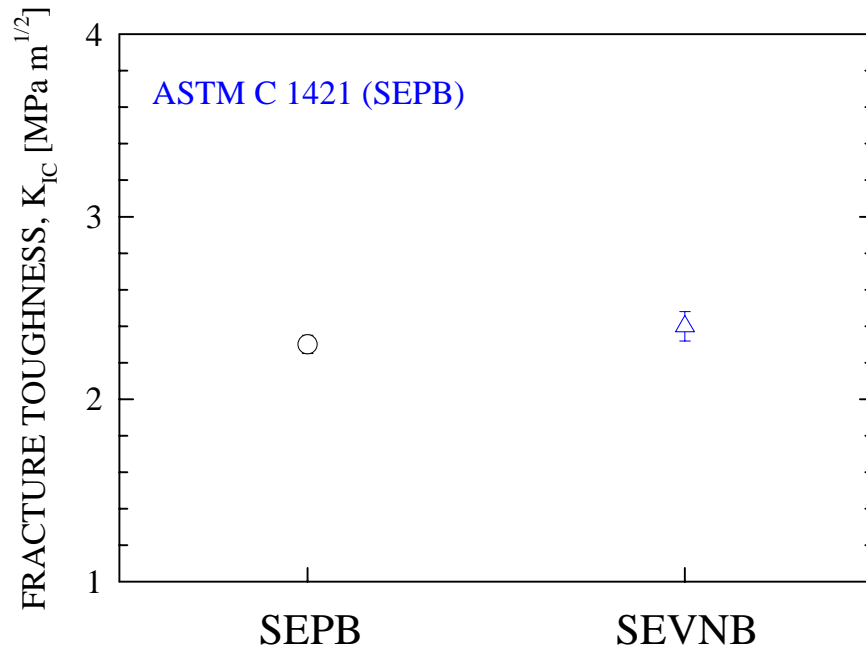


Figure A6-1.—Average fracture toughness of Pyroceram at room temperature, determined by SEPB and SEVNB methods. Error bars indicate ± 1.0 standard deviation.

6. Raw Elastic Modulus Data

Youngs Modulus by Impulse Excitation of Vibration

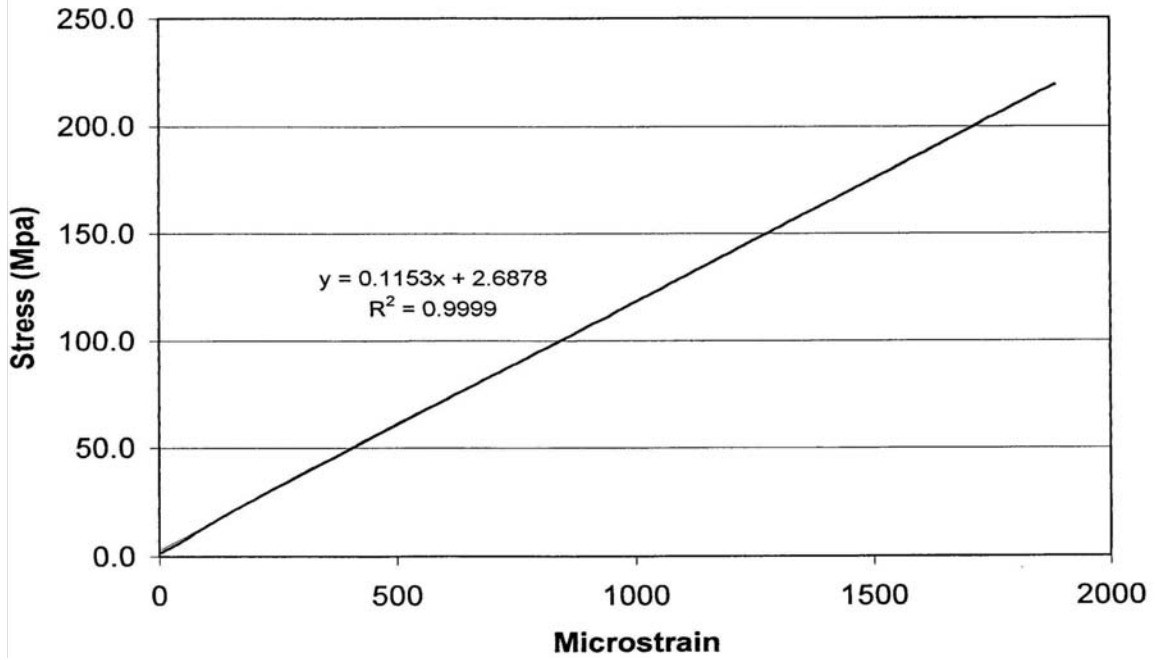
Flexure Beam

Poisson's: 0.29

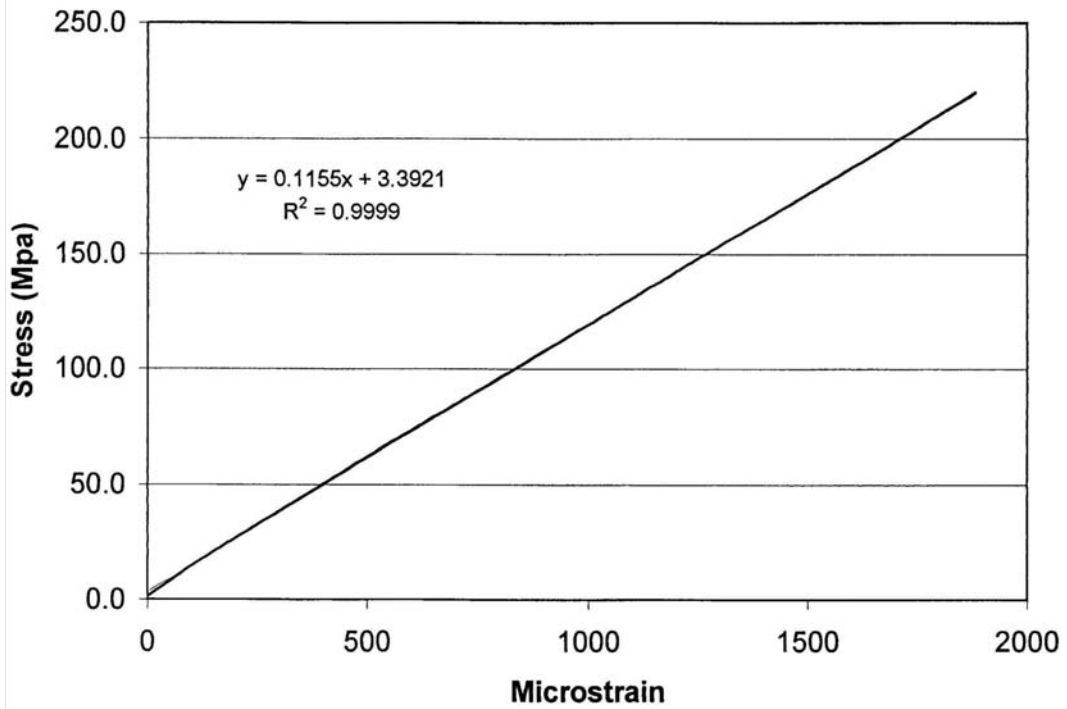
Date	Specimen	Temperature	Length (mm)	Height (mm)	Width (mm)	Mass (g)	Frequency (Hz)	Density (g/cm ³)	E (GPa)
6/20/2000	NF-1	rt	91.54	2.563	5.079	3.0985	2170	2.60	124.58
	NF-2	rt	91.52	2.553	5.081	3.1071	2170	2.62	126.26
	NF-3	rt	91.53	2.512	5.093	3.0293	2100	2.59	120.75
	NF-4	rt	91.54	2.52	5.118	3.0507	2110	2.58	121.05
	NF-5	rt	91.51	2.522	5.102	3.044	2120	2.59	121.91
	NF-6	rt	91.52	2.557	5.092	3.0825	2140	2.59	120.99
	NF-7	rt	91.51	2.552	5.079	3.101	2170	2.61	126.17
	NF-8	rt	91.53	2.589	5.081	3.1037	2170	2.58	120.99
	NF-9	rt	91.52	2.563	5.076	3.0963	2180	2.60	125.63
	NF-10	rt	91.53	2.529	5.094	3.0387	2120	2.58	120.96
	NF-11	rt	91.53	2.52	5.094	3.0313	2110	2.58	120.81
	NF-12	rt	91.53	2.567	5.076	3.1049	2170	2.60	124.29
	NF-13	rt	91.52	2.567	5.082	3.0813	2150	2.58	120.90
	NF-14	rt	91.53	2.523	5.108	3.034	2100	2.57	119.02
	NF-15	rt	91.53	2.503	5.097	3.0372	2110	2.60	123.45
	NF-16	rt	91.56	2.567	5.103	3.1241	2180	2.60	125.66
	NF-17	rt	91.53	2.512	5.098	3.0285	2120	2.58	122.91
	NF-18	rt	91.53	2.541	5.091	3.0818	2150	2.60	124.47
	NF-19	rt	91.53	2.545	5.095	3.0816	2150	2.60	123.78
	NF-20	rt	91.53	2.606	5.094	3.1052	2160	2.56	117.31
	NF-21	rt	91.54	2.504	5.096	3.0314	2110	2.60	123.13
	NF-22	rt	91.52	2.526	5.097	3.0405	2110	2.58	120.21
	NF-23	rt	91.53	2.608	5.082	3.1295	2190	2.58	121.54
	NF-24	rt	91.56	2.515	5.097	3.0517	2140	2.60	125.90
	NF-25	rt	91.52	2.5	5.098	3.0319	2120	2.60	124.78
	NF-26	rt	91.56	2.509	5.109	3.0456	2110	2.59	122.74
	NF-27	rt	91.53	2.539	5.081	3.0565	2140	2.59	122.83
	NF-28	rt	91.55	2.545	5.147	3.0915	2130	2.58	120.73
	NF-29	rt	91.59	2.501	5.094	3.018	2100	2.59	122.11
	NF-30	rt	91.53	2.563	5.076	3.1018	2160	2.60	123.59
	NF-31	rt	91.53	2.596	5.077	3.1091	2170	2.58	120.32
	NF-32	rt	91.52	2.596	5.077	3.1095	2160	2.58	119.19
	NF-33	rt	91.52	2.513	5.083	3.0252	2110	2.59	121.80
	NF-34	rt	91.57	2.525	5.096	3.046	2120	2.59	121.94
	NF-35	rt	91.52	2.511	5.095	3.0251	2100	2.58	120.64
	NF-36	rt	91.52	2.512	5.091	3.0413	2120	2.60	123.56
	NF-37	rt	91.53	2.51	5.098	3.0271	2100	2.58	120.83
	NF-38	rt	91.53	2.591	5.069	3.091	2170	2.57	120.50
	NF-39	rt	91.52	2.593	5.078	3.1045	2180	2.58	121.61
								Avg:	122.30
								St.Dev:	2.14

n: 39

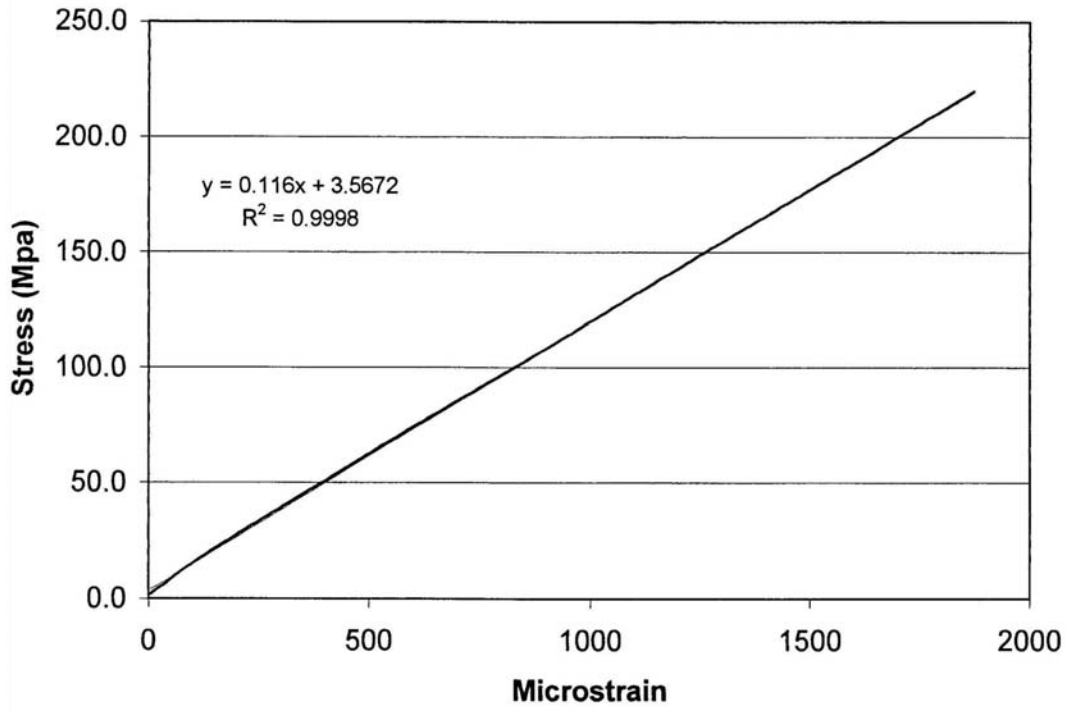
Pyroceram
Compression Direction 1 run 1



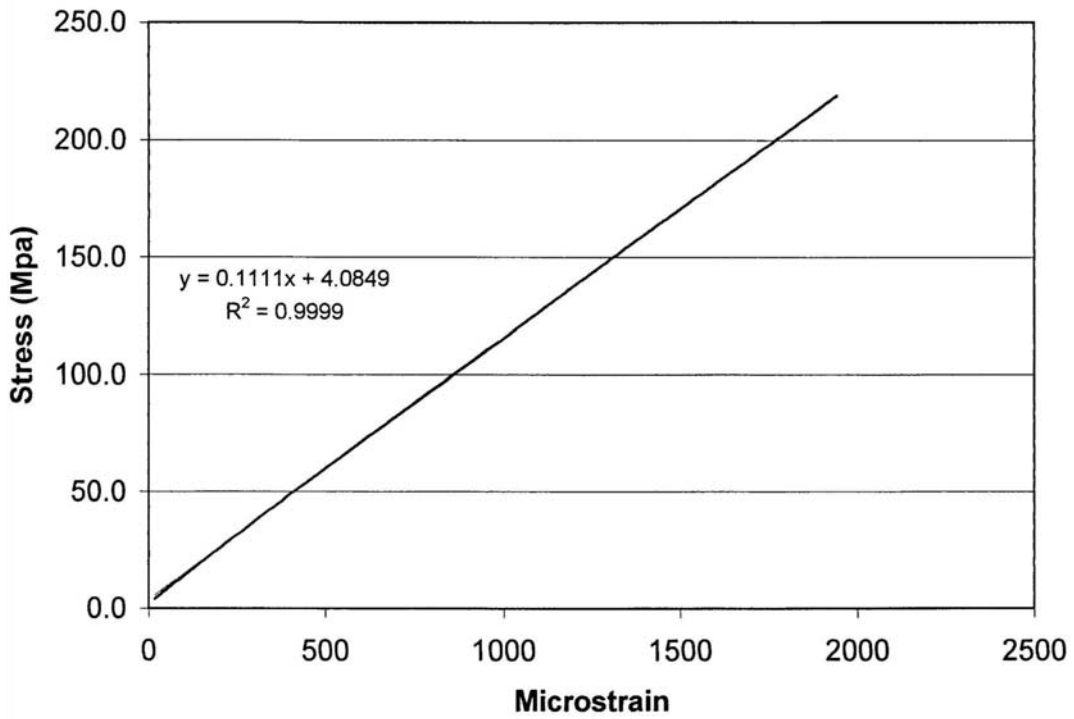
Pyroceram
Compression Direction 1 run 2



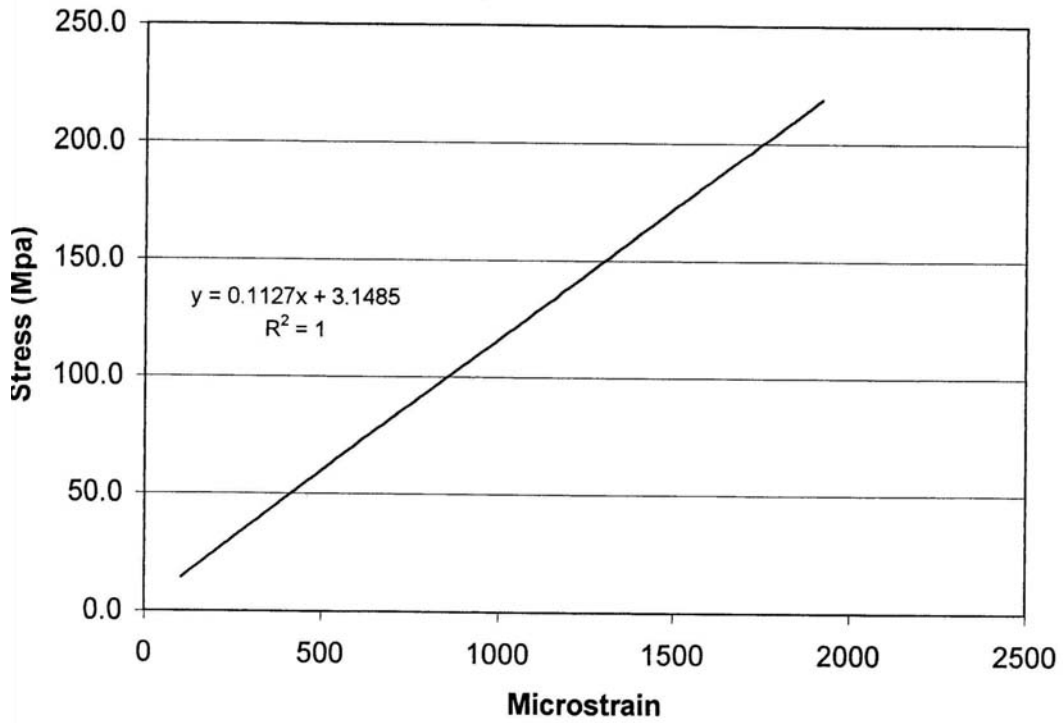
Pyroceram
Compression Direction 1 run 3



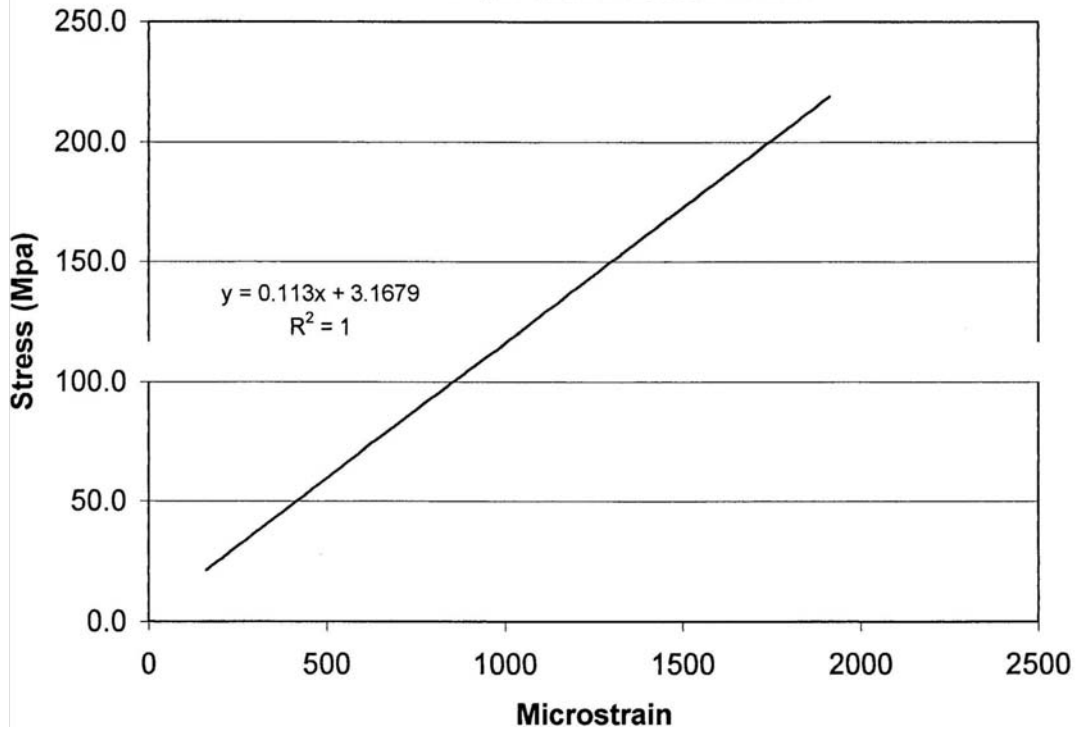
Pyroceram
Compression Direction 2 run 1



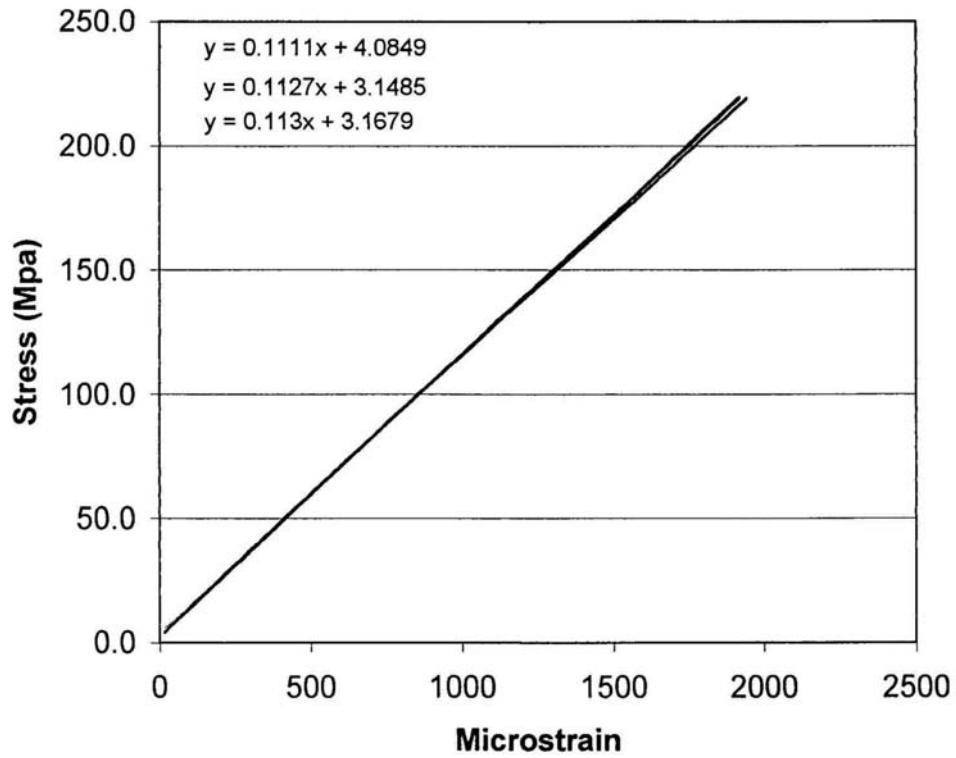
Pyroceram
Compression Direction 2 run 2



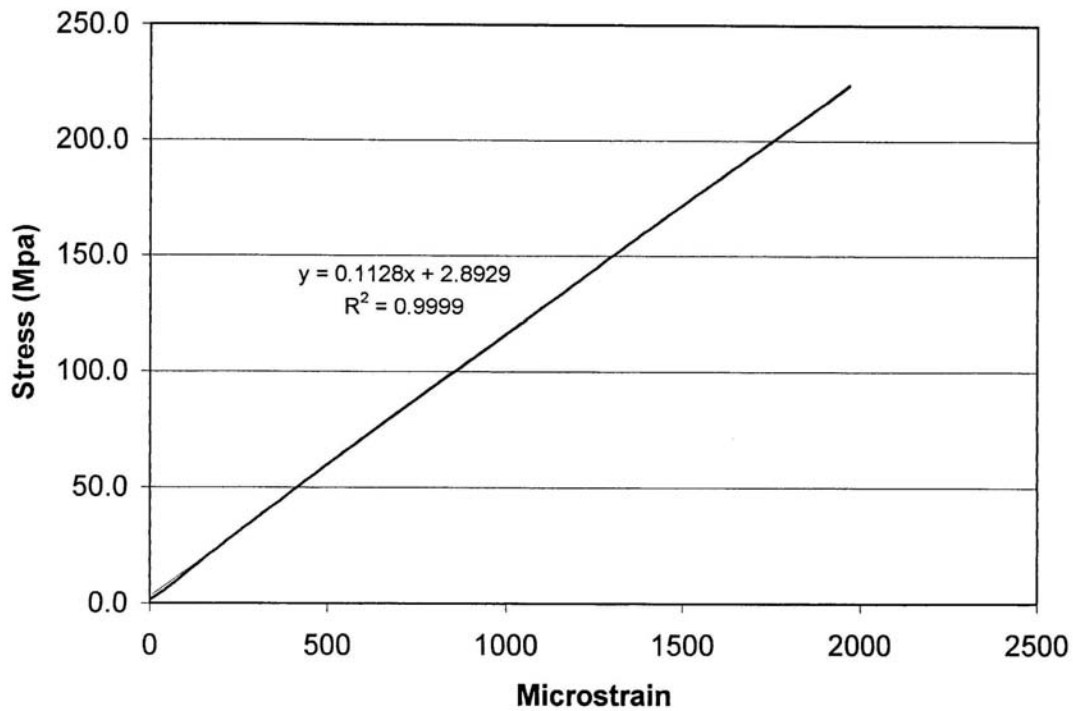
Pyroceram
Compression Direction 2 run 3



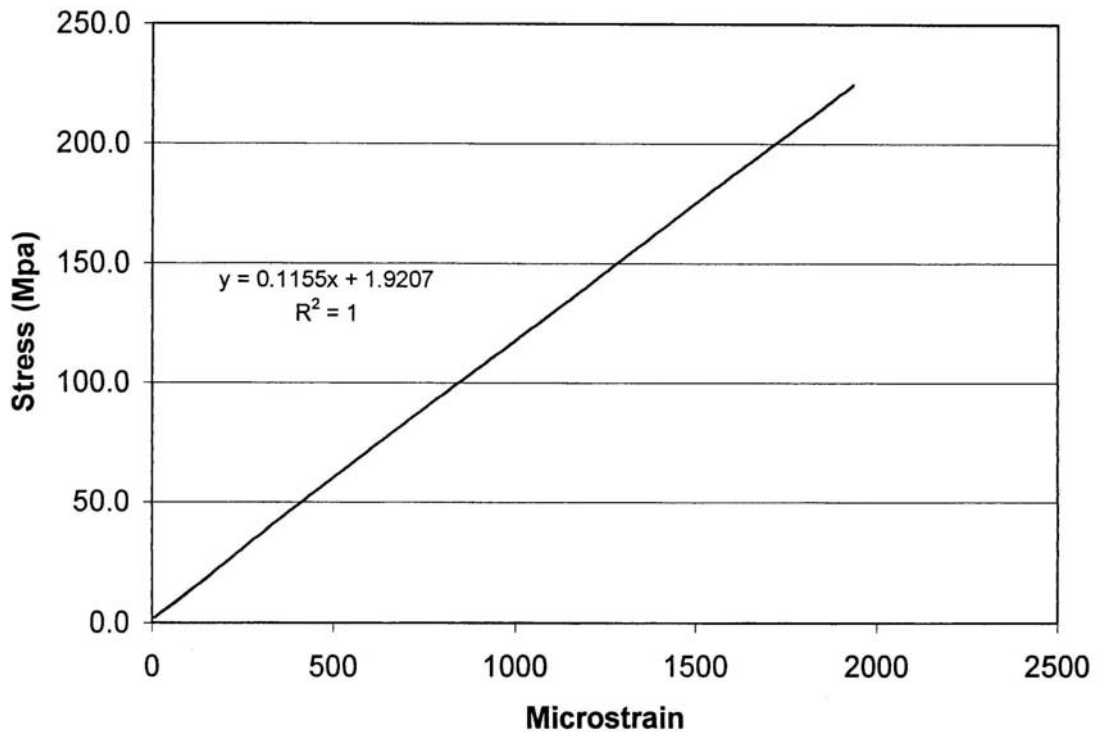
Pyroceram
Compression Direction 2 run All



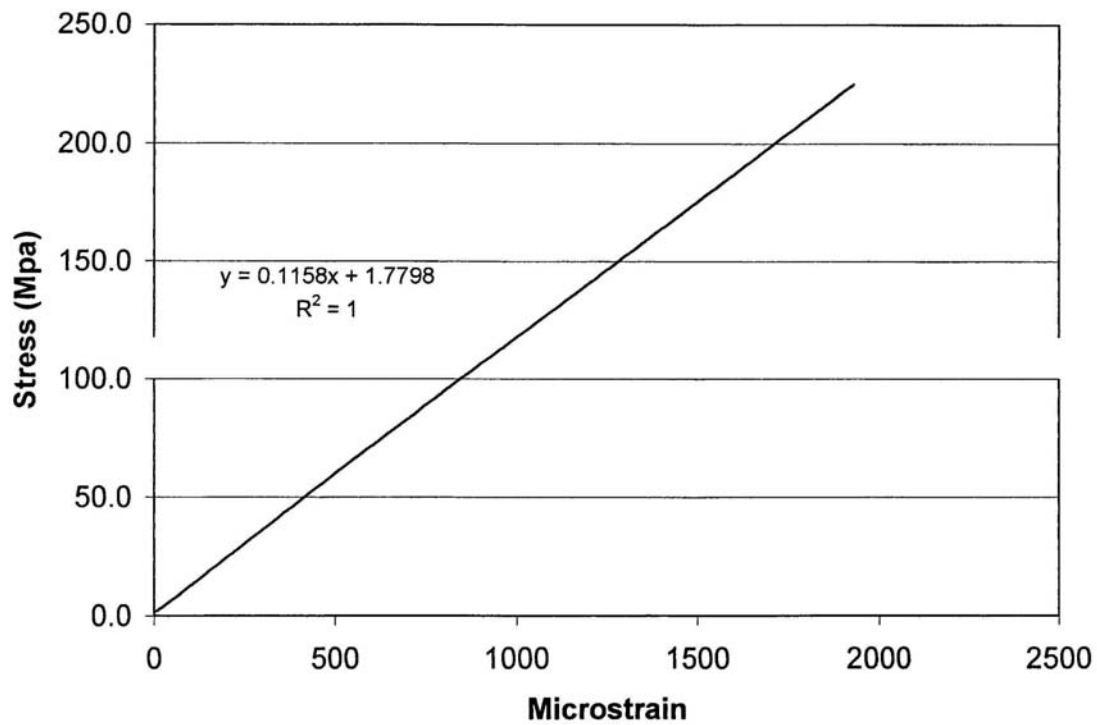
Pyroceram
Compression Direction 3 run 1



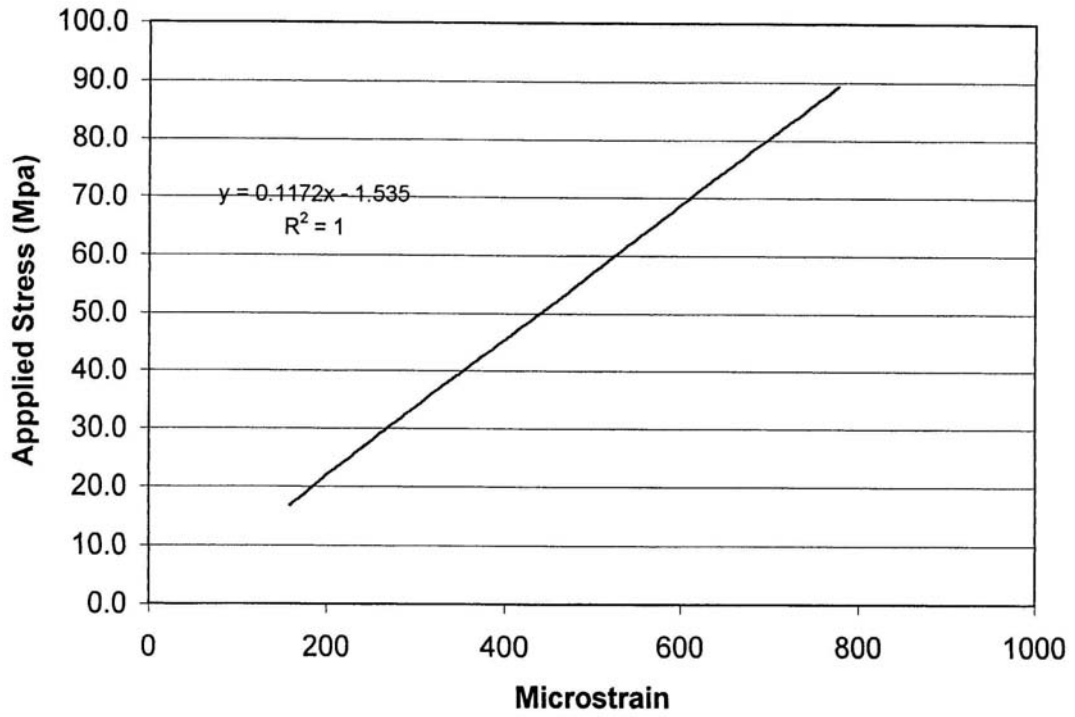
Pyroceram
Compression Direction 3 run 2



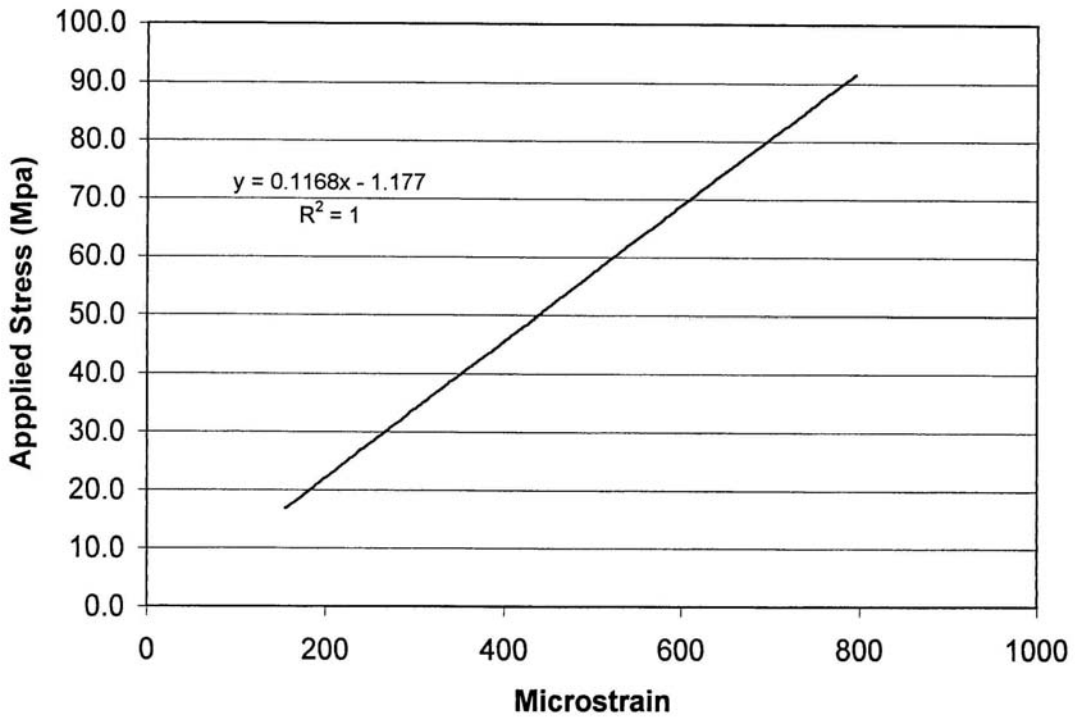
Pyroceram
Compression Direction 3 run 3



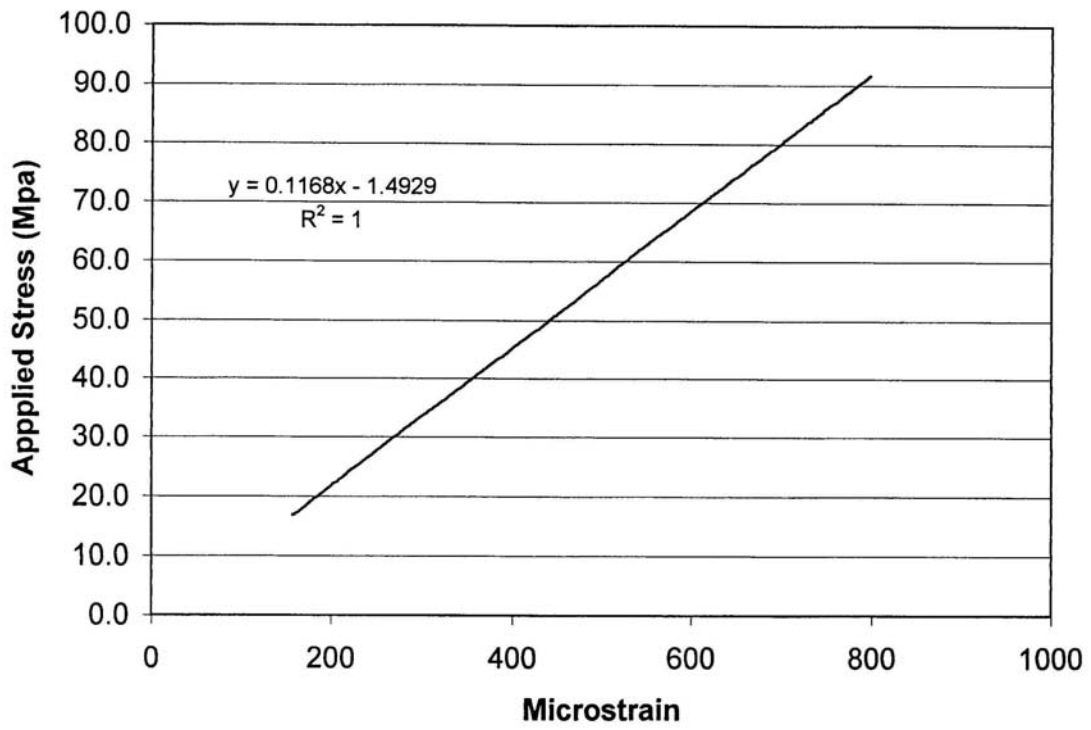
Pyroceram
Flexure Compression Direction 1 run 1



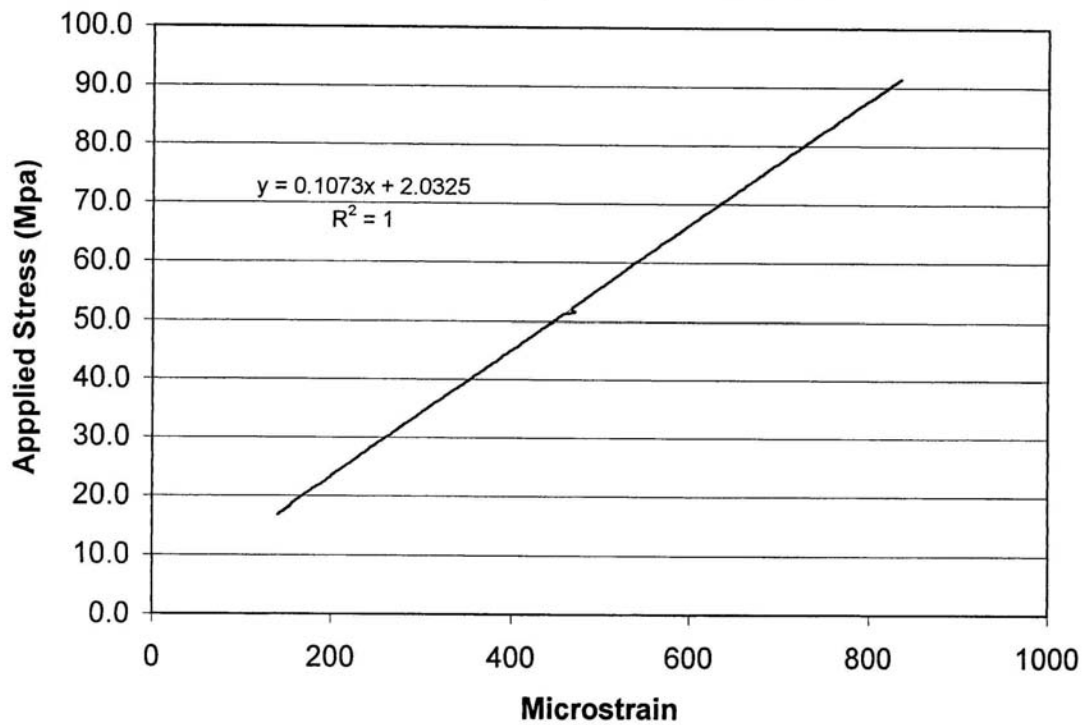
Pyroceram
Flexure Compression Direction 1 run 2



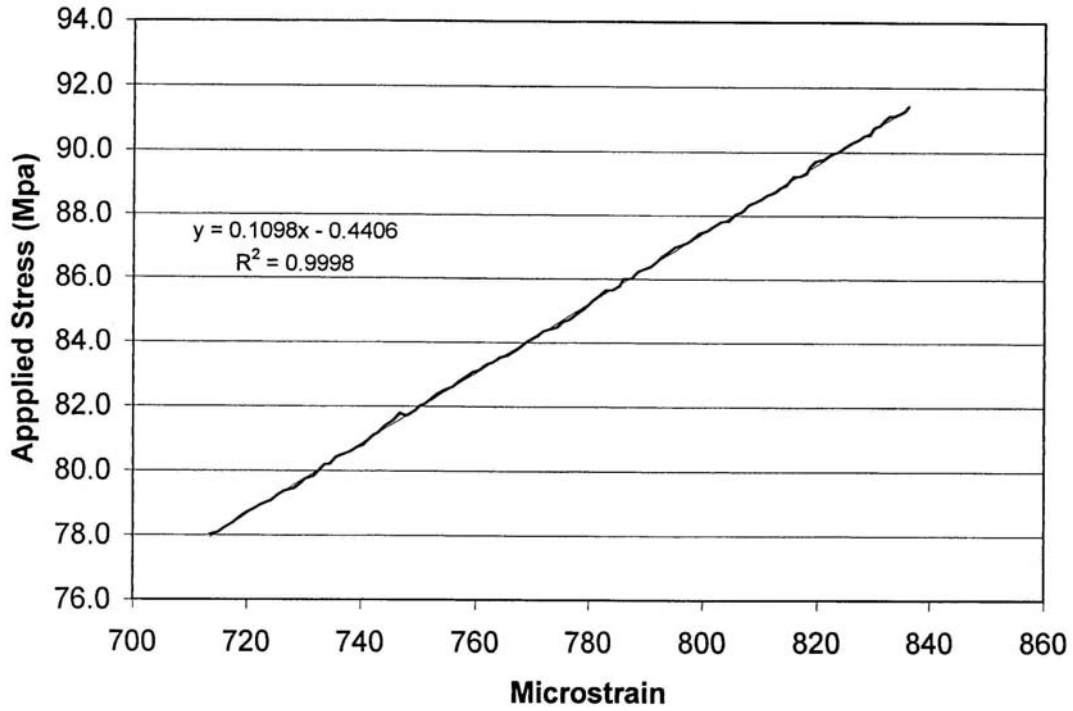
Pyroceram
Flexure Compression Direction 1 run 3



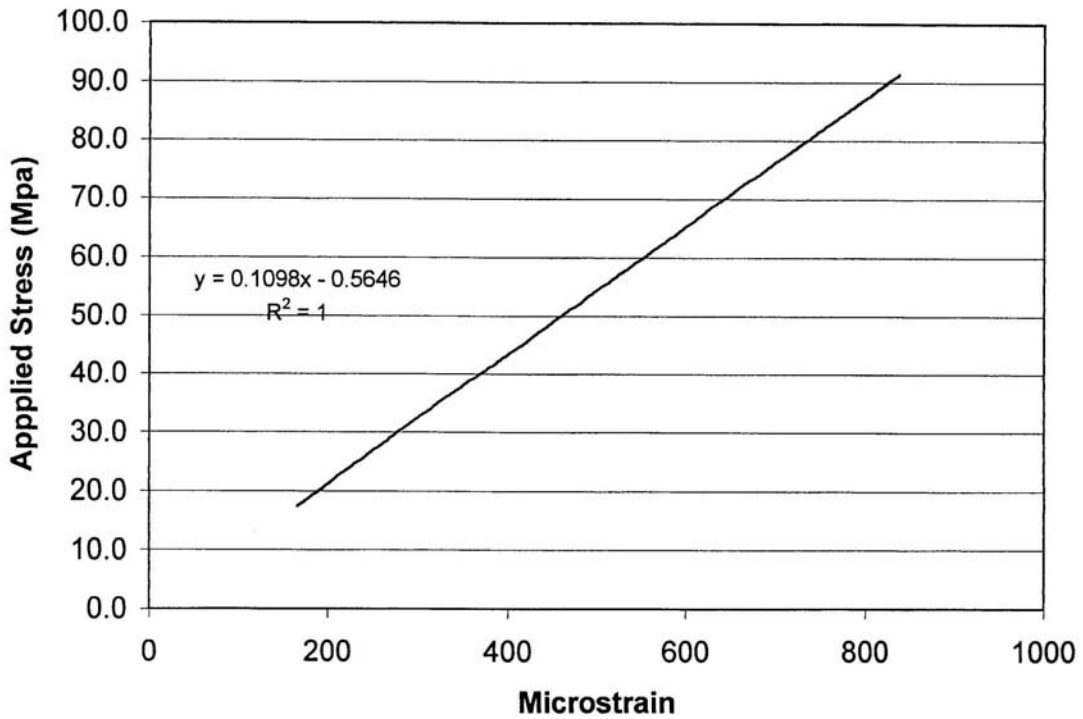
Pyroceram
Flexure Compression Direction 2 run 1



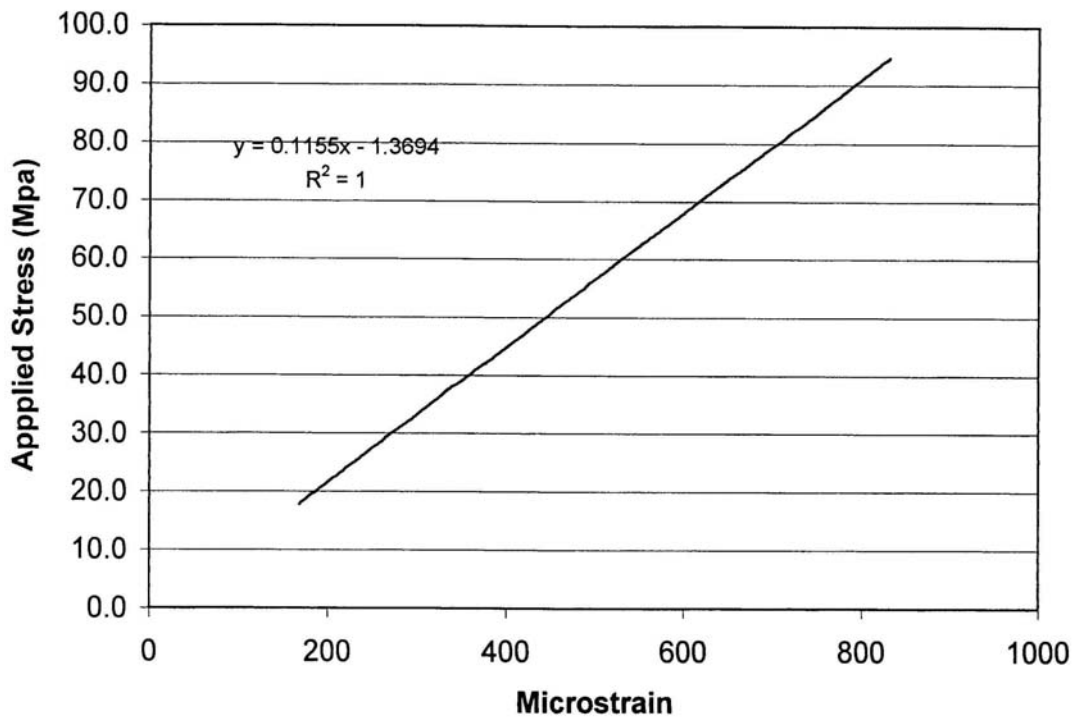
Pyroceram
Flexure Compression Direction 2 run 2



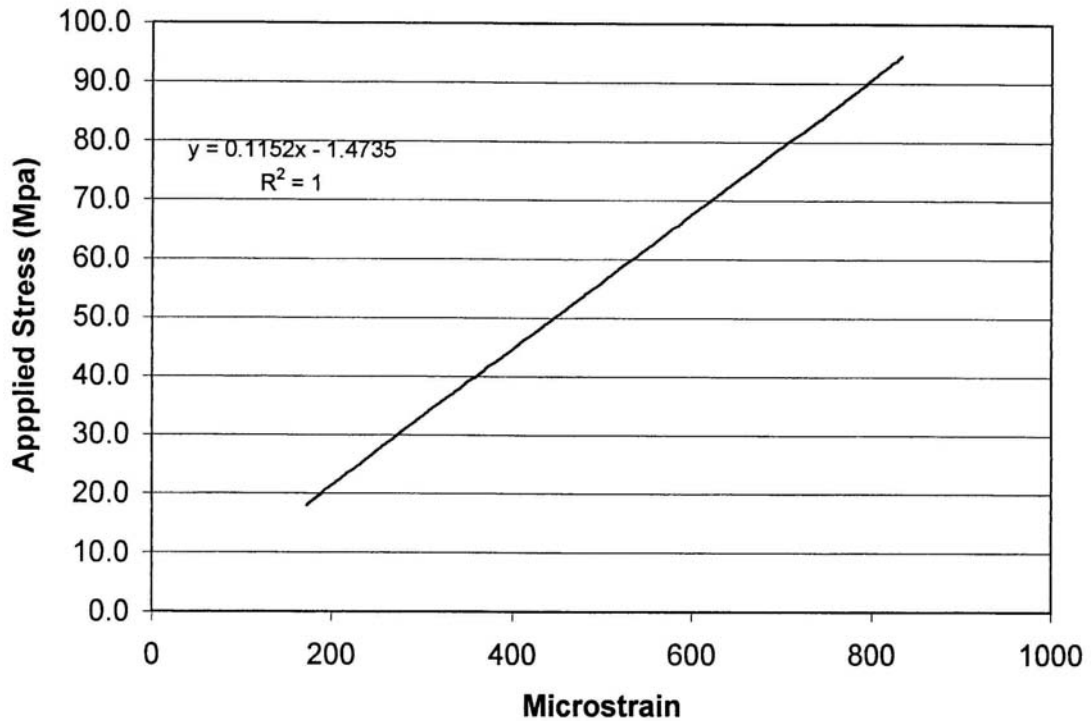
Pyroceram
Flexure Compression Direction 2 run 3



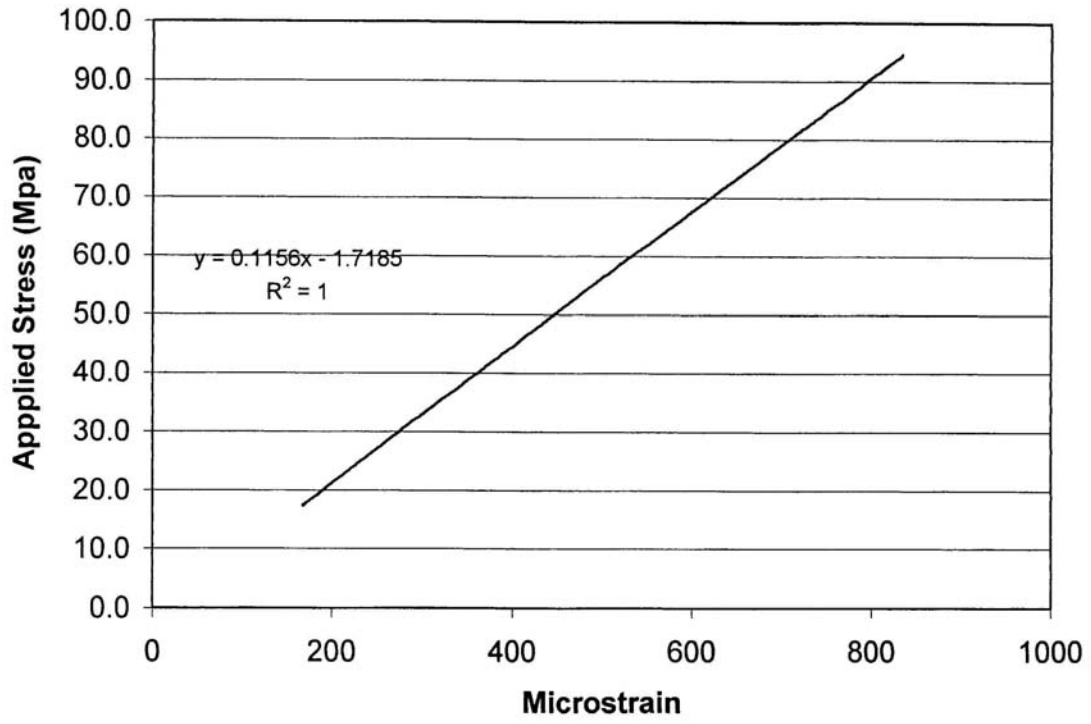
Pyroceram
Flexure Compression Direction 3 run 1



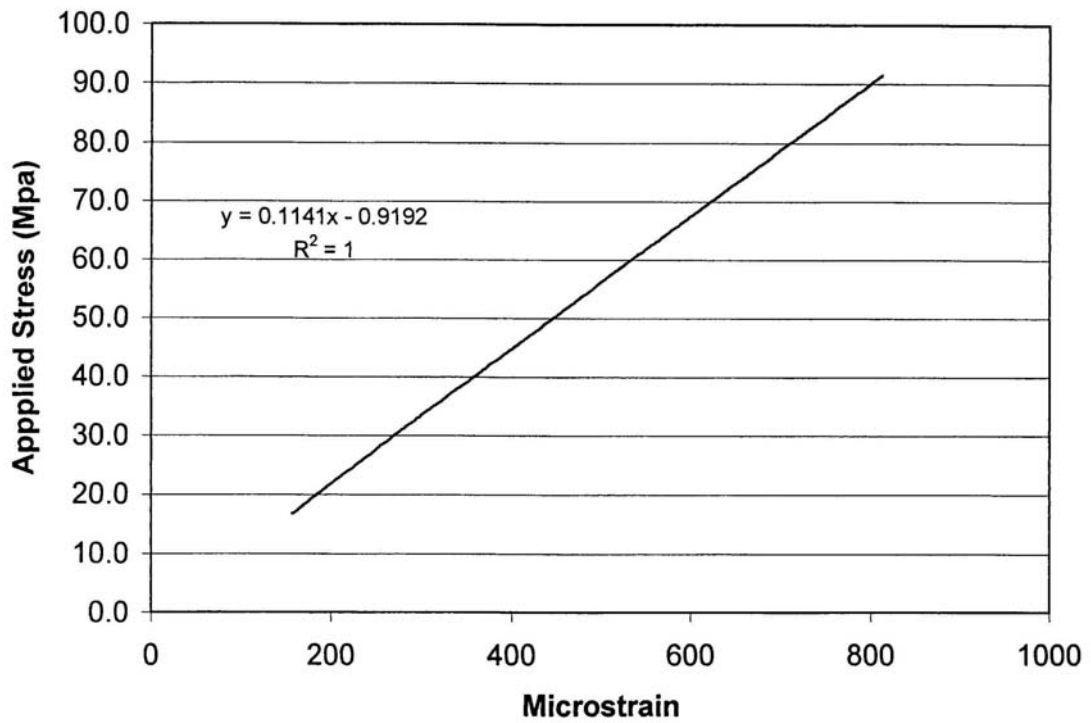
Pyroceram
Flexure Compression Direction 3 run 2



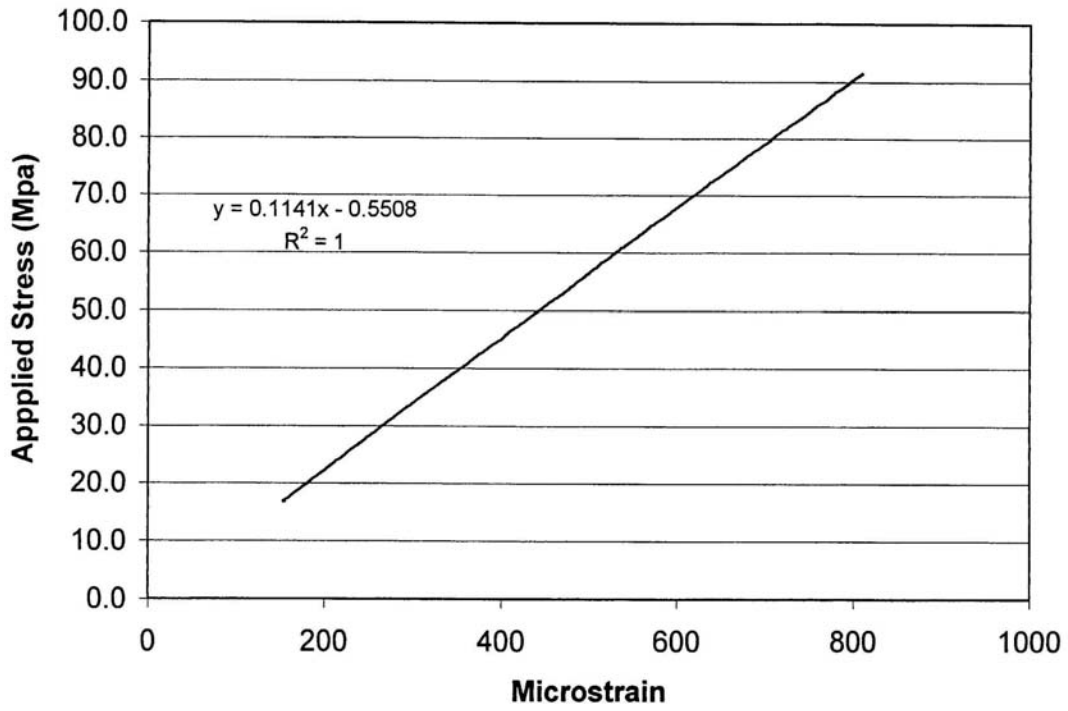
Pyroceram
Flexure Compression Direction 3 run 3



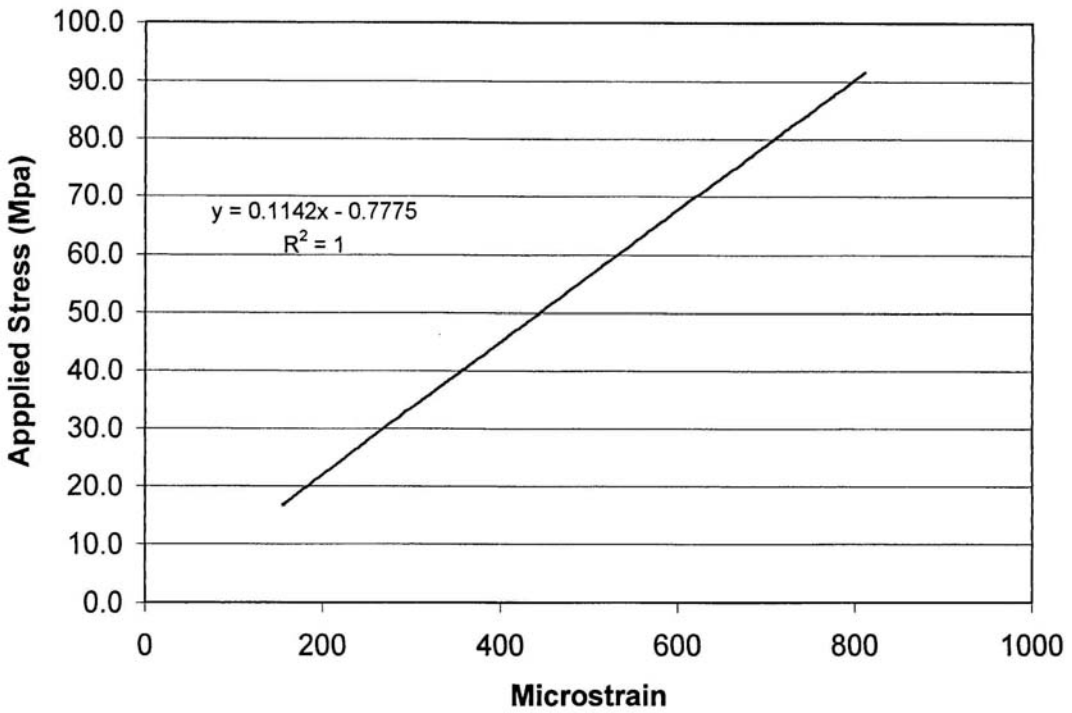
Pyroceram
Flexure Tensile Direction 1 run 1



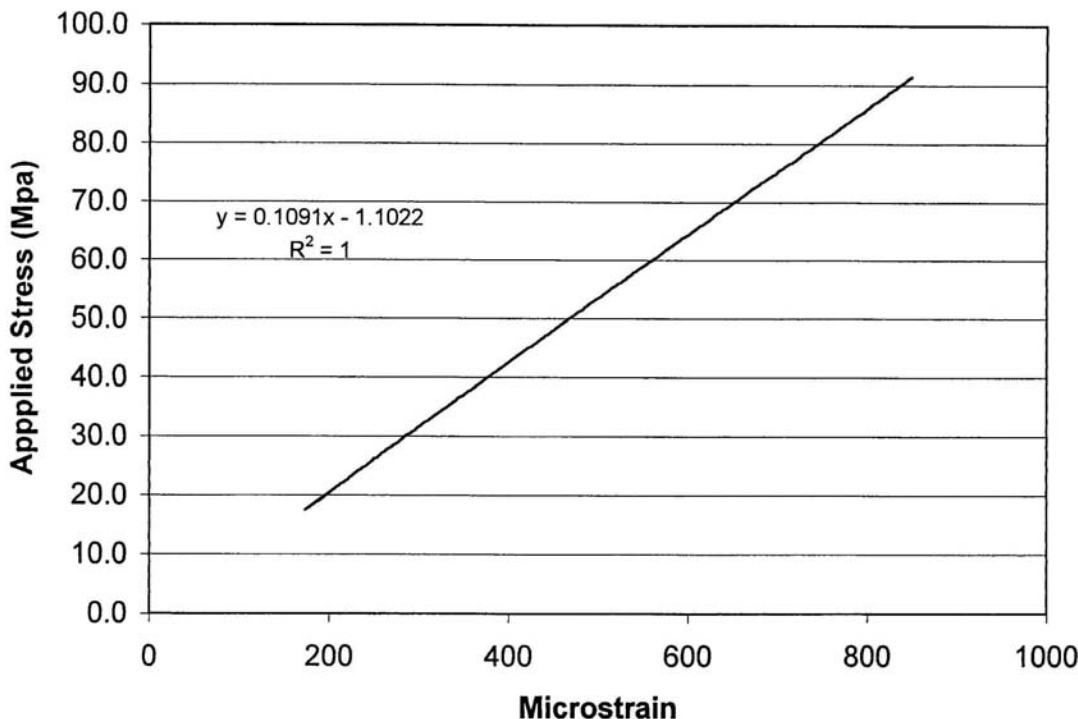
Pyroceram
Flexure Tensile Direction 1 run 2



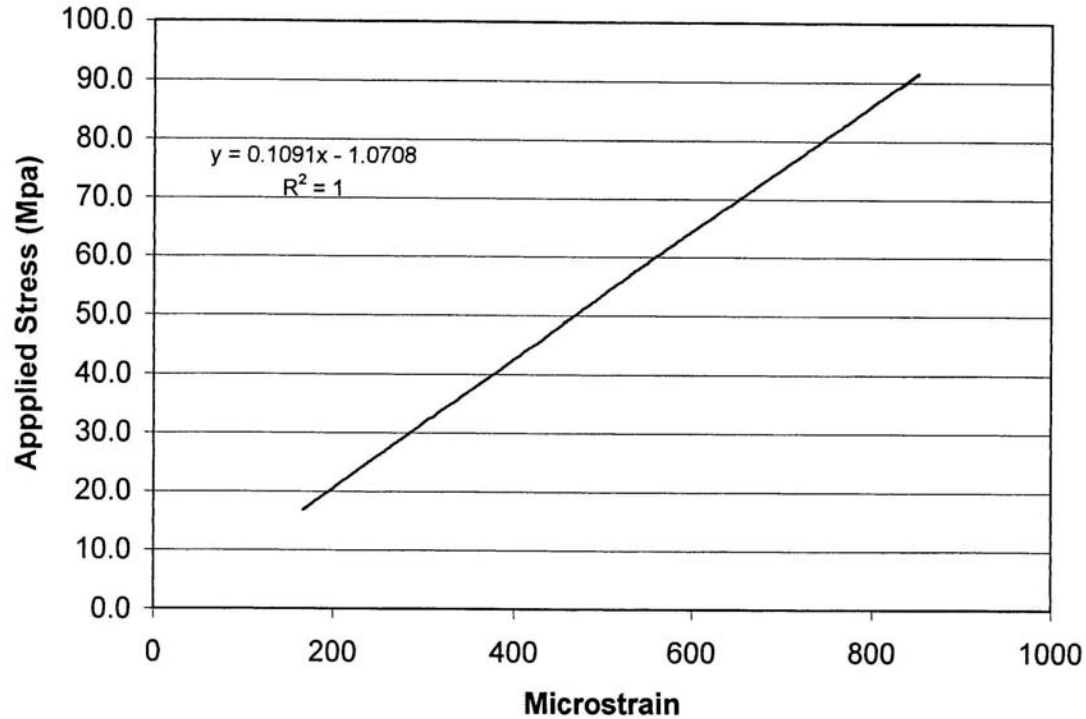
Pyroceram
Flexure Tensile Direction 1 run 3



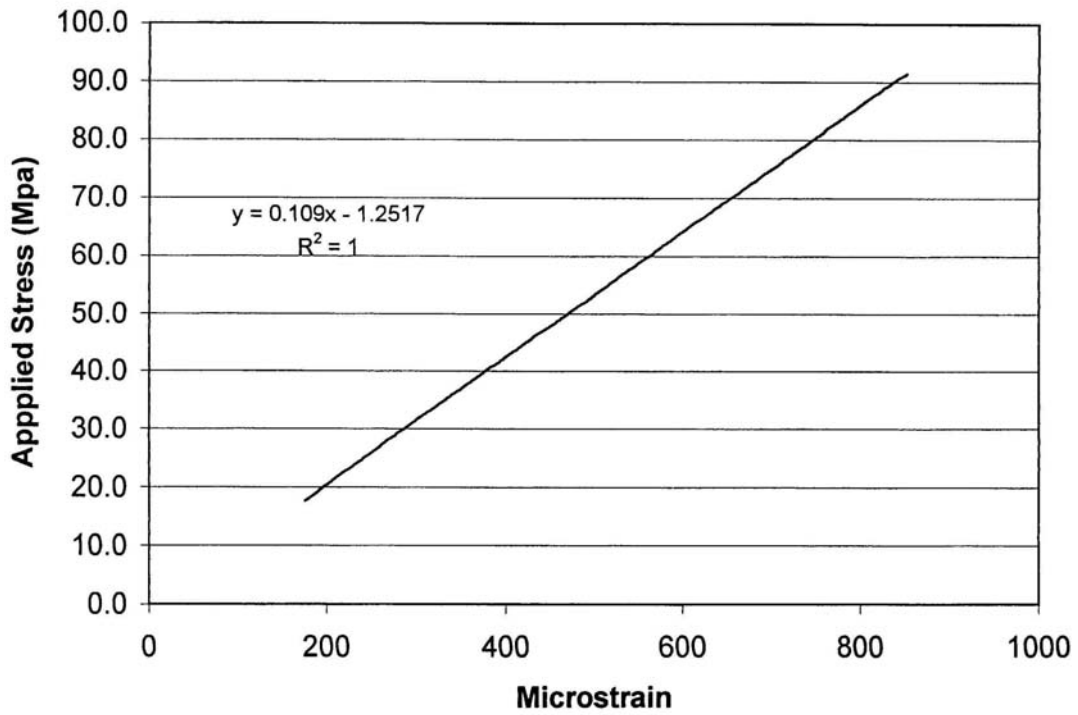
Pyroceram
Flexure Tensile Direction 2 run 1



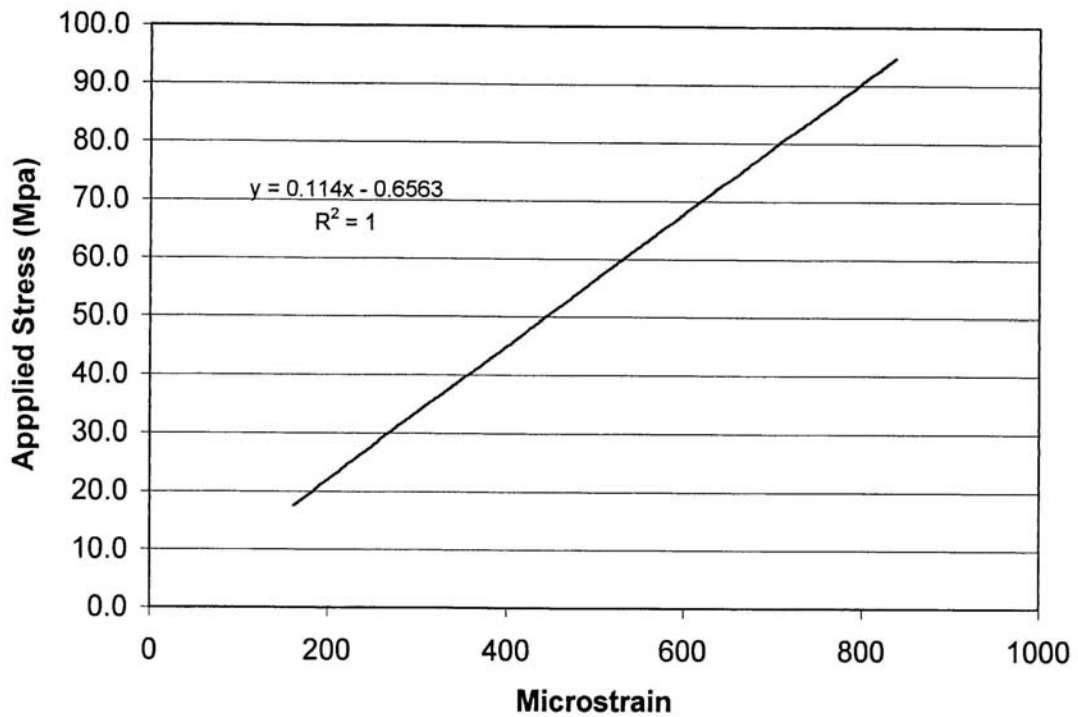
Pyroceram
Flexure Tensile Direction 2 run 2



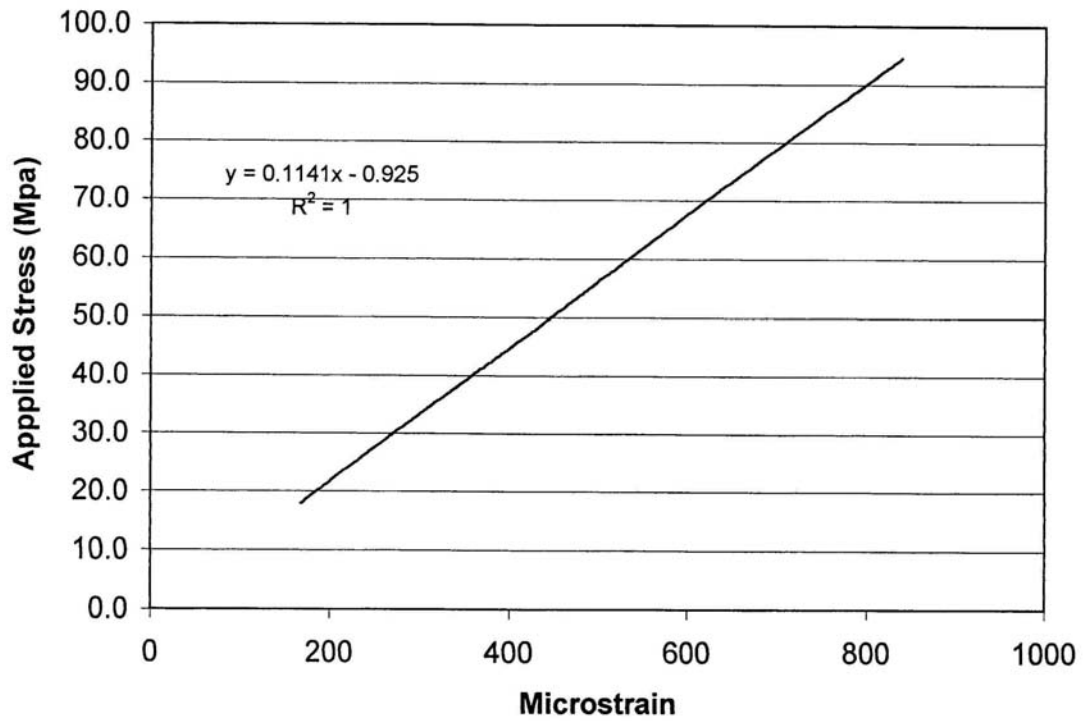
Pyroceram
Flexure Tensile Direction 2 run 3



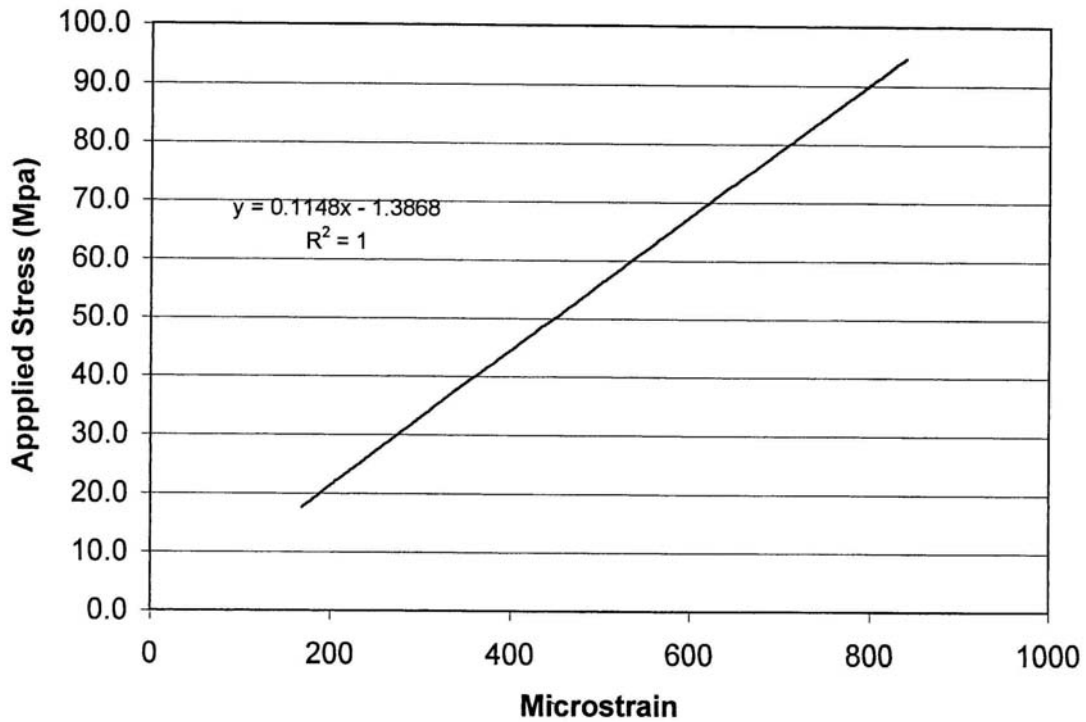
Pyroceram
Flexure Tensile Direction 3 run 1



Pyroceram
Flexure Tensile Direction 3 run 2



Pyroceram
Flexure Tensile Direction 3 run 3



REPORT DOCUMENTATION PAGE

Form Approved
OMB No. 0704-0188

Public reporting burden for this collection of information is estimated to average 1 hour per response, including the time for reviewing instructions, searching existing data sources, gathering and maintaining the data needed, and completing and reviewing the collection of information. Send comments regarding this burden estimate or any other aspect of this collection of information, including suggestions for reducing this burden, to Washington Headquarters Services, Directorate for Information Operations and Reports, 1215 Jefferson Davis Highway, Suite 1204, Arlington, VA 22202-4302, and to the Office of Management and Budget, Paperwork Reduction Project (0704-0188), Washington, DC 20503.

1. AGENCY USE ONLY (<i>Leave blank</i>)		2. REPORT DATE September 2003	3. REPORT TYPE AND DATES COVERED Technical Memorandum	
4. TITLE AND SUBTITLE Results of Mechanical Testing for Pyroceram™ Glass-Ceramic			5. FUNDING NUMBERS WBS-22-708-31-07	
6. AUTHOR(S) Sung R. Choi and John P. Gyekenyesi				
7. PERFORMING ORGANIZATION NAME(S) AND ADDRESS(ES) National Aeronautics and Space Administration John H. Glenn Research Center at Lewis Field Cleveland, Ohio 44135-3191			8. PERFORMING ORGANIZATION REPORT NUMBER E-14029	
9. SPONSORING/MONITORING AGENCY NAME(S) AND ADDRESS(ES) National Aeronautics and Space Administration Washington, DC 20546-0001			10. SPONSORING/MONITORING AGENCY REPORT NUMBER NASA TM-2003-212487	
11. SUPPLEMENTARY NOTES Sung R. Choi, Ohio Aerospace Institute, Brook Park, Ohio 44142; and John P. Gyekenyesi, NASA Glenn Research Center. Responsible person, Sung R. Choi, organization code 5920, 216-433-8366.				
12a. DISTRIBUTION/AVAILABILITY STATEMENT Unclassified - Unlimited Subject Category: 07 Available electronically at http://gltrs.grc.nasa.gov This publication is available from the NASA Center for AeroSpace Information, 301-621-0390.			12b. DISTRIBUTION CODE	
13. ABSTRACT (<i>Maximum 200 words</i>) Mechanical testing for Pyroceram™ 9606 glass-ceramic fabricated by Corning was conducted to determine mechanical properties of the material including slow crack growth (or life prediction parameters), flexure strength, tensile strength, compressive strength, shear strength, fracture toughness, and elastic modulus. Significantly high Weibull modulus in flexure strength, ranging from $m = 34$ to 52, was observed for the 'fortified' test specimens; while relatively low Weibull modulus (but comparable to most ceramics) of $m = 9$ to 19 were obtained from the 'unfortified' as-machined test specimens. The high Weibull modulus for the 'fortified' test specimens was attributed to the chemical etching process. The slow crack growth parameter n were found to be $n = 21.5$ from constant stress-rate ("dynamic fatigue") testing in flexure in room-temperature distilled water. Fracture toughness was determined as $K_{IC} = 2.3$ to 2.4 MPa√m (an average of 2.35 MPa√m) both by SEPB and SEVNB methods. Elastic modulus, ranging from $E = 109$ to 122 GPa, was almost independent of test temperature, material direction, and test method (strain gaging or impulse excitation technique) within in the experimental scope, indicating that the material was homogeneous and isotropic. The existence of the 'fortified' layer played a crucial role in controlling and determining strength, strength distribution, and slow crack growth behavior. It also acted as a protective layer. Valid testing was not achieved in tension, compression, and shear testing due to inappropriate test specimen configurations (in compression and shear) provided and primarily due to the existence of 'fortified' layer (in tension).				
14. SUBJECT TERMS Mechanical testing; Glass ceramic; Pyroceram; Strength; Fracture toughness; Elastic modulus; Slow crack growth; Dynamic fatigue; Life prediction			15. NUMBER OF PAGES 90	
			16. PRICE CODE	
17. SECURITY CLASSIFICATION OF REPORT Unclassified	18. SECURITY CLASSIFICATION OF THIS PAGE Unclassified	19. SECURITY CLASSIFICATION OF ABSTRACT Unclassified	20. LIMITATION OF ABSTRACT	